ADDIS ABABA UNIVERSITY
INSTITUTE OF TECHNOLOGY
CENTER OF ENERGY TECHNOLOGY

DESIGN AND ANALYSIS OF SOLAR THERMAL SYSTEM FOR HOT WATER SUPPLY TO MINILK II HOSPITAL NEW BUILDING

A thesis submitted to the School of Graduate Studies of Addis Ababa University Institute of Technology in partial fulfillment for the Degree of Masters of Science in Energy of Technology

By: **Dagim Kebede**

Advisor: **Dr. Yilma Tadesse**

June, 2016

Addis Ababa,

Ethiopia

CERTIFICATION

I, the undersigned, certify that I read and hear by recommend for acceptance by Addis Ababa University Institute of Technology Energy Center a thesis entitled "Design and Analysis of Solar Thermal System for Hot Water Supply to Minilik II Hospital New Building." This certificate used as in partial fulfillment of the requirements for the degree of Masters of Science in Energy Technology.

Signature: _____

Date: _____

Dr. Yilma Tadesse

(Supervisor)

DECLARATION

I, Dagim Kebede, First, I declare that this thesis is the result of my own work and that all source or materials used for this thesis have been duly acknowledged. This thesis is submitted in partial fulfillment of the requirements for Master's Degree in Energy Technology at Addis Ababa University and to be made available at the University's Library under the rule of the Library. I confidently declare that this thesis has not been submitted to any other institutions anywhere for the award of any academic degree, diploma, or certificate.

Signature: _____

Date: _____

Dagim Kebede

Addis Ababa University Institute of Technology

School of Graduate

Energy Center

Design and Analysis of Solar Thermal System for Hot Water Supply to Minilik II Hospital New Building

By: Dagim Kebede

Approved by Board of Examiners

Dr. Yilma Tadesse (Advisor)	**Signature**	**Date** 29/01/2016
Dr.-Ing. Demiss Alemu (Internal Examiner)	**Signature**	**Date** 02/10/2016
Dr. Tesfaye Dama (External Examiner)	**Signature**	**Date** 30/8/16
Dr. Solomon Abebe (Chairman)	**Signature**	**Date** 30/8/16

ACKNOWLEDGMENT

First I would like to give an Enormous thanks to the Almighty God who gives me patient, courage and wisdom to finish this project.

I would like to express the deepest sadness for my former adviser Dr.-Ing Abebayehu Assefa whom suddenly passes away. I am grateful for his support, kind help and encouragement. And also, I express my sincere gratitude to my new advisor Dr. Yilma Tadesse for giving me the opportunity to work on this project and for his guidance and encouragement without which this work could have not been completed. I am also grateful to Dr. Solomon Abebe head of Energy Center in Addis Ababa University, Institute of Technology, for his kind help on different occasions. Last but not least, I would like to thank my family and friends who were always besides me and played a great role in completion of my work.

TABLE OF CONTENTS

CERTIFICATION i
DECLARATION ii
ACKNOWLEDGMENT iv
LIST OF FIGURES ix
LIST OF TABLES xi
ABBREVIATION xii
NOMENCLATURE xiii
ABSTRACT xvii
CHAPTER 1 1
INTRODUCTION 1
1.1 Statement of the Problem 2
1.2 Objectives 3
1.3 Scope 3
1.4 Significance 4
1.5 Organization 4
CHAPTER 2 6
LITERATURE REVIEW 6
2.1 Background 6
2.2 Type of Solar Thermal Collector 7
2.3 Solar water heating system 9
2.4 Factors Affecting Solar Water Heating (SWH) Performance 11
2.5 Summary of Literature Review 13
CHAPTER 3 14
HOT WATER DEMAND OF MINILIK II HOSPITAL 14
3.1 Introduction 14
3.2 Data from Minilik II Hospital 15
3.3 Determining Hot water demand of the Hospital 15
3.4 Hot Water Consumption Pattern 19
3.5 Hot Water Storage Tank Capacity 20
3.6 Energy Capacity of a Storage Unit 21

CHAPTER 4 22
AVAILABLE SOLAR RADIATION DATA 22
4.1 Introduction 22
4.2 Incident Solar Radiation 23
4.3 Radiation Factors 27
4.4 Basic Sun-Earth Angles 28
CHAPTER 5 30
FLAT PLATE COLLECTOR DESIGN 30
5.1 Introduction 30
5.2 Component of Flat Plate Collector 30
5.3 Material Selection 31
5.4 Assumption for Design 33
5.5 Theoretical Designing of Collector 34
5.6 Area of a Collector 42
5.7 Pressure Drop in the Collector 44
5.8 Analysis Parameters 48
CHAPTER 6 50
THERMAL STORAGE TANK AND INSULATION 50
6.1 Introduction 50
6.2 Material Selection 50
6.3 Optimization of Thermal Storage Tank 51
6.4 Optimization of Insulation Thickness 53
6.5 Optimization of Storage Tank Thickness and Outer Diameter 56
6.6 Technical Data of Storage Tank 60
CHAPTER 7 61
TRANSIENT ANALYSIS OF FLAT-PLATE SOLAR COLLECTOR 61
7.1 Transient Analysis of Solar Water Heater 61
7.2 Assumptions for Transient Analysis of Flat Plate Collector 62
7.3 Basic Energy Balance Equation 63
7.4 Transient Temperature Analysis of Collector System 67
7.5 The Heat Transfer Correlations 69

CHAPTER 8 74

MATHEMATICAL MODEL PROGRAMING 74

8.1 MATLAB Input Parameters 74

8.2 Expected Output of MATLAB 75

8.3 Procedure for Simulation of Solar Thermal Water Heater 75

CHAPTER 9 79

RESULTS AND DISCUSSION 79

9.1 Solar Contribution to the Heating Load 79

9.2 Outlet Water Temperature Graph 80

9.3 Hourly Useful Heat Gain 83

9.4 Collector Efficiency 84

CHAPTER 10 85

PUMP AND CONTROL SYSTEM SELECTION 85

10.1 Arrays of Collectors 85

10.2 Pipe Length 88

10.3 Selection of Pump 91

10.4 Control Element 95

CHAPTER 11 98

FINANCIAL ANALYSIS 98

11.1 Costs of Solar Process Systems 98

11.2 Operating, Maintenance and Replacement Cost 100

11.3 Investment cost 101

11.4 Economic Analysis 102

11.5 Payback Period 104

CHAPTER 12 105

CONCLUSIONS AND RECOMMENDATIONS 105

12.1 Conclusion 105

12.2 Recommendation 106

REFERENCE 107

APPENDIX 109
ANNEX A: MATLAB PROGRAM CODE 109
ANNEX (A-1): Mass flow rate 109
ANNEX (A-2): Plate Thickness 109
ANNEX (A-3): Riser Tube Inner Diameter 110
ANNEX (A-4): Riser Tube Outer Diameter 112
ANNEX (A-5): Number of Riser Tube 113
ANNEX (A-6): Header Tube Diameter 114
ANNEX (A-7): Insulation Thickness Optimization 115
ANNEX (A-8): Storage Tank Thickness Optimization 116
ANNEX (A-9): Transient Analysis of Temperature 116
ANNEX B: GRAPHS OF OUTLET WATER TEMPERATURE ANALYSIS 123
ANNEX C: PROPERTIES OF VARIOUS MATERIALS 124
ANNEX D: MOODY CHART 127

LIST OF FIGURES

Figure 2.1: Typical Flat Plate Collectors 7
Figure 2.2: Evacuated tube collector (flooded evacuated tube and heat pipe evacuated tube) 8
Figure 2.3: Thermosyphon SWH system 10
Figure 2.4: Direct Active SWH System 11
Figure 3.1: Daily Hot Water Demand of each Appliance 19
Figure 3.2: Hot Water Demand Distribution over the Time of the Day 19
Figure 3.3: Daily Hot Water Consumption Pattern of Minilik II Hospital. 20
Figure 4.1: Average Monthly Global Radiations 24
Figure 4.2: Average Yearly Global Radiations 25
Figure 5.1: Components of Flat Plate Collector 31
Figure 5.2: The Relation of Mass Flow Rate with efficiency and outlet Temperature of water . 34
Figure 5.3: Sheet and tube dimensions 35
Figure 5.4: Relations of Absorber Plate Thickness and Efficiency 37
Figure 5.5: Relations between Inner Diameter of Riser Tube and Efficiency 38
Figure 5.6: Relations of Inner Diameter of Riser Tube with Pressure and Velocity 38
Figure 5.7: Relations of Outer Diameter of Riser Tube and Efficiency 39
Figure 5.8: Relation of Pressure Drop with Number of Riser Tube 40
Figure 5.9: Pressure Drop and Velocity with Header Diameter 41
Figure 5.10: Schematic Representation of the flow in the collector 44
Figure 6.1: Optimum Thickness of Insulation on the Basis of Minimum Total Cost. 55
Figure 6.2: Optimum Thickness of Storage Tank on the Basis of Minimum Total Cost. 58
Figure 6.3: Thicknesses of the Storage Tank and Side Insulation 59
Figure 7.1: Cross-Section of the Flat Plat Collector 61
Figure 7.2: Heat Energy Balance of Glass Cover. 64
Figure 7.3: Heat Energy Balance of Absorber Plate. 65
Figure 7.4: Energy balance of the working fluid in flat-plate solar collector 66
Figure 7.5: Energy balance in a control volume of storage tank. 67
Figure 7.6: Thermal Networks for a One-Cover Flat-Plate Collector 69

Figure 8.1 (a) Flowchart of Simulation Programme 77
Figure 8.1 (b) Flowchart of Simulation Programme (contd.), ... 78
Figure 9.1: Solar Radiations for Minilik II Hospital 79
Figure 9.2: Outlet Water Temperatures for Different Number of Nodes 80
Figure 9.3: Outlet Water Temperatures for Different time period 81
Figure 9.4: Simulated Hourly Outlet Water Temperatures for Various Seasons 82
Figure 9.5: Simulated Hourly Storage Tank Temperatures for Various Seasons 82
Figure 9.6: Hourly Useful Heat Gain 83
Figure 9.7: Efficiency for July 17 and November 14 84
Figure 10.1: Collector modules in parallel (a) and series (b). 85
Figure 10.2: Collector Array (a) and Collector Module with Connection Line (b) 86
Figure 10.3: Clearance of Collector Array System 87
Figure 10.4: Positioning of Differential Controller 96
Figure (B-1): Outlet Water Temperature for Winter Season 123
Figure (B-2): Outlet Water Temperature for Spring Season 123
Figure (B-3): Outlet Water Temperature for Summer Season 123
Figure (B-4): Outlet Water Temperature for Autumn Season 124
Figure (D-1): Moody Chart 127

LIST OF TABLES

Table 3.1: Data from Minilik II Hospital 15
Table 3.2: Standard Hot Water Demand for Hospital 15
Table 3.3: Hot Water Demand for each Appliance of the Hospital 16
Table 3.4: Hot water demand of the Hospital per Services 18
Table 3.5: Total Hot water demand of the Hospital per Services 18
Table 3.6: Summaries of Hot Water, Storage Tank and Energy Capacity Needed 21
Table 4.1: Average Monthly Global Radiation (AMGR) data from year (2010 to 2015) 24
Table 4.2: Average Yearly Global Radiations 25
Table 4.3: Average Monthly Diffuse Radiations 26
Table 4.4: Average Monthly Beam Radiations 27
Table 5.1: Collector Analysis Parameters 48
Table 6.1: Technical Data of Storage Tank 60
Table 9.1: Summery of Annual Fraction of Solar Contribution to Load 80
Table 9.2: Monthly Useful Heat Gain 83
Table 10.1: Summery of Length of Pipes 90
Table 10.2: Specification of Selected Pump 95
Table 11.1: Price for Solar Water Heating System 98
Table 11.2: Operating, Maintenance and Replacement Cost 101
Table 11.3: Economic Analysis Parameters 102
Table 11.4: Financial Analysis Summary 104
Table (C-1): Thermal Conductivities of Absorber Materials 124
Table (C-2): Properties of Glass Cover Materials 124
Table (C-3): Properties of Sealing Materials 125
Table (C-4): Properties of Insulation Materials 125
Table (C-5): Lists Properties of Some Selective Coatings 126

ABBREVIATION

AMBR	Average Monthly Beam Radiation
AMDR	Average Monthly Diffuse Radiation
AMGR	Average Monthly Global Radiation
AYGR	Average Yearly Beam Radiation
CGF	Cost of Glass Fiber
CHL	Cost of Heat Energy Loss
CI	Investment Cost
CMSP	Cost of Mild Steel Plate
DHWSS	Domestic Hot Water Solar System
EEPCo	Ethiopian Electric Power Corporation
ES	Energy Saving
HWDKs	Hot Water Demand of Kitchen for Shower
HWDKw	Hot Water Demand of Kitchen for Washing
HWDRs	Hot Water Demand of Restaurant for Shower
HWDRw	Hot Water Demand of Restaurant for Washing
ICS	Integral Collector Storage
LCC	Life Cycle Cost
LCCS	Life Cycle Cost Saving
LCSE	Life Cycle Saving of Energy
PTCs	Parabolic Through Collectors
PV	Photovoltaic
ST	Solar Time
TC	Total Cost
TDHWD	Total Daily Hot Water Demand
TDHWS	Total Daily Hot Water Supplied
THWDK	Total Hot Water Demand of Kitchen
THWDR	Total Hot Water Demand of Restaurant
THWDS	Total Hot Water Demand of Shower

NOMENCLATURE

Notations

A	Area
C_b	Bond Conductance
Cp	Heat Capacity of Water
D	Diameter
Dr	Diffuse Radiation
F	Fin Efficiency Factor
F'	Collector Efficiency Factor
F_R	Collector Heat Removal Factor
Gr	Global Radiation
g	Gravity
H	Total Head
h	Height
h_c	Convective Heat Loss Coefficient
h_r	Radiative Heat Loss Coefficient
h_{fi}	Heat Transfer Coefficient inside Tube
I	Solar Radiation
Isc	Solar Constant
K	Thermal Conductivity
K_T	Clearness index
K_f	Pressure Loss Factor
L	Length
m	Mass
$\dot{m}$	Mass Flow Rate
N	Number of Day in a Year
Nr	Number of Riser Tube
Nu	Nusselt Number
n	Number of Node
P	Pressure Drop
Pr	Prantdl Number
Q	Heat Energy

$\dot{Q}$	Volume Flow Rate
q_{ab}	Solar Energy Absorbed by the Plate
R	Radiation Factor
Ra	Rayleigh Number
R_e	Reynolds Number
T	Temperature
t	Thickness
U	Heat Transfer Coefficient
V	Volume
V	Velocity
V_w	Average Wind Speed
W	Distance between Riser Tubes
w	Width
Y	Total Specific Work
z	Collector Row Clearance

Greek Symbols

θ_i	Incident Angle
θ_z	Zenith Angle
$\emptyset$	Latitude Angle
ω	Hour Angle
δ	Declination Angle
β	Collector Tilt Angle
α_A	Altitude Angle
γ	Collector Azimuth Angle
ε	Emissivity
α	Absorptivity
η	Efficiency
π	Pi
μ	Dynamic Viscosity
ϑ	Kinematic Viscosity
β'	Volumetric Expansion coefficient
σ	Steven Boltzmann Constant

Subscripts

a	Ambient
ap	Aperture
av	Average
b	Beam Radiation
bi	Beam Radiation on Inclined Surface
bz	Beam Radiation on Horizontal Surface
c	Collector
cn	Connection Pipe
d	Diffuse Radiation
e	Collector Edge
f	Fluid
g	Glass Cover
ga	From Glass to Ambient
h	Header Tube
i	Inlet
im	Intake Manifold
in	Insulation
L	Overall
o	Outlet
p	Absorber Plate
pab	From Plate to Back Insulation
pae	From Plate to Edge Insulation
pg	From Plate to Glass Cover
pw	From Plate to Water Stream
r	Riser Tube
rm	Return Manifold
rp	Return Pipe
sp	Supply Pipe
st	Storage Tank
T	Total
u	Useful Heat Gain

Units

A	Ampere
℃	Degree Celsius
h	Hour
H_z	Herz
J	Joule
K	Kelvin
K_g	Kilogram
KJ	Kilo Joule
KWh	Kilo Watt Hour
lt	Liter
m	Meter
min	Minute
mm	Millimeter
MWh	Mega Watt Hour
N	Newton
P_a	Pascal
s	Second
V	Voltage
W	Watt

ABSTRACT

Solar energy technology has led to the development of a number of solar appliances used for lighting, electricity, cooking and solar thermal systems. The most hopeful among them is the solar thermal system, to achieve the energy necessity for different applications at domestic as well as at the industry level. In this research work an attempt has been made to design and analyses solar thermal system for hot water supply to Minilik II Hospital new building. The selected solar collector and the heat storage are also designed based on: the amount of hot water supplied to the hospital throughout the day and the energy needed to heat the demanded hot water. Mechanical system of hot water distribution in the hospital, building structure, array of solar collector and thermal storage system of the project will be investigated.

Transient performance of the system is computed using a numerical heat transfer model of a single glass cover flat plate collector solar water heater with riser and header type active system. The various design parameters are gathered from the inside country solar water heater manufacturers and dealer companies and also from the world experience. The meteorological data for simulation was prepared by taking the average of six years starting from 2010 - 2015. From the annual contribution of solar energy to the heating load and solar fraction the estimated values of investment cost, the unit solar energy cost and the pay-back period of the system was calculated.

It was found that for Minilik II hospital of total daily hot water consumption of 30.475 m^3, a total of 108 collectors with two storage tanks of each capacity 18.3 m^3 are needed with initial capital cost of 1,006,865 Birr per project, which will cost a total of 1,864,054 Birr per project through-out its life time and the life cycle cost saving will be 1,869,571 Birr per project. The unit price of solar thermal energy is 0.033 Birr per KWh and the payback period of the project is 2.2 year.

Since the unit cost of solar energy (0.033 Birr/KWh) is less than the unit cost of electricity (0.46 Birr/KWh) in Ethiopia, therefore water heating by solar energy is a viable alternative to heating by electricity and fossil fuel (furnace oil).

CHAPTER 1

INTRODUCTION

Today, solar thermal systems are regarded as a well-established, low -tech technology with an enormous potential for energy production. Solar thermal technologies for low-to medium temperature applications can be used all over the world, cold climates to hot climates. A large variety of solar-thermal components and systems, mostly for residential, hospital, hotel, commercial building and industrial applications, are available on the market. The products are reliable and have a high technical standard in the low temperature regime (below 100 °C). Solar thermal systems in larger buildings, multi-family houses and apartment blocks and as well as in district heating plants are now emerging onto the market [1].

Solar water heating systems use the energy from the sun to heat water using a store of water in a hot water cylinder. Often a boiler or electric immersion heater will still be used to heat the stored water further ready for use. Using solar energy from the sun to 'pre-heat' stored water means that less gas is used, oil or electricity, saving money and reducing the amount of carbon produced.

In the United Kingdom, a solar thermal hot water system will work all year round, although as would be expected, more heat is generated in summer months with clear sunny days, often meeting the full hot water heating demand without further topping up. In autumn or winter months when it is overcast or cloudy, the system will rely more on a boiler or electrical supply to top-up the temperature of the water. As energy from the sun is 'free', once the installation costs have been met, a solar thermal hot water system can reduce fuel bills and in addition, using less gas or oil will reduce the carbon footprint [2].

Low temperature solar water heating system is one of essential process in hospital, residential, hotel, industry and domestic services. Many services and processes in hospital needs hot water for different applications such as washing and boiling medical equipment, washing clothes, for bath application, kitchen processes, etc.. Low temperature hot water supply system is an energy intensive process. Mainly for hospitals, the energy consumed for hot water production system is electrical and fossil fuel energy. Global environmental pollution, human health problem, increasing cost and depletion of fossil fuel, dramatically increase current demand and future

dependence of the world on electricity: leads the world to seek an efficient, effective, environmental friendly and more sustainable energy [1, 2].

This research "Solar Thermal System for Hot Water Supply to Minilik II Hospital New Building" is aimed at the development of low temperature hot water supply systems for the hot water demand of Minilik II hospital focusing on solar-thermal energy. In this project, the potential of solar thermal system to provide low temperature process hot water to the hospital will be investigated. The typical issues generated by applying solar thermal energy for hot water supply system in hospital building will be discussed. Also to maximize overall collector efficiency or to achieve the desired output temperature, how the solar collector system can be operated would be revised. Mechanical system of hot water distribution in the hospital, building structure, array of solar collector and thermal storage system of the project will be investigated. Finally the methodology employed and financial analysis of the research will be discussed.

1.1 Statement of the Problem

Ethiopia is one of the fastest growing countries by medical control in the Africa and planned to improve medical treatment of the country. Accordingly, many hospitals are launching in the country each year and the majority of newly established hospitals are using energy intensive thermal processes. Almost all of those hospitals are dependent on the electrical power supplied by EPECO, fuel and natural gases imported from abroad.

More than 50-60% of energy is used for thermal energy application in the hospital [3]. But the country has limited capacity of power production which is around 2267MW from hydropower and wind energy resources without involving the biggest renascence dam, of which more than 30% of the power is supplied for hospital sector and domestic use, the remaining 70% for industry sector. This shows the country uses electrical energy for the purpose of electrical thermal heating system [4]. More energy is demanded by industry and now a day's new industry emerges in the country. Therefore, the country needs to implement other form of renewable energy for thermal hot water production systems.

Country like Ethiopia which has 13 month of sun shined, solar thermal system which is environmental friendly and sustainable source of energy is the best alternative. Ethiopia has high potential of solar irradiation and average sun light length of more than 10 hour per day

throughout the year and has high amount of solar energy potential [5]. But, this enormous amount of solar energy is not used as expected in the country.

Solar thermal systems for hot water supply system have been identified with a number of technical defaults that have become the problem to the promotions of the system, e.g., low existing efficiency, difficulty on hot water delivery system in the building, high heat loss from the system and poor capability of solar collector to harvest solar energy. Design and analysis of solar thermal system for hot water supply to hospitals is necessary to fill the above gap.

1.2 Objectives

The general objective of this research is analyzing and designing of a solar thermal system for low temperature hot water supply to Minilik II hospital new building and designing of hot water distribution system in the building. Finally simulation of the system is expressed using MATLAB software

The specific objectives of this thesis are, therefore,

i. Analyzing the hourly temperature variation of a flat plate solar thermal system for the area.
ii. Designing the flat plate collector solar thermal system to meet the required outlet temperature of hot water demand of the hospital and determining the collector area.
iii. Designing thermal energy storage tank to meet the required outlet temperature of hot water load, selecting tank and insulation material, optimizing thermal storage tank diameter and height, determining total storage tank area and optimizing storage tank and storage insulation thickness.
iv. Designing hot water distribution system in the building and analyzing the alignment of flat plate collector array on the top of the building.
v. Financial analysis of the designed solar thermal system and the hot water distribution system. Finally the payback time of the system.

1.3 Scope

The analysis and design of this research will be based on the solar energy data available in Ethiopia Addis Ababa (Minilik). The analysis of solar thermal system encompasses a wide range

of application (for residential, hotel, hospital, industrial, etc.) but this study focus on analyzing and designing of solar thermal system for low temperature hot water supply system to Minilik II hospital new building. The characteristic and impact of this research will be identified and a range of techniques applied to perform the design and analysis of solar thermal system for hot water supply system based on implemented analysis procedures will be examined. Finally proposing optimal techniques to perform the analysis and design of the solar thermal system for hot water supply to Minilik II hospital new building is the scope of this research.

1.4 Significance

This study contributes a new form of solar thermal system for low temperature hot water supply system to the hospital processes which requires hot water. It works by renewable energy focuses on solar radiation as the power source of the system will minimizes the electric and fossil fuel energy consumption of the hospital for hot water supply system and it will improve energy consumption pattern of the hospitals. Also it will form a clean environment and free from different hazards which affects human health.

The results of this research will open an opportunity for further application of solar thermal system for hot water supply system in the country. In addition, the result can be used as reference and base for future expansion plans and by policy-maker. Also this study could suggest some points for further improvement of the system based on theoretical point of views.

1.5 Organization

The thesis is organized as twelve different chapters. The rest of the paper is organized as follows. The next chapter is devoted to literature review gives an overview of the history, present and future trends of the solar thermal system and low temperature hot water supply system.

Chapter three is hot water demand of Minilik II hospital presents the total daily hot water demand of the hospital, water consumption pattern of the hospital and appliance used hot water in the hospital new building.

Chapter four is available solar radiation data dial with solar radiation data organization, determining beam and diffuse radiation of the area, determining hourly, monthly and yearly global radiation and calculating basic sun angles.

Chapter five is flat plate collector design presents theoretical design of collector components, selection of collector material and listing design parameters.

Chapter six is storage tank and insulation dial with the selection of storage tank and insulation material, optimization of storage tank volume, area height and diameter, and optimization of insulation and storage tank thickness.

Chapter seven is transient analysis of solar thermal system presents the transient analysis of collector system, energy balance of collector and transient analysis of temperature of collector systems.

Chapter eight is mathematical model programing presents the analysis of temperature, useful heat gain and instantaneous efficiency by using MATLAB simulation software.

Chapter nine is results and discussion presents the brief discussion of the results from MATLAB simulation programing software.

Chapter ten is pump and control system selection dial with the selection of pump based on flow rate and head, selection of control system and arrays of collector system.

Chapter eleven is financial analysis presents the cost of component and installation, total investment cost, life cycle cost of the system, unit price of the solar thermal energy and payback period of the system.

The last chapter is conclusion and recommendation presents the summary and main conclusions of this thesis. The topics for future work are also discussed in the end.

CHAPTER 2

LITERATURE REVIEW

2.1 Background

First solar water heaters were invented in the 1890"s in California. By 1954, Florida had over 100,000 solar hot water systems. Popularized nation-wide in the 1970's but industry faded in the 1980's. There is a re-emerging market today with the need for renewable sources of energy. Today's technology is superior and well regulated. Many countries around the world use solar energy as a primary source of thermal system for hot water supply. The U.S. only accounts for 1% of the global solar thermal market, a $4 Billion dollar industry [6].

Ethiopia is known to have an annual mean average solar radiation of about 5.2 KWh/m2, with the minimum being 4 KWh/m2 and the maximum estimated to be 6 KWh/m2. With this suitable solar radiation resource, it is expected that this section of the guidelines and tariff methodology, which will apply to grid connected solar PV or solar thermal energy resource, will serve as catalyst to attract private sector capital into Ethiopia's solar electricity generation [4].

Ethiopia has substantial solar energy resource. However, less than 1% of the potential has been exploited so far. According to the recent data collected by energy information administration and development follow up core process, within the last 6 years, the total generated energy from solar photovoltaic is more than 35 MWh, more than 6MW than the installed capacity. Solar water heating systems with the total energy generation of 299 MWh and ten water pumps with pumping installed capacity of 10 kW have been installed in different parts of the country by governmental and nongovernmental organizations [4].

Solar heaters, or solar thermal systems, provide environmentally friendly heat for industry water heating, commercial building water and space heating, hospital water and space heating and household water and space heating, and the heating of swimming pools. Such systems collect the sun's energy to heat a fluid. The heated water is then stored in a tank similar to a convectional gas or electric water tank. Some systems use an electric pump to circulate the fluid through the collectors [7].

2.2 Type of Solar Thermal Collector

A solar collector is a special kind of heat exchanger that transforms solar radiant energy into heat. A solar collector differs in several aspects from most conventional heat exchangers. The latter usually accomplish a fluid-to-fluid exchange with high heat transfer rates and with radiation as an unimportant factor. In the solar collector, energy transfer is from a distant source of radiant energy to a fluid [7].

There are basically two types of solar collectors;

1. **Non-concentrating or stationary collectors:** has the same area for intercepting and for absorbing solar radiation. Unlike concentrating collectors it has no sun-tracking.
2. **Concentrating solar collector:** has a concave reflecting surface to intercept and focus the sun's beam radiation to a smaller receiving area, by increasing solar radiation flux.

2.2.1 Flat Plate Collector

Flat-plate collectors can be designed for applications requiring energy delivery at moderate temperatures, up to perhaps 100°C above ambient temperature. They use both beam and diffuse solar radiation, and do not require tracking of the sun, with little maintenance required. They are mechanically simpler than concentrating collectors. The major applications of these units are in solar water heating, building heating, air conditioning, and industrial process heat [8].

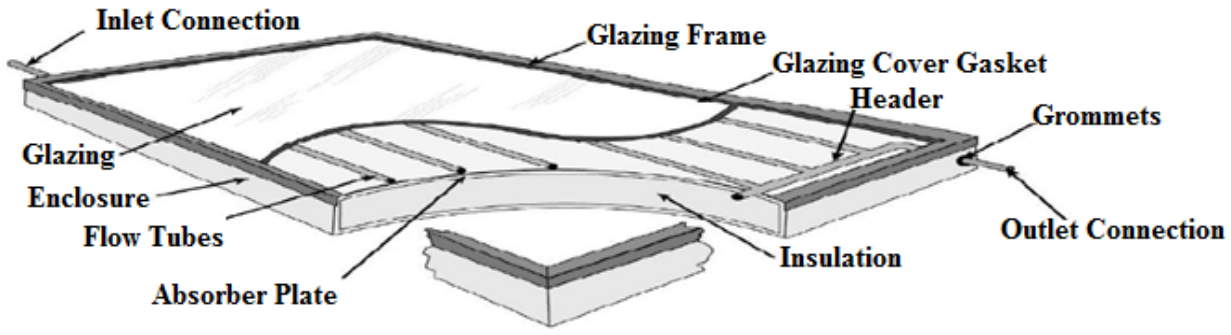

Figure 2.1 Typical Flat Plate Collectors

2.2.2 Evacuated Tube Collector

Evacuated tube collectors are mostly used to heat water that requires higher temperature than flat plate collector. Sunlight enters through the outer glass tube and strikes the absorber tube(s) and

changes to heat. The heat is transferred to the liquid flowing through the absorber tube. Evacuated-tube collectors generally have a smaller solar collecting surface because this surface must be incased by an evacuated glass tube [8].

In "***flooded***" evacuated-tube collectors the absorber itself forms a tube through which the heat collection fluid is pumped and typically used in passive Thermosiphon systems.

In a "***heat pipe***" evacuated-tube collector, a flat absorber plate running the length of the tube covers a heat pipe filled with a fluid that evaporates at relatively low temperatures. As the fluid is heated, it evaporates and raises to the top of the tube to transfers the heat to water in a manifold and condensed heat-collection fluid then return by gravity to the bottom of the heat pipe. These systems can be active or passive [8].

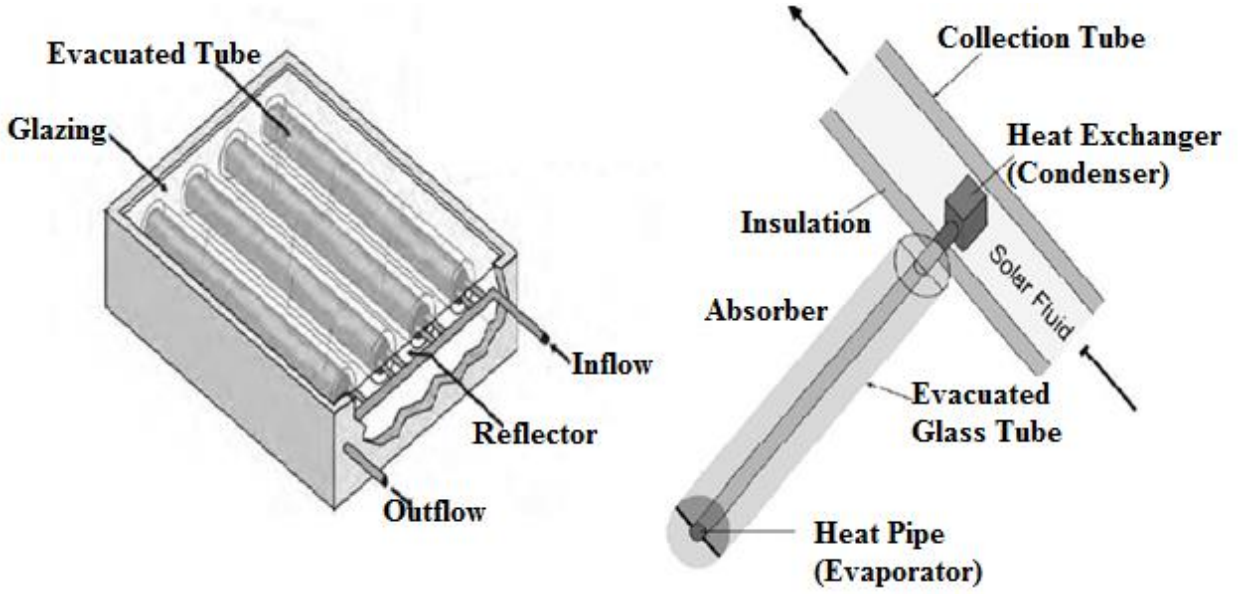

Figure 2.2: Evacuated tube collector (flooded evacuated tube and heat pipe evacuated tube)

2.2.3 Concentrating Collectors

Concentrating collectors make use of curved reflectors to concentrate sunlight on a receiver. The intensity of sunlight falling on the receiver can be up to 60 times the intensity of normal sunlight. The parabolic reflector concentrates sunlight on a tube running along the reflector's focal line, thereby heating the water passing through the tube. Usually, the reflector is controlled by a tracking system that keeps the reflector facing direct sunlight throughout the day [8].

In order to deliver high temperatures with good efficiency, a high performance solar collector is required. Systems with light structures and low cost technology for process heat applications for hot water temperatures up to 400 °C could be obtained with a type of concentrating collector called parabolic trough collectors. PTCs can effectively produce heat at temperatures between 50 and 400 °C [8, 9].

2.3 Solar water heating system

Solar water heating systems are classified depending on how the domestic water is heated or how the heat transfer fluid (water or antifreeze fluid) flows through the collector. Factors that influence the selection of a specific system type include the amount of water that needs to be heated, relative cost and efficiency, simplicity of operation, and climate conditions in which the system will be used [9].

2.3.1 Passive Systems

In passive systems, hot water is either stored in the collector itself or is transferred to a storage tank located above the collectors by means of a Thermosiphon. Passive systems do not employ pumps to circulate water or collector fluid. This makes them generally more reliable, easier to maintain, and possibly long lasting than active systems. There are two types of passive systems; Thermosiphon systems and Integral collector storage systems [7, 8, 9].

a) Integral Collector Storage (ICS) Systems (Batch Systems)

In integral collector storage or batch systems, water is heated directly by the sun and the storage tank serves as the solar collector. Batch water heaters are almost always passive systems in which hot water is delivered from the solar heated tank to a backup tank or the point of use by the water pressure in the house. Most designs use local main water pressure to circulate water in the collector. Water may also flow due to buoyancy forces set up due to differential heating on the collector and valves control the flow direction. Hot water is drawn from the top, which is the hottest, and replacement water flows into the bottom. These systems are relatively cheaper than thermosyphon systems [8, 9].

b) Thermosyphon Systems

As the sun shines on the collector, the water inside the collector flow-tubes is heated. As it heats up, this water expands slightly and becomes lighter than the cold water in the solar storage tank

mounted above the collector. Gravity then pulls heavier (cold water) down from the tank and into the collector inlet. The cold water pushes the heated water through the collector outlet and into the top of the tank, thus heating the water in the tank. A thermosyphon system requires neither pump nor controller [7, 9].

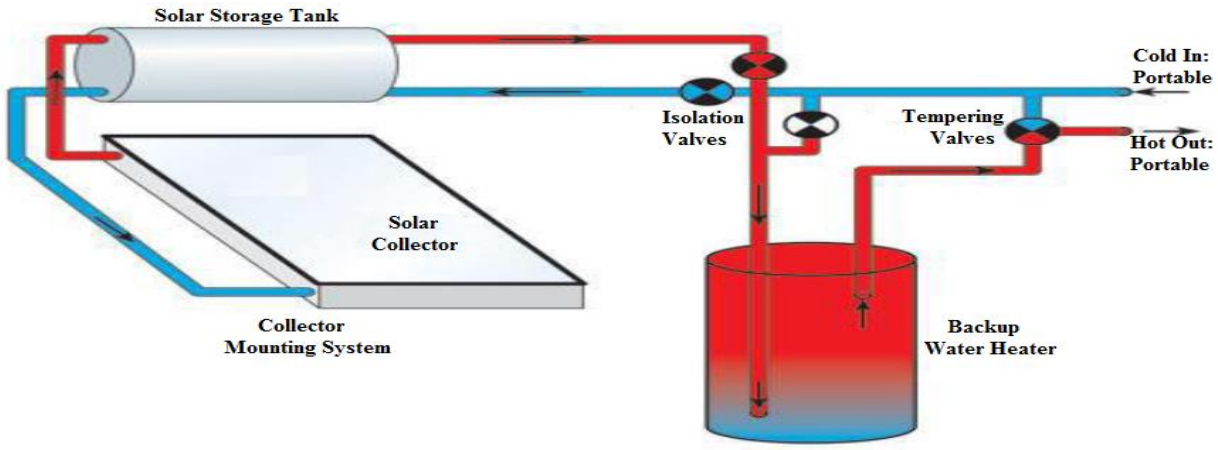

Figure 2.3: Thermosyphon SWH system

2.3.2 Active Systems

Active systems use pumps, valves, and controllers to circulate water or other heat-transfer fluids through the collectors. They are usually more expensive than passive systems but are also more efficient. Active systems are usually easier to retrofit than passive systems because their storage tanks do not need to be installed above or close to the collectors. But because they use electricity for pumping, they will not function in a power outage [7, 8, 9].

i. Direct (Open Loop) Active Systems

Direct (Open Loop) Active Systems are similar to thermosyphon systems in that they are direct systems that use a solar collector separate from the storage tank. The difference with direct active systems is that they use an electric pump to circulate water from the storage tank to the collector, and back to the storage tank. Direct System is the most common systems in use in tropical and sub-tropical climates where temperatures do not often go below 0°C [7, 8, 9].

a) Recirculation Systems

These are a specific type of open-loop system that provides freeze protection. They use the system pump to circulate warm water from storage tanks through collectors and exposed piping when temperatures approach freezing [7].

b) Photovoltaic Operated Systems

The main difference of this system and recirculation system is the energy to power the pump; for this system energy provided by a photovoltaic (PV) panel [7, 9].

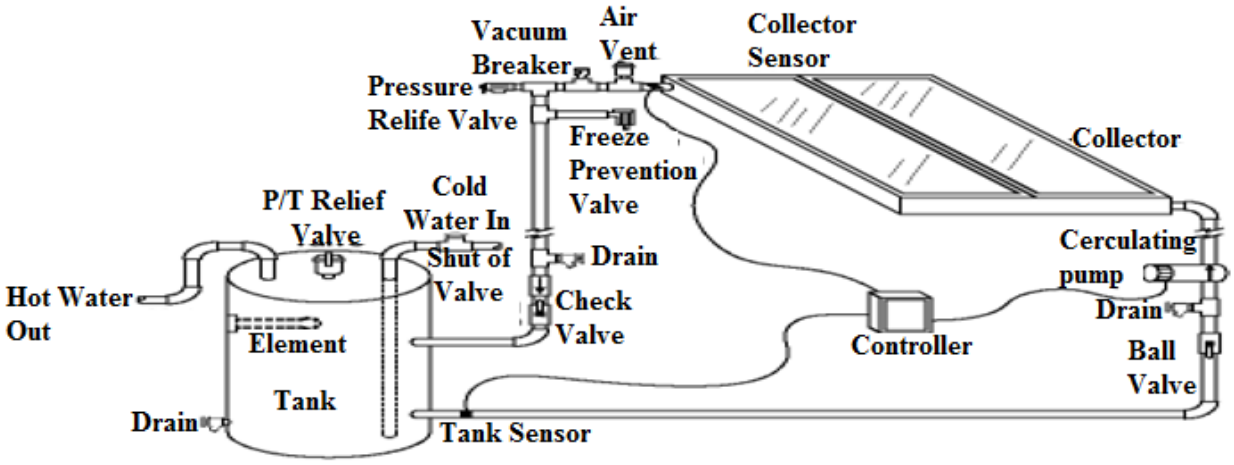

Figure 2.4: Direct Active SWH System

ii. Indirect (Closed Loop) Active Systems (Glycol Antifreeze Systems)

Closed-loop (***Indirect Systems***) active systems are designed for use in climates where freezing weather can occur more frequently. These systems, also known as closed loop systems, are the most commonly used in cold climates where temperatures often go below 0°c. A solar collector, filled with an anti-freeze solution (heat-transfer fluids), is used to collect the thermal energy in sunlight. Typically a propylene glycol or ethylene glycol and water mixture is used. Glycol antifreeze systems are active, indirect systems with a heat exchanger [7, 8, 9].

1. Drain Back Systems

Drain back systems are used in cold climates to reliably ensure that the collectors and the piping never freeze. In drain back mode all of the liquid in the collectors and piping is drained back into an insulated reservoir tank when the system is not producing heat. An indicator on the reservoir tank shows when the collector is completely drained and each time the pump shuts off the solution in the collector is drained into the reservoir tank [7].

2.4 Factors Affecting Solar Water Heating (SWH) Performance

The performance of a solar water heating system depends on the following factors

2.4.1 Ambient Conditions

The amount of incident radiation determines the absorbed solar radiation by the collector while the ambient temperature determines the thermal losses from the collector. Cloudy conditions limit the beam insolation levels and thus the radiation absorbed by the collector especially the concentrating collectors [1, 5].

2.4.2 Collector Orientation and Tilt

Geographic orientation and collector tilt can affect the amount of solar radiation received by system. Collector orientation is critical in achieving maximum performance from a solar energy system. In general, the optimum orientation for a solar collector in the northern hemisphere is true south (azimuth of 180°). However, recent studies have shown that, depending on the location and collector tilt, the collector can face up to 90° east or west of true south without significantly decreasing its performance [1, 5].

2.4.3 Transport Fluid Flow Rate

Low collector fluid flow rates of about $(0.005 - 0.02 m^3/min)$ increases the thermal performance of the collector by increasing the degree of storage tank thermal stratification. In a stratified tank, the temperature of fluid at the bottom of the storage tank is lower than at the top. Collector inlet temperature is reduced because the collector inlet fluid is fed from the bottom portion of the tank that reduces thermal losses and increased useful energy gain [1, 5].

2.4.4 Collector Array Arrangement

The performance of the collector array depends on how the collector modules are connected. In parallel connection, module inlet and outlet ports are fed to the common respective headers. Assuming identical modules, fluid inlet temperature is the same to all modules in the array and also true to fluid outlet temperature. The performance of the collector array is thus the same as the performance of the individual collector. Unlike parallel connection; in series connection, the performance of the second and subsequent modules will not be the same as the first because its inlet temperature is the outlet temperature of the first [1, 5].

2.4.5 Collector Characteristics

Collector area, its absorber plate absorbents property and its glass cover optical properties affect the amount of the incident solar irradiation that can be absorbed while collector insulation thickness and its thermal conductivity affect the overall heat loss coefficient and thus the thermal losses [1, 5].

2.5 Summary of Literature Review

A solar water heater is a long-term investment that will save money and energy for many years. Like other renewable energy systems, solar water heaters minimize the environmental effects. In addition, they provide insurance against energy price increases, help reduce our dependence on imported oil, and are investments in everyone's future.

The proposed solar water heating system would be of the active system type where flat plate collector thermal performance would be analyzed because it is the most used collector in Africa. The solar collector modules would be better if identical and parallel connected so as to have the same fluid inlet and outlet temperatures in all the modules in the array. Low inlet temperature of a collector would be preferred, to reduce thermal losses and increase useful energy gain and thermal performance.

CHAPTER 3

HOT WATER DEMAND OF MINILIK II HOSPITAL

3.1 Introduction

Hospitals and health care buildings traditionally have high energy demands for both mechanical power and heat. Heat is required for space heating needs, sanitary hot water, and steam production. Among the heat required system of the hospital, water heating system is one of the most energy extensive process. Demand for Hot water consumption in hospital is very high. Also, because of the big size of the buildings, there is important loss of heat in the pipeline [3].

That's why the needs in hot water must be determined with accuracy, since they differ from one hospital to another, in order to avoid unnecessary energy consumption for water heating. To reduce energy use and greenhouse gas emissions by hospital facilities, the health care sector needs energy efficient solutions operating at the lowest cost and free from environment pollution gas emission.

Generally almost all hospitals in the world require water for different appliance that Depending on the type and size of a facility, hospitals typically use 15% of their water for non-domestic use (sterile processing and radiology) and 85% for domestic use including (boilers, chillers, food services to the patient and pantry service for guests, operating rooms, laundry facilities, kitchen equipment, sinks, tubs and showers, washing basing and toilets). Daily water demand of the hospital about 90% is hot water and 10% is cold water application [3].

In Ethiopia most of hospitals requires hot water for the appliance including kitchen equipment washing, laundry facilities, showering purpose, food service to the patient and hospital restaurants, sterile processing, boilers and radiology. Few private hospitals have higher standard, which riches to the typical standard hospital hot water demand and appliance used.

This chapter manly concentrates on hot water demand calculation of Minilik II hospital. This hospital uses electricity as sources of energy for water heating, to meet daily hot water demand of the hospital. The appliance considered for this study includes kitchen equipment, laundry facilities, shower and restaurant of Minilik II hospital new building.

3.2 Data from Minilik II Hospital

In developing countries such as Ethiopia, due to absence or malfunction of measuring instruments and misinformation about hospital hot water system, reliable data of the hospital is not found. In the absence and scarcity of reliable hot water system of the hospital data, assumption and estimation are made based on the standard hot water delivery system of hospital. Data gathered methods are inspection (the hospital building) and interview (the workers of the hospital).

Table 3.1: Data from Minilik II Hospital

Parameters	Appliance					
	Kitchen	Shower			Restaurant	Laundry
		Patient 1	Patient 2	Medical Stuff 3		
Number of Room	2	72	48	28	1	1
Person per Room	10	4	2	10	8	10
Occupancy	100%	95%	90%	35%	100%	100%

3.3 Determining Hot water demand of the Hospital

The hot water demand is decisive for the dimensioning of a domestic hot water solar system (DHWSS). However, this depends on the users' habits. For example, if a person is used to have a shower rather than a bath, the daily hot water demand is significantly lower than if a bath is frequently taken. For developed countries, it is better to assume that the daily hot water requirement for based on the developed countries requirement.

Table 3.2: Standard Hot Water Demand for Hospital

Demand	Standard Hot Water Demand for Different Uses			
	Kitchen	Shower	Restaurant	Laundry
Hot Water	320 $l/kitchen$	60 $l/person$	160 $l/restaurant$	530 $l/laundry$
Temperature	48℃	43℃	48℃	60℃

For this study; determination of the hospital hot water demand per day; is performed by make assumptions. Depending on Ethiopian condition it is good to assume that the daily hot water

requirement for shower will be determined by multiplying the developed countries hot water requirement for shower by the ratio (**3:4**). Final hot water demand for each appliance is listed in table 3.3.

Table 3.3: Hot Water Demand for each Appliance of the Hospital

Demand	Appliance of the Hospital			
	Kitchen	**Shower**	**Restaurant**	**Laundry**
Hot Water (lt/day)	320	45	260	500
Temperature (℃)	50	45	50	60
Energy Source	Electrical	Electrical	Electrical	Electrical

Determination of hot water demand of the hospital for different appliance is done by considering only hot water needs of hospital new building. There is one hot water consumption systems in the hospital that is the daily hot water consumption system, used for determination of solar thermal water heating system and to optimize storage tank and collector area.

Hot water demand for each appliance is given by:

$$HWD = (Number\ of\ room) * (Water\ per\ appliance) \quad ---------- \quad (3.1)$$

Hot water demand for showering service is given by:

$$HWDKs = (Number\ of\ room) * \left(\frac{person}{room}\right) * \left(\frac{water}{person}\right) * (Occupancy\ rate) \quad ------ \quad (3.2)$$

Total daily hot water demand of the hospital is determined as:

$$TDHWD = HWDK + HWDR + HWDL + HWDS \quad ---------- \quad (3.3)$$

3.3.1 Hot Water Required for Kitchen

In the kitchen hot water is required for cooking equipment washing and shower service for cookers.

By applying equation (3.1), daily hot water demand for the kitchen is:

$$HWDK = 2 * 320lt = \mathbf{640\ liter\ per\ day}$$

3.3.2 Hot Water Required for Restaurant

For the hospital restaurant hot water is required for cooking and café equipment washing and shower service for restaurant servant.

Hot water demand of the restaurant is determined by applying equation (3.1):

$$HWDR = 1 * 260lt = \mathbf{260\ liter\ per\ day}$$

3.3.3 Hot Water Required for Laundry Service

Hot water is required for laundry service of the hospital is for cloth washing and shower service of workers in the room.

Hot water demand for laundry service is determined by applying equation (3.1):

$$HWDL = 1 * 530lt = \mathbf{530\ liter\ per\ day}$$

3.3.4 Hot Water Required for Shower

Shower service is required for the patients, workers and medical staffs of the hospital. Based on the rate of occupancy shower service is divided in to four and hot water demand for shower service is determined by using equation (3.2).

Shower service for kitchen worker is:

$$HWDKs = 2 * 10 * 45lt * 1 = \mathbf{900\ liter\ per\ day}$$

Shower service for patient 1 is:

$$HWDS1 = 72 * 4 * 45lt * (0.95) = \mathbf{12{,}312\ liter\ per\ day}$$

Shower service for patient 2 is:

$$HWDS2 = 48 * 2 * 45lt * (0.90) = \mathbf{3{,}888\ liter\ per\ day}$$

Shower service for medical staff is:

$$HWDS3 = 28 * 10 * 45lt * (0.40) = \mathbf{5040\ liter\ per\ day}$$

Shower service for restaurant worker is:

$$HWDRs = 1 * 8 * 45lt * (1) = \mathbf{360\ liter\ per\ day}$$

Shower service for laundry worker is:

$$HWDLs = 1 * 10 * 45lt * (1) = \mathbf{450\ liter\ per\ day}$$

Total daily hot water demand for shower service is determined by using equation (3.3):

$$THWDS = 900lt + 12{,}312lt + 3{,}888lt + 5040lt + 360lt + 450lt = \mathbf{22{,}950\ liter\ per\ day}$$

3.3.5 Total Hot Water Demand of the Hospital

Therefore, the total amount of hot water demand of the hospital is ($THWD$):

$$THWD = 640lt + 260lt + 530lt + 22{,}950lt = \mathbf{24{,}380\ liter\ per\ day}$$

Table 3.4: Hot water demand of the Hospital per Services

Demand	Services				Total
	Kitchen	Shower	Restaurant	laundry	
Hot Water (lt/day)	640	22,950	260	530	24,380

The daily and weekly hot water consumption of the hospital can be increase or decrease from the calculated value, so to compensate the error created the calculated value can be multiplied by same factor 1.25. The factor is one fourth of the total calculated daily and weekly hot water demand of the hospital [10].

Total hot water should be supplied ($THWS$) is:

$$THWS = \left(Daily\ Hot\ Water\ Consumption\ \frac{liter}{day}\right) * 1.25 \quad (3.4)$$

Table 3.5: Total Hot water demand of the Hospital per Services

Demand	Services				Total
	Kitchen	Shower	Restaurant	Laundry	
Hot Water ($liter/day$)	**800**	**28,687.5**	**325**	**662.5**	**30,475**

The variation of total daily hot water demand of each appliance is shown by the figure 3.1.

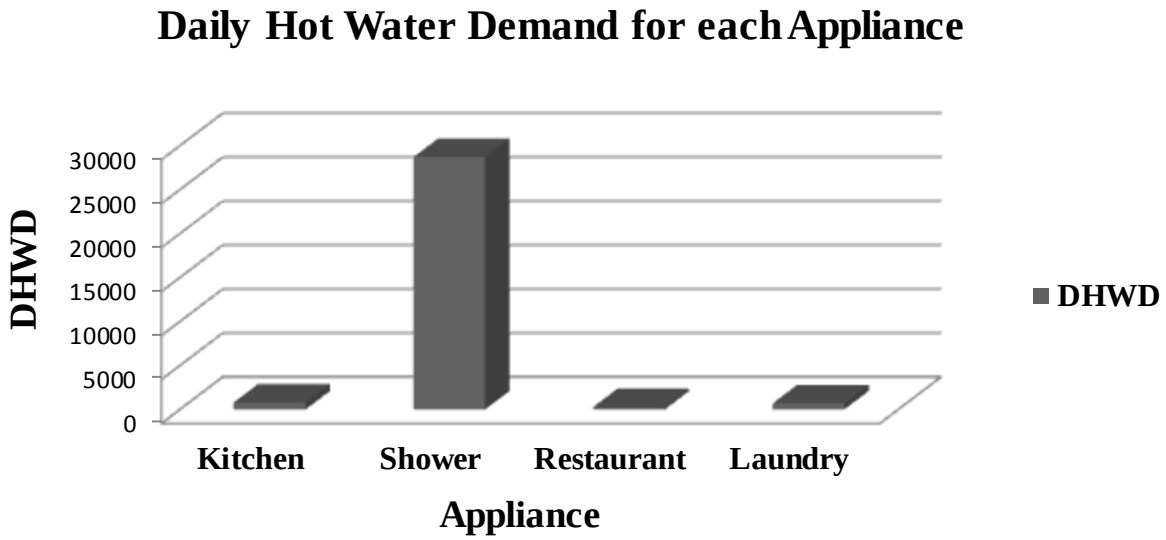

Figure 3.1: Daily Hot Water Demand of each Appliance

3.4 Hot Water Consumption Pattern

Daily hot water requirement for Minilik II hospital will be 30,475 liter per day. This daily hot water consumption can be distributed as 75% in the morning, 9% at the mid-day and the rest 16% will be distributed in the evening time.

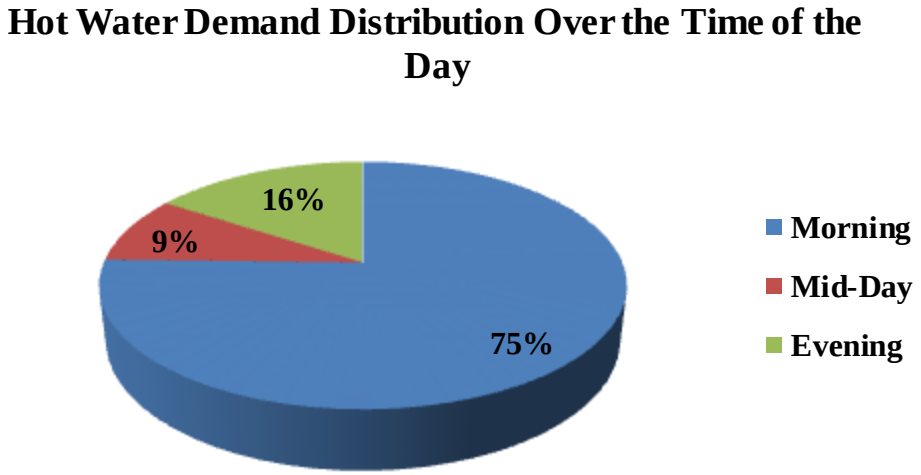

Figure 3.2: Hot Water Demand Distribution over the Time of the Day

Hot water consumption pattern of the selected hospital is summarized by fig. 3.3.

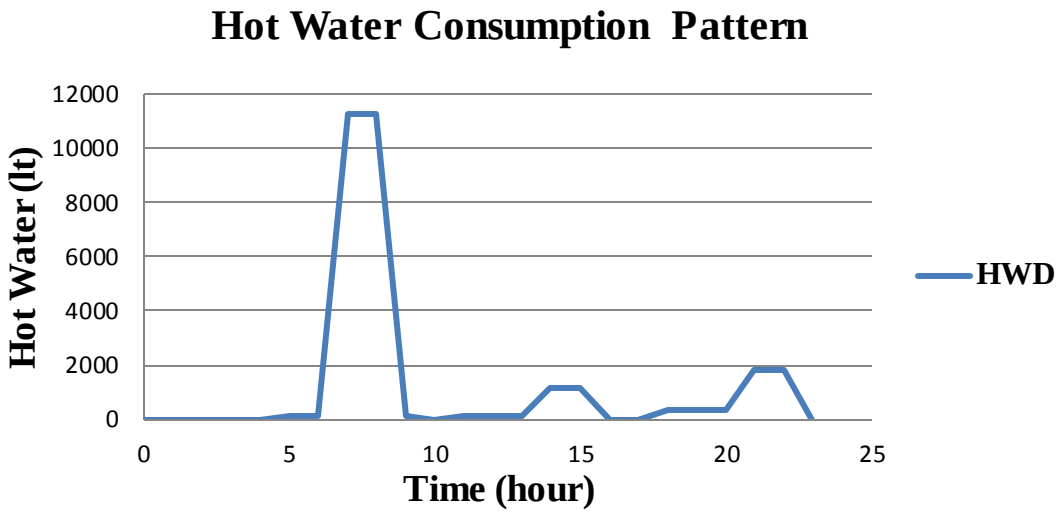

Figure 3.3 Daily Hot Water Consumption Pattern of Minilik II Hospital.

Hot water requirement of the hospital reaches maximum demand (pick demand) at the morning time of the day and the minimum demand is at mid-day time of the day.

3.5 Hot Water Storage Tank Capacity

When the daily hot water demand has been determined, the volume of the storage tank can be specified. It should be some 0.8 to 1.2 fold the daily demand for regions with high solar radiation and 2 to 2.5 fold the daily demand for regions with lower solar radiation respectively, so that consumption peaks can be met well and cloudy days can be compensated [3].

The volume of the storage tank (V_{St}) is thus calculated as follows:

$$V_{St} = THWD * 1.2 \quad (3.5)$$

For total daily hot water demand volume of the storage tank (V_{St}) is:

$$V_{St} = 30{,}475lt * 1.2 = \mathbf{36{,}570\ liter}$$

As the manufacturers do not offer tanks in every possible size, the choice has to be made among those generally available on the market. However, it is recommended that the storage tank capacity is not less than 90% and not more than 120% of the calculated volume [3].

3.6 Energy Capacity of a Storage Unit

The energy storage capacity of a water storage unit at uniform temperature is given by [5]:

$$Q_S = (\dot{m} C_p)\Delta T \quad (3.6)$$

Where: Q_S = total heat capacity of the storage tank [KWh]

$\dot{m}$ = volume of the storage tank [m^3]

$C_p = 4.2 \frac{\text{KWh}}{\text{m}^3\,\text{K}}$ heat capacity of water

ΔT = temperature difference − hot and cold water temperature [K]

Total daily energy demand (Q_S) is:

$$Q_S = 36.6m^3 * 4.2 \frac{KWh}{m^3 K} * (333 - 293)K = \mathbf{6,148.8KWh}$$

Table 3.6: Summaries of Hot Water, Storage Tank and Energy Capacity Needed

Summaries of Hot Water, Storage Tank and Energy Capacity			
Total Demand	**Daily Hot Water Consumption**	**Storage Tank**	**Energy Capacity**
Daily	30,475 lt	36.6 m^2	6.2 MWh

CHAPTER 4

AVAILABLE SOLAR RADIATION DATA

4.1 Introduction

Solar power is the flow of energy from the sun. The primary forms of solar energy are heat and light. Sunlight and heat are transformed and absorbed by the environment in a multitude of ways. Some of these transformations result in renewable energy flows such as biomass, wind and waves. Effects such as the jet stream, the Gulf Stream and the water cycle are also the result of solar energy's absorption in the environment [5].

Interest in solar energy has prompted the accurate measurement and mapping of solar energy resources of the globe. Solar radiation data are available in several forms. Most radiation data available for horizontal surfaces include both direct and diffuse radiation. This is normally done by using solar-meters. Most solar-meters measurements are recorded simply as total energy (global radiation) incident on the horizontal surface; other measurements separate the direct (beam) and the scattered (diffuse) radiation.

Radiation data are the best source of information for estimating average incident radiation and for the proper designing of a solar water heating system. A precise analysis and design of a solar water heating system requires knowledge of the solar thermal system, the availability of global solar radiation and its components at the location of project site. Since the solar radiation reaching the earth’s surface depends upon climatic conditions of the place, a study of solar radiation under local climatic conditions is essential [5, 10].

Due to absence or malfunction of measuring instruments, reliable solar radiation data is not available. In the absence and scarcity of trustworthy solar radiation data, the use of an empirical model to predict and estimate solar radiation seems inevitable. This study uses data of solar radiation and ambient temperature from Ethiopian metrological agency for the project location (around Minilik II hospital). Solar radiation data available in Ethiopian metrological agency is only global radiation. Beam and diffuse solar radiation data calculated by using solar energy empirical relations, available global radiation data at project site, location (latitude and longitude) of Minilik II hospital and weather condition of the area.

4.2 Incident Solar Radiation

The solar radiation energy incident on the collector surface which is inclined at an angle of (β) to the horizontal surface is defined in terms of global, diffuse, beam and reflectivity radiation. Total solar radiation incident on a surface consists of beam, diffuse and reflected solar radiation from the ground and surrounding. Total radiation on a surface can be evaluated by arbitrary orientation from knowledge of beam, diffuse and global radiation on horizontal surface [5].

The total incident radiation on this surface can be written as:

$$I_T = R_b I_b + R_d D_r + \rho R_r G_r \quad (4.1)$$

The flux incident beam radiation collected by the absorber per unit time is given by:

$$I_c = I_T(\tau_g \alpha_p) \quad (4.2)$$

4.2.1 Global Radiation (G_r)

Global solar radiation is the sum of the beam and the diffuse solar radiation on a surface (the most common measurements of solar radiation are total radiation on a horizontal surface, often referred to as global radiation on the surface.

Available global radiation on a given area can be determined in two ways:

- First one is estimating the radiation data using solar energy empirically relations and
- Second one is measuring the radiation data by using solar-meters instrument called pyranometers, that most of available solar radiation data are obtained.

Generally for this study, analysis of available temperature at project location to heat water uses measured global radiation by Ethiopian metrology agency. Global radiation data gained from metrological agency is read from automatic station within 15 minutes.

a) Average Monthly Global Radiation

The monthly average global radiation on a horizontal surface can be calculated from the meteorological data of hourly and daily global radiation on a horizontal surface and global radiation on an inclined surface is determined multiplying global radiation on horizontal surface by same angle (β). Average monthly global radiation of project site gained from metrological for 6 year (2010-2015) is given in the table 4.1.

Table 4.1: Average Monthly Global Radiation (AMGR) data from year (2010 to 2015)

Average Monthly Global Radiation (W/m^2)												
Year	Months of the Year											
	Jan	Feb	Mar	Apr	May	Jun	Jul	Aug	Sep	Oct	Nov	Dec
2010							382	438	507	593	513	542
2011	543	592	549	492	486							
2012	585	603	589	499	507	451	421	428	512	613	564	551
2013	599	607	600	514	513	480	423	436	542	606	581	569
2014	604	620	616	524	529	513	432	441	547	608	595	598
2015	613	631	628	597	556	524	465	470	611	615	632	638

Radiation data on Minilik II hospital location is taken from nearest metrology agency station (bole Ethiopia). Global radiation was evaluated in grades after every 15 minutes and then the mean value of the hourly and daily will be calculated.

Average monthly global radiation data listed on table 4.1 for different year is graphically expressed as:

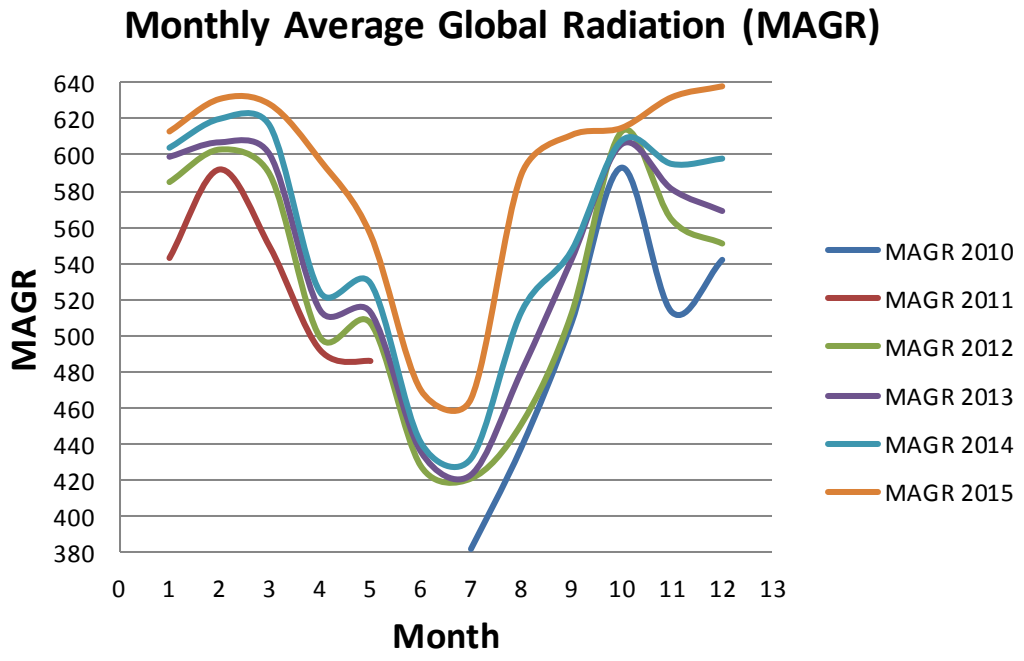

Figure 4.1: Average Monthly Global Radiations

Average monthly global radiation decreases from January up to July and increases from July up to October finally decreases up to December. Minimum radiation is received in July month for each year and reaches maximum from January up to March and for October up to November months almost for all years.

b) Average Yearly Global Radiation

Average yearly global radiation (AYGR) on horizontal surface can be calculated from monthly average listed in table 4.1. Average yearly global radiation shows available solar radiation energy distribution over different years on the given location.

Table 4.2: Average Yearly Global Radiations

Average Yearly Global Radiation (W/m^2)						
Year	**2010**	**2011**	**2012**	**2013**	**2014**	**2015**
AYGR	**496**	**532**	**527**	**539**	**552**	**587**

Average yearly global radiation listed in table 4.2 is used to understand yearly variation of global solar radiation on the given location and help to predict or estimate the coming year global radiation on the project site.

Graphical expression of average yearly global radiation listed in table 4.2 is given as:

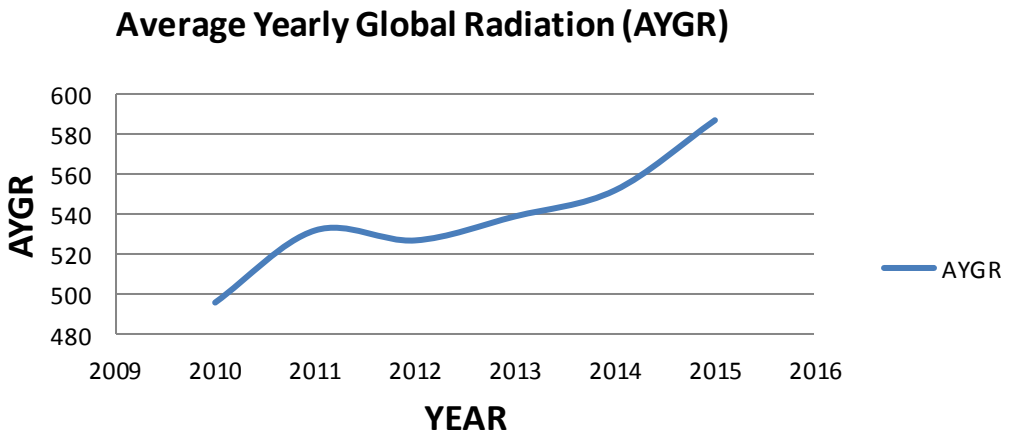

Figure 4.2: Average Yearly Global Radiations

Average yearly global radiation increases from one year to the coming year as shown in fig 4.2. This implies there is a change of solar radiation energy and weather condition of the location as year increases that indicates environmental change at the location through the year increases. For

the analysis of this study, available global radiation data on the year of 2015 is selected by predicting the coming year global radiation also increases.

4.2.2 Extraterrestrial Radiation (I_o)

Extraterrestrial Radiation is the solar radiation outside of the earth's atmosphere. By integrating the instantaneous radiation over the hour angle is given by [5]:

$$I_o = I_{sc}\left[1.0 + 0.033cos\left(\frac{360N}{365}\right)\right] cos(\theta_z)\ \left[\frac{KJ}{m^2 h}\right] \quad (4.3)$$

4.2.3 Diffuse Radiation (D_r)

The solar radiation received from the sun after its direction has been changed by scattering the atmosphere. Diffuse radiation is referred to in some meteorological literature as sky radiation or solar sky radiation. The hourly diffuse radiation on a horizontal plane correlated to the hourly clearness index (k_T). Diffuse radiation can be determined from the product of clearness index and global radiation, and the equation for the correlation is given by [5]:

$$\frac{D_r}{G_r} = \begin{cases} 1.0 - 0.249k_T & for \quad k_T < 0.35 \\ 1.557 - 1.84k_T & for \quad 0.35 < k_T < 0.75 \\ 0.177 & for \quad k_T > 0.75 \end{cases} \quad (4.4)$$

Therefor:

$$D_r = G_r * k_T \quad (4.5)$$

Hourly clearness index (k_T) during a particular hour is the ratio of the hourly global radiation on surface to the hourly extraterrestrial radiation on surface during the same time period.

$$k_T = \frac{G_r}{I_o} \quad (4.6)$$

Hourly global radiation is gain from metrology agency and hourly extraterrestrial radiation of a given area is calculated using the location (latitude and longitude), basic sun angle and solar constant with number of days.

Table 4.3: Average Monthly Diffuse Radiations

Average Monthly Diffuse Radiation (W/m^2)												
Month	**Jan**	**Feb**	**Mar**	**Apr**	**May**	**Jun**	**Jul**	**Aug**	**Sep**	**Oct**	**Nov**	**Dec**
AMDR	**223**	**208**	**197**	**205**	**202**	**195**	**192**	**189**	**125**	**127**	**115**	**126**

4.2.4 Beam Radiation (I_b)

The solar radiation received from the sun without having been scattered by the atmosphere. Beam radiation is often referred to as direct solar radiation. The beam radiation incident on a surface is the deference between global radiation and diffuse radiation is given by [5]:

$$I_b = G_r - D_r \quad (4.7)$$

Table 4.4: Average Monthly Beam Radiations

Average Monthly Beam Radiation (W/m^2)												
Month	**Jan**	**Feb**	**Mar**	**Apr**	**May**	**Jun**	**Jul**	**Aug**	**Sep**	**Oct**	**Nov**	**Dec**
AMBR	**390**	**423**	**431**	**392**	**354**	**275**	**273**	**400**	**486**	**488**	**517**	**512**

4.3 Radiation Factors

4.3.1 Beam radiation factor (R_b)

Beam radiation factor (R_b) is defined as the ratio of beam radiation incident on an inclined surface to that on a horizontal surface [5].

- The flux of beam radiation incident on a horizontal surface is given by:

$$I_{bz} = I_N \cos(\theta_z) \quad (4.8)$$

- The flux of beam radiation incident on an incline surface is given by:

$$I_{bi} = I_N \cos(\theta_i) \quad (4.9)$$

Therefore beam radiation factor (R_b) can be determined as:

$$R_b = \frac{I_N \cos(\theta_i)}{I_N \cos(\theta_z)} = \frac{\cos(\theta_i)}{\cos(\theta_z)} \quad (4.10)$$

4.3.2 Diffuse radiation factor (R_d)

Diffuse radiation factor (R_d) is the ratio of the flux of diffuse radiation falling on the tilted surface to that on the horizontal surface [5].

$$R_d = \frac{(1+\cos(\beta))}{2} \quad (4.11)$$

4.3.3 Reflectivity factor (R_r)

Reflectivity factor (R_r) the reflected component comes mainly from the ground and other surrounding objects, then [5]:

$$R_r = \frac{(1-\cos(\beta))}{2} \quad (4.12)$$

4.4 Basic Sun-Earth Angles

The position of a location on the earth's surface is defined by the coordinate's latitude and meridian or longitude angles. Depending on the orientation of the inclined surface, the expression for $\cos(\theta_i)$ and $\cos(\theta_z)$ can be obtained as:

4.4.1 Angle of incidence$(\boldsymbol{\theta_i})$

Angle of incidence is the angle between the beam radiation on a surface and the line normal to surface [5].

$$\mathrm{Cos}(\theta_i) = (\cos(\emptyset)\cos(\beta) + \sin(\emptyset)\sin(\beta))\cos(\delta)\cos(\omega) + \sin(\delta)(\Big(\sin(\emptyset)\cos(\beta) - \big(sin(\beta)cos(\emptyset)\big)\Big) \quad (4.13)$$

4.4.2 Zenith angle$(\boldsymbol{\theta_z})$

Zenith angle is the angle between the sun's ray and the perpendicular line to a horizontal plane [5].

$$\cos(\theta_z) = \cos(\emptyset)\cos(\delta)\cos(\omega) + \sin(\delta)\sin(\emptyset) \quad (4.14)$$

Where: latitude $(\emptyset)$, collector tilte (β), declination (δ) and hour (ω) angles

4.4.3 Latitude $(\emptyset)$

The latitude of a location is the angle made by the radial line joining the given location to the center of the earth with its projection on the equatorial plane. The project site Minilik II hospital is located on:

$$\boldsymbol{latitude\ \emptyset = 9.033\ due\ to\ north}$$

Therefore the latitude angle is positive.

4.4.4 Hour angle (ω)

The hour angle of a point on the earth's surface is defined as the angle through which the earth would turn to bring the meridian of the point directly under the sun. Hour angle and solar time in hour are related as [5]:

$$\omega = (ST - 12) * 15^0 \quad (4.15)$$

Where: ST = is solar time (from1 to 24) hours.

4.4.5 Declination angle (δ)

Declination angle is the angle between the earth's equatorial plane and the line drawn between the center of the earth and the sun. Declination angle of the sun varies daily and is calculated from the following relation [5]:

$$\delta = 23.45 \sin\left[\frac{360}{365}(284 + N)\right] \quad (4.16)$$

4.4.6 Collector Tilt

The tilt of a collector is the angle between the collector and the local horizontal. In most solar water heating applications, a tilt of approximately latitude plus 10º to 15º is near optimum because it is necessary to favor the summer season, when the collector operates under adverse conditions (due to lower ambient temperature) and load is greatest [8].

$$\beta = \emptyset + 12.5° \quad (4.17)$$

For Addis Ababa latitude ($\emptyset = 9.033$), the collector tilt is:

$$\beta = 9.033° + 12.5° = 21.533° \approx 22°$$

4.4.7 Collector Azimuth

The azimuth is the angle the collector faces relative to south. The maximum heating performance is occurred at azimuth of 0º [5, 8].

4.4.8 Altitude Angle

Altitude angle is known as sun rays angle and given by [8]:

$$\alpha = 90° - \theta_z \quad (4.18)$$

CHAPTER 5

FLAT PLATE COLLECTOR DESIGN

5.1 Introduction

Many of the systems, which utilize solar energy, first collected the energy as heat and converting the radiation to thermal energy then transfers this heat to a working fluid. It must be converted to heat before it can be used in practical heating and cooling systems. Solar energy collectors are the device used to convert the sun's radiation to heat, usually consist of a surface that efficiently absorbs radiation and converts this incident flux to heat which raises the temperature of the absorbing material. Part of this energy is then removed from the absorbing surface by means of a heat transfer fluid that may be either liquid or gaseous [5].

The underside of the absorber plate and the side of casing are well insulated to reduce conduction losses. The liquid tubes can be welded to the absorbing plate, or they can be an integral part of the plate. The liquid tubes are connected at both ends by large diameter header tubes. Since the absorber plate has a temperature greater than its environment, unrecoverable heat losses occur from the entire absorbing surface of the collector to the environment. Consequently, 100% collector efficiency cannot be realized in practice [5].

This chapter deals about the designing of flat plate collector which fulfill the hot water demined of Minilik II hospital. The design concerns; optimization of collector based on cost of manufacturing, efficiency of collector, outlet temperature of water, weather condition and location of project site, properties of selected material and area of the building roof for the installation is essential. Each component of the collector design perfectly for higher efficiency and component material is selected to receive higher solar energy and to minimize the initial cost of the whole system.

5.2 Component of Flat Plate Collector

The components of a solar collector that enhances heat transfer are;

- **Glazing:** One or more sheets of glass (radiation-transmitting) material.
- **Tubes:** To conduct or direct the heat transfer fluid from the inlet to the outlet.
- **Absorber plates:** Flat, corrugated, or grooved plates, integral with the tubes.

- **Headers:** To admit and discharge the fluid.
- **Insulation:** To minimize the heat loss from the back and sides of the collector.
- **Casing and sealing**: To surround the aforementioned components and keep them free from dust, moisture, etc.

A typical flat plate collector generally consists of the following components

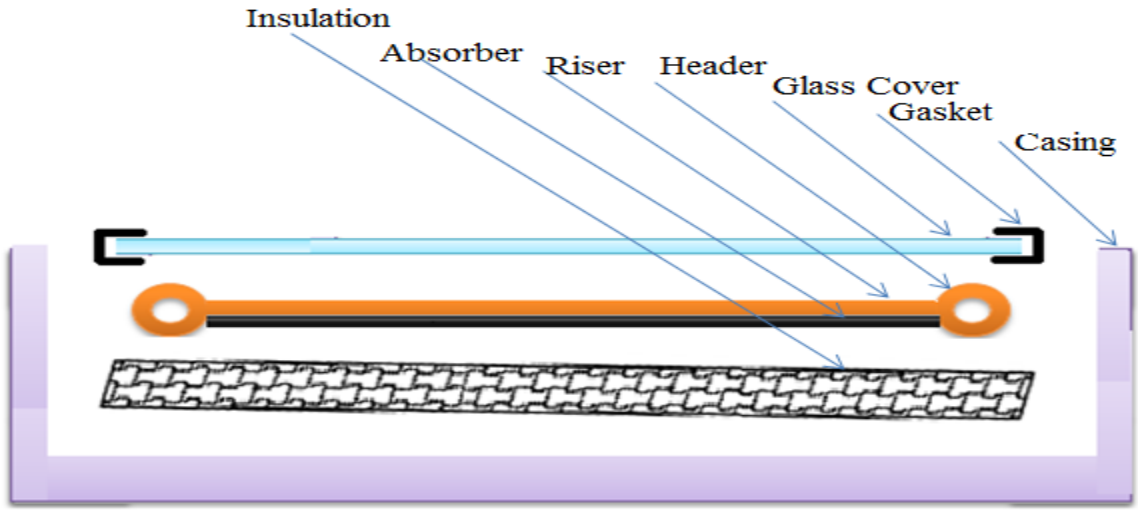

Figure 5.1: Components of Flat Plate Collector

5.3 Material Selection

Collector material selection is made based on collector efficiency, strength of material and cost of material. For this collector design; absorber plate, riser and header tube, glass cover and insulation materials are selected.

5.3.1 Absorber Material

An absorber may be made from a wide range of materials. Collector heat losses can be substantially reduced by the use of selective coatings, which have a high absorbance greater than 0.95 for solar radiation, but a low emissivity of around 0.1 for thermal radiation. Collectors with selective coating have high efficiency either in increased operating temperature of the collector [5]. Properties of different absorber plate materials are listed in **ANNEX C (Table (C-1))** and selective coating materials are listed in **ANNEX C (Table (C-5))**.

In this study, **Black chrome** coated on plated **copper** is considered as the absorber material because of the following reasons:

- Due to its high thermal conductivity.
- higher absorbance
- low emissivity of the material
- Has lower cost per heat energy transfer rate
- High thermal and corrosion resistance and
- High durability and strength.

5.3.2 Riser and Header Tube Material

Copper tubes are the most common material used for the fluid passageways, while mild steel or stainless steel and mild steel tubes are also in use. Tubes are bonded to an absorbing plate with high accuracy to increase system smoothness and efficiency of collector. For riser and header tubes; selected material should be have high heat transfer rate [9]. Properties of different riser and header tube materials are listed in **ANNEX C (Table (C-1))**.

For this design, **copper** is considered as fluid passageways tube (riser and header tube) material because of the following reasons:

- Its higher thermal conductivity.
- High absorbance of material
- Low emissivity of material
- Suitability to high temperatures
- long life
- Higher corrosion resistant
- High durability and strength.
- Lower cost per the rate of heat energy transfer

5.3.3 Glass Cover Material

The most widely used transparent cover material in solar collectors is the common glass, which has most of the required properties. From the standpoint of the utilization of solar energy, the important characteristics are reflection **(ρ),** absorption **(α),** and transmission **(τ).** The first two should be as low as possible and the latter as high as possible for maximum efficiency [8]. Properties of different glass cover materials are listed in **ANNEX C (Table (C-2))**.

In this study, **Low iron, tempered glass** is selected for the following reasons:

- mechanical strength: (it has higher mechanical strength (lower failure rates) than the common glass)
- for safety : (tempered glass breaks into a large number of relatively harmless bits of glass and so it is safer during its use)
- for higher collector efficiency: (It has higher transmittance to the solar energy)
- It is readily available everywhere and its cost is reasonable

5.3.4 Insulation Material

Heat losses from the back and sides of a collector are reduced by the use of insulation. It should be resistant to the maximum stagnation temperature of the collector usually about 150°C in collectors with matt black paint absorbers and about 200°C when selectively coated absorbers are used [9]. Properties of different insulation materials are listed in **ANNEX C Table (C-4)**.

Rockwool insulation material is selected for the following reasons:

- higher resistance to the water
- Low thermal conductivity properties
- Higher durability in the presence of moisture.
- Higher thermal resistance
- Because of the risks of water penetration in solar collectors

5.4 Assumption for Design

Different assumptions are made for the designing of the collector which is [5]:

- Steady state system
- Unit area of absorber plate
- 50% efficiency of the system
- 60^0C outlet water temperature
- 20^0C daily average water inlet temperature
- 100^0C absorber plate temperature
- Average daily solar radiation $I = 754.3\ W/m^2$ from metrology agency
- Specific heating capacity of water $C_p = 4200 J/KgK$
- Over all heat transfer coefficient $U_L = 6\ W/m^2K$
- Ambient air temperature from metrology agency

5.5 Theoretical Designing of Collector

5.5.1 Analysis of Mass Flow Rate

Collector systems can be operated with different specific flow rates. At the same collector output, a higher flow rate means a lower temperature spread and higher efficiency in the collector circuit; a lower flow rate means a higher temperature spread and lower efficiency.

Efficiency of collector is given by:

$$\eta = \frac{\dot{m}C_p\,(T_o - T_i)}{I * A_c} \quad \text{(5.1)}$$

Outlet water temperature is given by:

$$T_o = \frac{\eta * I * A_c}{\dot{m}C_p} + T_i \quad \text{(5.2)}$$

I is per unit area, assuming ($\eta = 75\%$), applying equation (5.1) and (5.2) and mass flow rate range (0.009:0.001:0.03) the relation of efficiency and outlet water temperature with mass flow rate is shown by fig 5.2. The detailed MATLAB code developed for the graph is presented in ANNEX (A-1).

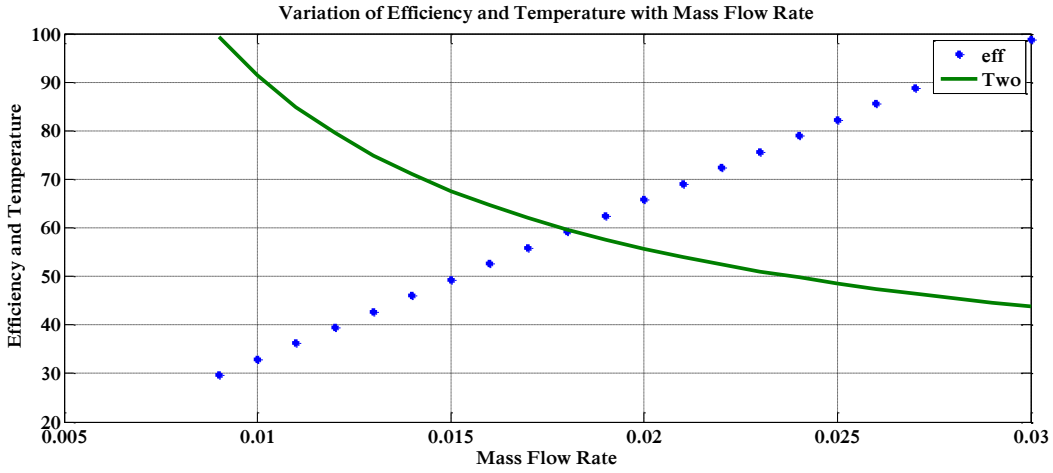

Figure 5.2: The Relation of Mass Flow Rate with efficiency and outlet Temperature of water

As shown in fig. 5.2, as mass flow rate increases; outlet water temperature decreases and Collector efficiency increases. However, lower flow rates mean; less auxiliary energy is expended for operating the pump, low pressure drop in the pipe line, and smaller connection lines are possible, outlet water temperature increases, and Collector efficiency decreases.

For the design of the collector system, mass flow rate is selected for outlet water temperature above (60℃) and collector efficiency is greater than (75%), by considering above listed mass flow rate selection criteria's and mass flow rate per second and per unit collector area is $\dot{m} = \mathbf{0.015}\ \boldsymbol{Kg/s}$

5.5.2 Theoretical Analysis of Collector Factors

The collector efficiency factor is essentially a constant for any collector design and fluid flow rate. Also used for optimization of riser tube diameter, plate thickness and space between two riser tubes. As expected, the collector efficiency factor decreases with increased tube center-to-center distances and increases with increases in both material thickness and thermal conductivity. Increasing the overall loss coefficient decreases collector efficiency factor [5].

a) Fin Efficiency Factor

Consider the sheet-tube configuration shown in Fig. 5.3. The distance between the tubes is *W*, the tube diameter is *D*, and the sheet is thin with a thickness δ. Because the sheet material is a good conductor, the temperature gradient through the sheet is negligible. The region between the centerline separating the tubes and the tube base can then be considered as a classical fin problem [10].

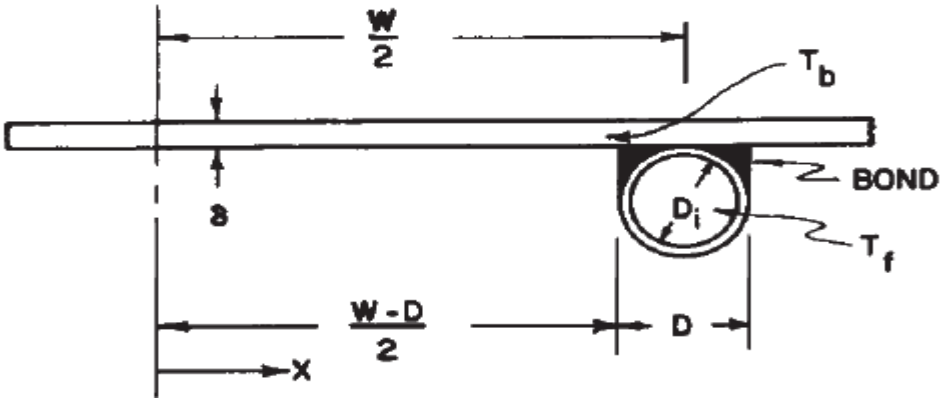

Figure 5.3: Sheet and tube dimensions

The function *F* is the standard fin efficiency for straight fins with rectangular profile is given by:

$$F = \frac{tanh[m(W-D)/2]}{m(W-D)/2} \quad (5.3)$$

For convenience, variables m defined as:

$$m = \sqrt{\frac{U_L}{k\delta}} \quad (5.4)$$

b) Collector Efficiency Factor

At a particular location, collector efficiency factor represents the ratio of the actual useful energy gain to the useful gain that would result if the collector absorbing surface had been at the local fluid temperature [5].

Where the collector efficiency factor F' is given as:

$$F' = \frac{{}^{1}/_{U_L}}{W\left[\frac{1}{U_L[D+(W-D)F]}+\frac{1}{C_b}+\frac{1}{\pi D_i h_{fi}}\right]} \quad (5.5)$$

Notice: Assumption made for calculation of collector efficiency factor is:

- The bond conductance was assumed to be very large; therefore $\frac{1}{C_b} = 0$ and
- The heat transfer coefficient inside the tube (h_{fi}) may be assumed: 300 W/m2 ºC for natural convection (Thermosiphon heaters), and 1500 W/m2 ºC for forced circulation; therefore $h_{fi} = 1500 W/m^2$°C is selected.

c) Collector Heat Removal Factor

Collector heat removal factor (*FR) is* quantity that relates the actual useful energy gain of a collector to the useful gain if the whole collector surface were at the fluid inlet temperature [5].

The collector heat removal factor can be expressed as:

$$F_R = \frac{\dot{m}C_p}{A_c U_L}\left[1 - exp\left(\frac{-A_c U_L F\prime}{\dot{m}C_p}\right)\right] \quad (5.6)$$

The collector heat removal factor times this maximum possible useful energy gain is equal to the actual useful energy gain (Q_u):

$$Q_u = A_c F_R [I(\tau\alpha) - U_L(T_i - T_a)] \quad (5.7)$$

The collector efficiency:

$$\eta_i = F_R(\tau\alpha) - \frac{U_L F_R(T_i - T_a)}{A_c I} \quad (5.8)$$

Pressure drop inside tube is given by:

$$\Delta P_h = f\left(\frac{L}{D_h}\right)\left(\frac{\rho V_{avh}{}^2}{2}\right) \quad (5.9)$$

5.5.3 Absorber Plate Thickness

The effect of absorber thickness on collector efficiency was studied and the results are shown in Fig.5.4. For mass flow rate $\dot{m} = 0.015\,Kg/s$, plate thickness range ($\delta = 0.1{:}\,0.1{:}\,2.4mm$) and by assuming; riser tube diameter ($D_r = 10mm$), space between riser tubes ($W = 75mm$) and applying equation (5.8) absorber plate thickness selected. The detailed MATLAB code developed for the graph is presented in ANNEX (A-2).

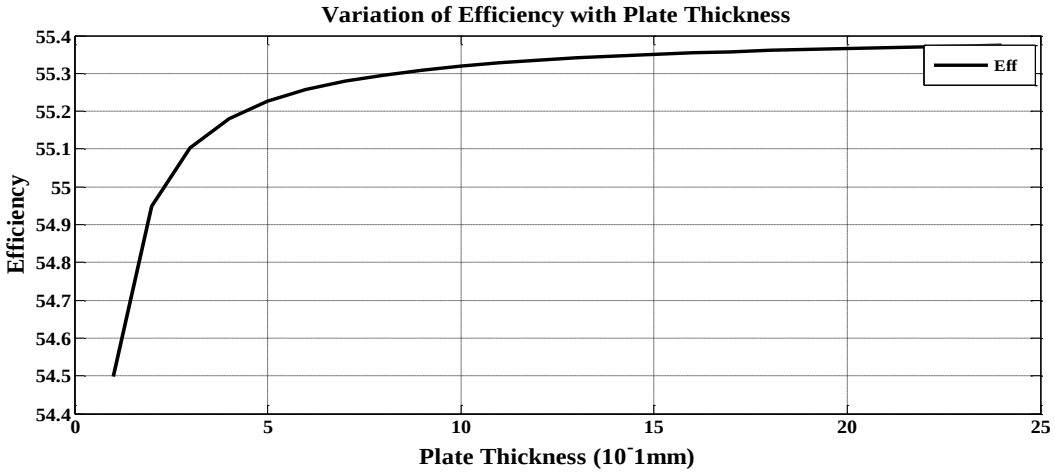

Figure 5.4: Relations of Absorber Plate Thickness and Efficiency

As shown in fig. 5.4, the collector efficiency increases by increasing the absorber plate thickness, based on the result increasing the absorber thickness from 0.1mm to 0.5 mm, the efficiency increases up to 1.05% and further increasing plate thickness the efficiency increases only 0.07%.

The cost of absorber plate increases when the thickness increases and collector efficiency increases almost negligible. Also the weight of a collector increases as plate thickness increases which increases the load on the roof top and the supporting structure. Decreasing plate thickness causes expansion of plate for higher temperature, low strength to hold the riser tubes and it is difficult for bond conductance with riser tube; therefore, the absorber plate thickness ($\boldsymbol{\delta = 0.5mm}$) is selected for the design.

5.5.4 Inner Diameter of a Riser Tube

Riser tubes used as a heat exchanger device that heat is transferred from the absorber plate to the water through riser tube. Also, used as directing the heat transfer fluid (water) from the inlet to the outlet of a collector. The effect of riser tube inner diameter on collector efficiency was studied and the results are discussed based on Fig.5.5 and Fig.5.6. For mass flow rate $\dot{m} =$

$0.015\,Kg/s$, absorber plate thickness ($\delta = 0.5mm$), riser tube inner diameter range ($D_{ri} = 1{:}1{:}30mm$) and by assuming; riser tube outer diameter ($D_{ro} = D_{ri} + 10mm$), space between riser tubes ($W = 75mm$) and applying equation (5.8, 5.9) riser tube inner diameter selected. The detailed MATLAB code developed for the graph is presented in ANNEX (A-3).

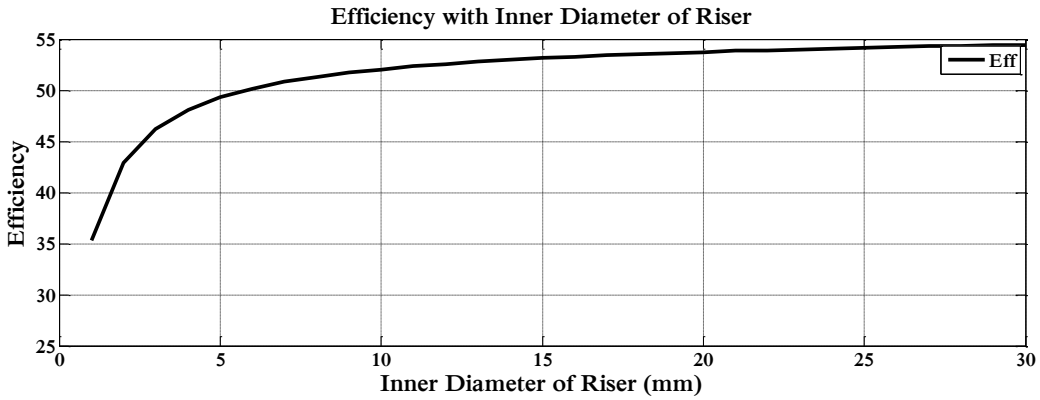

Figure 5.5: Relations between Inner Diameter of Riser Tube and Efficiency

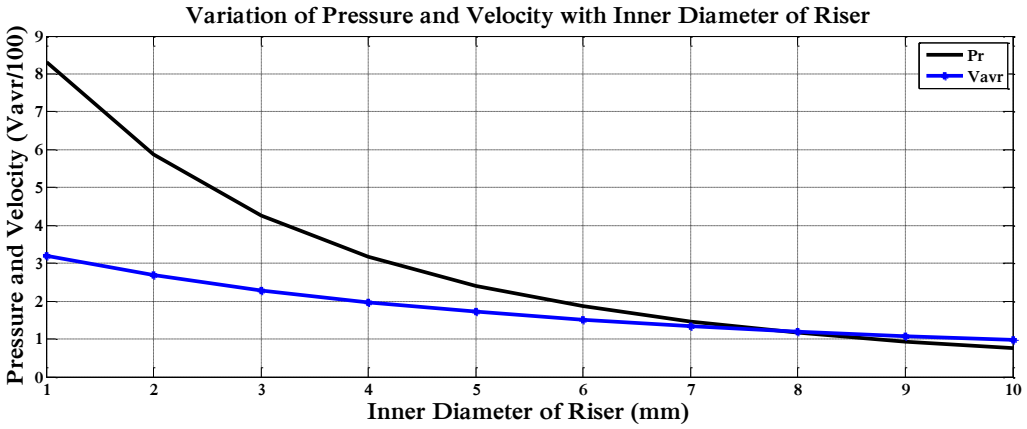

Figure 5.6: Relations of Inner Diameter of Riser Tube with Pressure and Velocity

As shown in fig. 5.5 and fig. 5.6, when inner diameter of riser tube increases collector efficiency increases, pressure drop inside riser tube and velocity of water decreases, based on the result increasing the diameter from 1mm to 15 mm, the efficiency increases up to 18% and pressure drop decreases up to $1.22*10^5$Pa, further increasing diameter the efficiency increases only 2% and pressure drop decreases only 2.26Pa. Amount of outlet water per a collector increases which minimize outlet water temperature.

The cost of riser tube increases when the inner diameter increases and further increasing diameter beyond 15mm collector efficiency increases and pressure drop decreases almost

negligible compering to the cost per diameter. Decreasing diameter of riser tube increases the velocity of water that increases pressure drop inside the riser tube, the thickness of tube increases to over-come pressure drop which increases cost of the tube and decreases the rate of heat transfer from plate to water stream. So, by considering the above reasons riser tube diameter ($D_{ri} = \mathbf{15}\boldsymbol{mm}$**)** is selected.

5.5.5 Outer Diameter of Riser

The absorber consists of a flat fin with a welded-on absorber pipe. Tubes with direct flow employ a parallel pipe. A heat transfer medium is routed from the return into the inner pipe; the medium returns through the outer pipe welded to the absorber.

The effect of riser tube inner diameter on collector efficiency was studied and the results are discussed based on Fig.5.7. For mass flow rate $\dot{m} = 0.015\,Kg/s$, absorber plate thickness ($\delta = 0.5mm$), riser tube inner diameter ($D_{ri} = 15mm$), riser tube outer diameter range ($D_{ro} = 15.1{:}\,0.1{:}\,16mm$) and ($D_{ro} = 16{:}\,1{:}\,25mm$) and by assuming; space between riser tubes ($W = 75mm$) and applying equation (5.8) riser tube outer diameter selected. The detailed MATLAB code developed for the graph is presented in ANNEX (A-4).

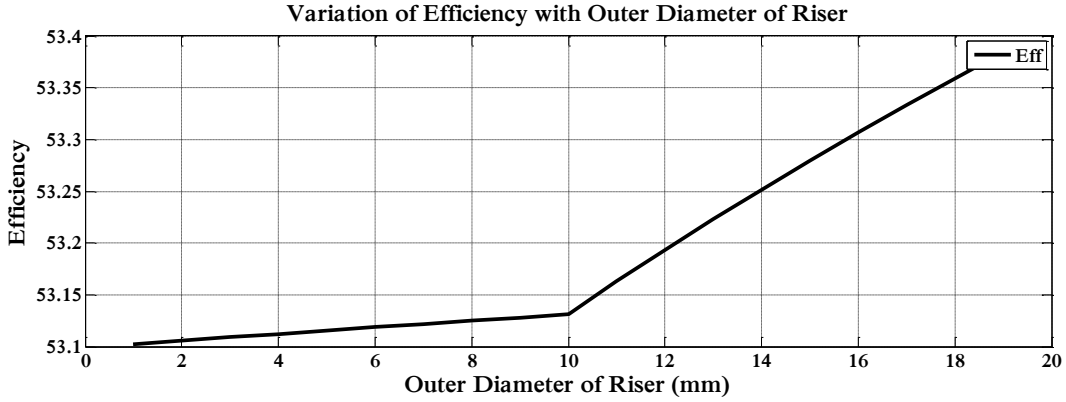

Figure 5.7: Relations of Outer Diameter of Riser Tube and Efficiency

As shown in fig. 5.7 when outer diameter of riser tube increases collector efficiency increases, based on the result increasing the diameter from 1mm up to 16 mm, the efficiency increases up to 0.15%, further increasing diameter the efficiency increases 0.2%.

The cost of riser tube thickness increases when the outer diameter increases and further increasing thickness beyond 1mm collector efficiency increases almost negligible compering to the cost per tube thickness. Further increasing riser tube thickness decreases the rate of heat

transfer from plate to water stream through tube thickness. Also the collector area determines the thickness of riser tube. Decreasing thickness (outer diameter) of riser tube causes expansion of tube for higher temperature, low strength to resist the pressure developed inside riser tube and it is difficult for bond conductance with absorber plate. So, by considering the above reasons riser tube outer diameter (thickness) $D_{ro} = \mathbf{16}\boldsymbol{mm}$ is selected.

5.5.6 Number of Tube

The effect of number of riser tube on pressure drop inside tube was studied and the results are shown in Fig.5.8. For mass flow rate $\dot{m} = 0.015\ Kg/s$, riser tube inner diameter ($D_r = 15mm$), length of riser tube ($L_r = 1.9m$), density of water ($\rho = 988Kg/m^2$) at temperature (50℃) and applying equation (5.9) number of riser tube should be optimized. The detailed MATLAB code developed for the graph is presented in ANNEX (A-5).

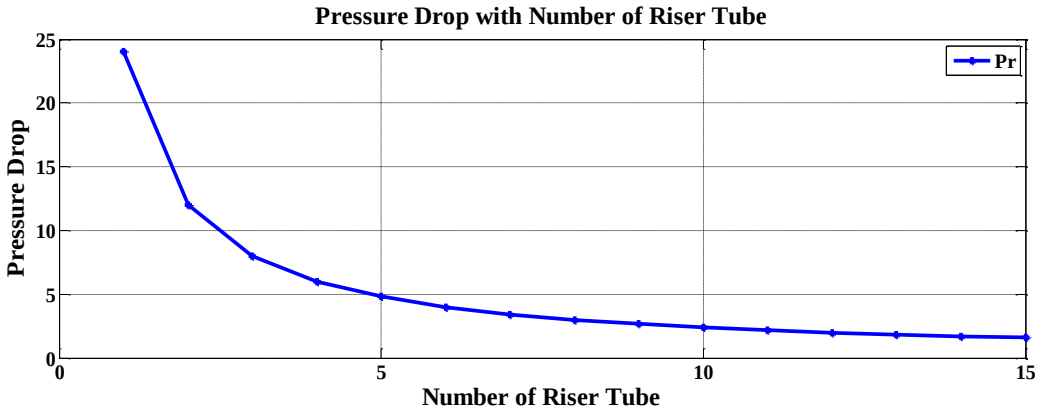

Figure 5.8: Relation of Pressure Drop with Number of Riser Tube

As shown in fig. 5.8, pressure drop inside header decreases by increasing the number of riser tube, based on the result increasing the number of riser tube from 1 to 10, pressure drop inside tube decreases up to 21.66Pa and further increasing header tube diameter pressure drop decreases up to 0.802Pa.

The cost of riser tube increases when the number of tube increases. Further increasing number of tube beyond 10 pressure drop decreases almost negligible compering to the cost per tube increases. As the number of tube decreases; velocity per tube increases, heat transfer surface area decreases and the rate of heat transfer from plate to water stream decreases. Considering mass flow rate, outlet temperature of water, efficiency and absorber area of the collector; number of riser tube fixed to **10** tubes per unit area of absorber plate.

5.5.7 Header Tube

Header tubes connected to the riser tube. Below header tube uses to distribute inlet water to the risers and top header uses to receive hot water from the riser and deliver to the storage tank.

The effect of header tube diameter on pressure drop rise inside the tube was studied and the results are discussed based on Fig.5.9. For mass flow rate $\dot{m} = 0.015\,Kg/s$, density of water ($\rho = 988Kg/m^3$) at temperature (50°C), number of header tubes is 2 in a single collector, length of header tube ($L_h = 0.736m$), header tube diameter range ($D_h = 15:1:40mm$), and applying equation (5.9) header tube diameter should be selected. The detailed MATLAB code developed for the graph is presented in ANNEX (A-7).

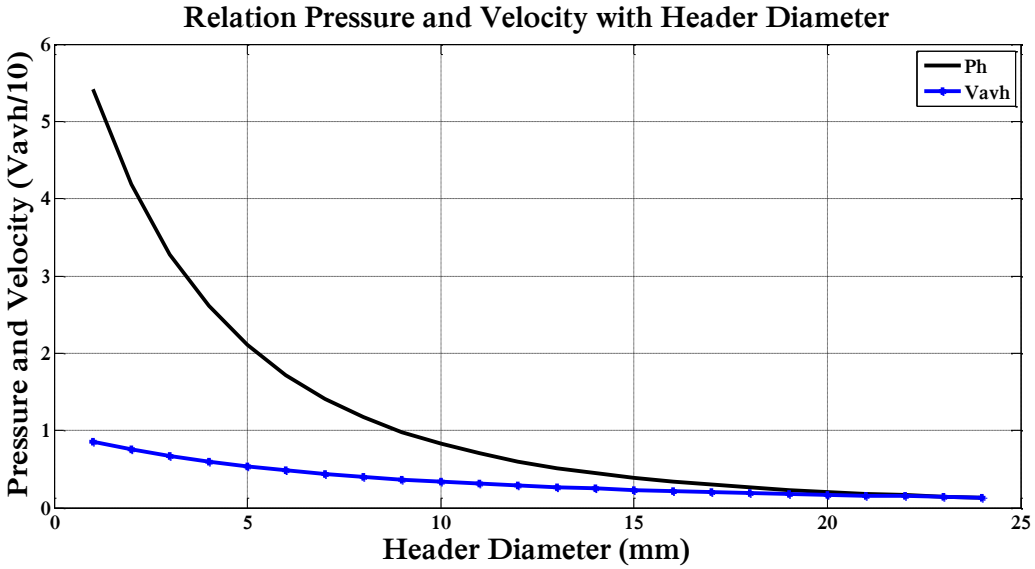

Figure 5.9: Pressure Drop and Velocity with Header Diameter

As shown in fig. 5.9, pressure drop and velocity inside header decreases by increasing the tube diameter, based on the result increasing the diameter from 15mm to 24mm, pressure drop inside tube decreases up to 4.44Pa and further increasing header tube diameter pressure drop decreases up to 0.96Pa.

The cost of header tube increases when the diameter increases and pressure drop decreases almost negligible compared to 4.44Pa. Decreasing header diameter causes pressure drop to rise inside tube and velocity of water increases, this needs hither pump and pump power to overcome created pressure drop inside tube, which is additional cost to the investment cost of system. So, for this reasons the header tube diameter optimized to ($\boldsymbol{D_h = 24mm}$).

5.5.8 Insulation Thickness

Heat losses from the back and sides of a collector are reduced by the use of insulation. To minimize heat losses from the collector, the collector must be 100 percent insulated in accordance with the requirements of heating circuit system.

Heat is lost to the surroundings from the plate through insulation is:

- Edge heat loss and
- Bottom heat loss

Insulation heat loss coefficient is the sum of bottom and edge loss coefficient is given as [10]:

$$U_{in} = U_b + U_e \quad ---------- (5.10)$$

The bottom loss coefficient is given by:

$$U_b \approx \frac{K_{in}}{L_{in}} ---------- (5.11)$$

The edge loss coefficient is given by:

$$U_e = U_b \left(\frac{A_e}{A_c}\right); \quad A_c = A_b ---------- (5.12)$$

Where: $L = 1m$ and $W = 0.09m$

$A_e = 4(L * W) = 4(1 * 0.09) = 0.36m^2$ And $A_c = 1m^2$

By assuming heat loss coefficient through insulation ($U_{in} = 1W/Km^2$), then insulation thickness is:

$$\boldsymbol{U_{in}} = U_e + U_b = \frac{K_{in}}{L_{in}}\left(\left(\frac{A_e}{A_c}\right) + 1\right)$$

$$L_{in} = \frac{K_{in}\left(\left(\frac{A_e}{A_c}\right)+1\right)}{\boldsymbol{U_{in}}} ---------- (5.13)$$

$$L_{in} \approx \boldsymbol{0.05m}$$

5.6 Area of a Collector

For collectors, three different area designations are used as the reference variable for output and yield details.

5.6.1 Absorber Area

The absorber area refers exclusively to the absorber. Unit area of absorber plate is assumed for the design analysis to get ($\mathbf{0.015Kg/s}$) per unit area of mass flow rate of water. For constant outlet temperature of water and efficiency of a collector, to double the mass flow rate of water to ($\mathbf{0.03Kg/s}$) the absorber area of the collector should be two times the assumed area, which is equals to $\mathbf{2m^2}$.

5.6.2 Aperture Area

In the case of flat-plate collectors, the aperture area is the visible part of the glass panel, in other words that area inside the collector frame through which light can enter the appliance.

Aperture area (A_{ap}) is given as:

$$A_{ap} = W * L \quad (5.14)$$

Where: $W = 1 - 0.04 = 0.96m$ and $L = 2 - 0.04 = 1.96m$

Therefore aperture area is equal to: $A_{ap} = \mathbf{1.88m^2}$

5.6.3 Gross Collector Area

The gross collector area describes the external dimensions of a collector. As regards the output of such appliances or their assessment, the gross collector area is irrelevant. However it is important when planning the installation and when calculating the roof area required.

Gross collector area (A_{gca}) is given as:

$$A_{gca} = W * L$$

Where: $W = (W_p) + (t_{in}) + (t_{cs}) = 1 + 0.05 + 0.004 = 1.054m$

$$L = L_p + t_{in} + t_{cs} = 2 + 0.05 + 0.004 = 2.054m$$

Therefore gross collector area is equal to: $A_{gca} = \mathbf{2.165m^2}$

5.6.4 Collector Edge Area

The edge collector area describes the external edge dimensions of a collector.

Edge collector area is equal to (A_e):

$$A_e = P(t_c - t_e) \quad (5.15)$$

$$A_e = 6 * (0.09 - 0.05) = \mathbf{0.24m^2}$$

5.6.5 Riser Tube Surface Area

The riser tube area describes the area of water riser tube of a collector.

Water riser tube area is equal to (A_e):

$$A_w = \pi d_i L_t \quad (5.16)$$

$$A_w = \pi * 0.015 * 1.6 = \mathbf{0.0895 m^2}$$

5.7 Pressure Drop in the Collector

Based on the designed diameter of riser and header tube, number of riser tubes, mass flow rate and flow pattern the pressure drop inside the collector can be calculated with the help of the schematic diagram shown by fig. 5.10.

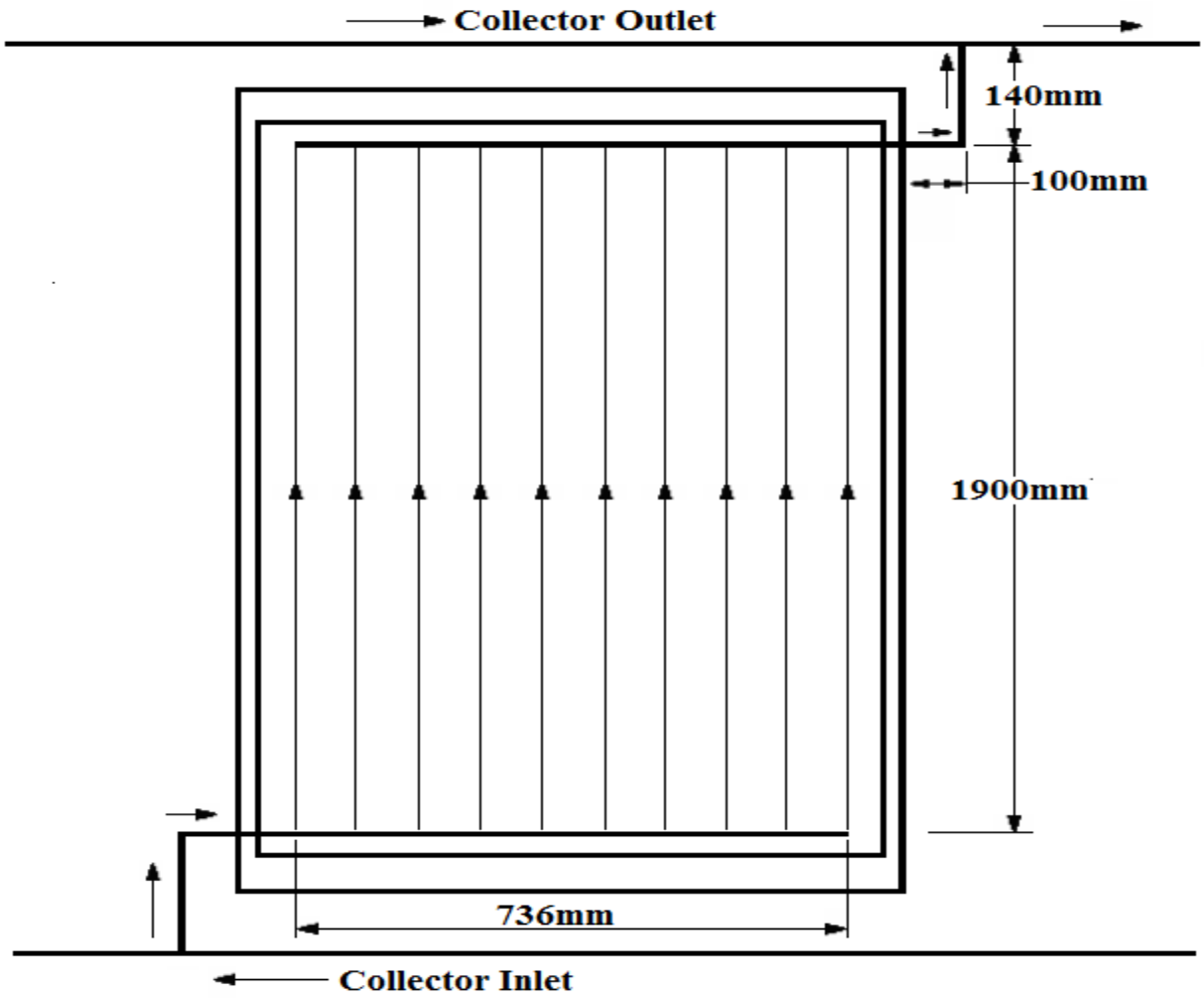

Figure 5.10: Schematic Representation of the flow in the collector

At average temperature of (50°C) of the property of water is:

$\rho = 988\ Kg/m^3$

$\mu = 5.47 * 10^{-4}\ N.s/m^2$

$\dot{m} = 0.015Kg/s.m^2 = 0.015Kg/s.m^2 * 2m^2 = \mathbf{0.03Kg/s}$

Volume flow rate:

$$\dot{Q} = \frac{\dot{m}}{\rho} \quad (5.17)$$

$$\dot{Q}_i = \frac{0.03Kg/s}{988Kg/m^3} = \mathbf{3.04 * 10^{-5}\ m^3/s}$$

Average velocity of fluid in a tube:

$$V_{av} = \frac{\dot{Q}_i}{A} \quad (5.18)$$

Reynolds Number:

$$R_e = \frac{\rho V_{av} d}{\mu} \quad (5.19)$$

(5.19)

If $R_e < 2300$ it is laminar flow

$$f = \frac{64}{R_e} \quad (5.20)$$

If $R_e > 2300$ it is turbulent flow

For turbulent flow f is read from moody chart.

Pressure drop inside tube is given as:

$$\Delta P = f\left(\frac{L}{d}\right)\left(\frac{\rho {V_{av}}^2}{2}\right) \quad (5.21)$$

5.7.1 Pressure Drop Inside the Risers

Assuming uniform flow rate in each riser the volume flow rate per riser is:

$$\dot{Q} = \frac{\dot{Q}_i}{N} = \frac{3.04 * 10^{-5} m^3/s}{10} = \mathbf{3.04 * 10^{-6} m^3/s}$$

Where: N is the number of risers.

Area of single riser tube:

$$A_r = \frac{\pi d_i}{4} = \frac{\pi * (0.015m)^2}{4} = \mathbf{1.767 * 10^{-4} m^2}$$

Average velocity in a riser;

$$V_{avr} = \frac{3.04 * 10^{-6} m^3/s}{1.767 * 10^{-4} m^2} = \mathbf{0.0172 m/s}$$

Reynolds Number;

$$R_e = \frac{988 * 0.0172 * 0.015}{5.47 * 10^{-4}} = \mathbf{466}$$

Since the $R_e < 2300$ it is laminar flow

Where: $f = \frac{64}{466} = \mathbf{0.137}$

$$\Delta P_r = 0.137 * \left(\frac{1.9}{0.015}\right) * \left(\frac{988 * (0.0172)^2}{2}\right)$$

$$\Delta P_r = \mathbf{2.536 Pa}$$

5.7.2 Pressure Drop Inside the Headers

Taking the average volume flow rate:

$$\dot{Q}_{avh} = \frac{\dot{Q}}{2} = \frac{3.04 * 10^{-5} m^3/s}{2} = \mathbf{1.52 * 10^{-5} m^3/s}$$

Ares of single header tube:

$$A_h = \frac{\pi {d_h}^2}{4} = \frac{\pi * (0.024m)^2}{4} = \mathbf{4.524 * 10^{-4}\ m^2}$$

Average velocity in the header:

$$V_{avh} = \frac{1.52 * 10^{-5} m^3/s}{4.524 * 10^{-4}\ m^2} = \mathbf{0.0336 m/s}$$

Reynolds Number;

$$R_e = \frac{988 * 0.0336 * 0.024}{5.47 * 10^{-4}} = \mathbf{1456.47}$$

Since the $R_e < 2300$ it is laminar flow

For laminar flow pressure drop is:

Where: $f = \frac{64}{1456.47} = \mathbf{0.044}$

$$\Delta P_h = 0.044 * \left(\frac{0.736}{0.024}\right) * \left(\frac{988 * (0.0336)^2}{2}\right)$$

$$\Delta P_h = \mathbf{0.753}\boldsymbol{Pa}$$

For the two headers, $\Delta P_H = 2 * \Delta P_h = \mathbf{1.506}\boldsymbol{Pa}$

5.7.3 Pressure Drop Inside the Fitting

Based on the figure (5.11) there are 24 bends.

Pressure loss in the fitting:

$$\Delta P_f = K_f \frac{\rho {V_1}^2}{2} - (5.22)$$

For 90° bend, laminar flow $K_f = 0.9$

Average velocity in the tube up stream of the fitting is given as:

$$V_1 = \frac{1.52 * 10^{-5} m^3/s}{4.524 * 10^{-4}\ m^2} = \mathbf{0.0336}\boldsymbol{m/s}$$

Pressure drop in the fitting is:

$$\Delta P_f = 0.9 * \frac{988 * 0.0336^2}{2}$$

$$\Delta P_f = \mathbf{0.501}\boldsymbol{Pa}$$

5.7.4 Pressure Drop Inside the Connection Pipes

The total connection pipes length for a single collector is $L = 0.744m$

Pressure drop in the pipe is given by:

$$\Delta P_c = f \frac{L}{d_h} \frac{\rho V^2 avh}{2} - (5.23)$$

$$\Delta P_c = 0.044 * \left(\frac{0.744}{0.024}\right) * \left(\frac{988 * 0.0336^2}{2}\right)$$

$$\Delta P_c = \mathbf{0.761}\boldsymbol{Pa}$$

5.7.5 Total Pressure Drop in a Single Collector

The total pressure loss due to viscous effect of the fluid in a single collector is the sum of all the above losses.

$$\Delta P_{TC} = \Delta P_R + \Delta P_H + \Delta P_f + \Delta P_c - (5.24)$$

$$\Delta P_{TC} = 2.536Pa + 1.506Pa + 0.501Pa + 0.761Pa$$

$$\Delta P_{TC} = \mathbf{5.304}\boldsymbol{Pa}$$

5.8 Analysis Parameters

The data of designed collector which can be used for water heating system design is given as follows.

Table 5.1: Collector Analysis Parameters

Technical Collector Analysis Parameters	
Parameters	**Technical Specification**
Type	Flat Plate Collector
Casing Material	Aluminium Case
Sealing Material	Silicone
Mass Flow Rate	$0.03Kg/s$
Different Areas of Collector	
Gross Area (Ag)	$2.165m^2$
Aperture Area (Ap)	$1.88m^2$
Absorber Area (Ac)	$2m^2$
Water Riser Tube Area (Aw)	$0.0895m^2$
Edge Insulation Area (Ae)	$0.24m^2$
Absorber Plate	
Material	Black chrome on copper
Thickness	$0.5mm$
Absorption	0.95
Emission	0.03
Riser Tube	
Material	Copper
Outer diameter	$16mm$
Inner Diameter	$15mm$
Tube Thickness	$1mm$
Number of Riser Tube	10
Tube Pitch	$80mm$
Header	

Material	Copper
Outer Diameter	$25mm$
Inner Diameter	$24mm$
Thickness	$1mm$
Glass Cover	
Material	Low Iron Tempered Glass
Transmittance	0.94
Emissivity	0.04
Absorption	0.02
Thickness	$4mm$
Insulation	
Material	Rockwool
Thermal Conductivity	$0.037W/mK$
Heat Capacity	$0.84KJ/KgK$
Thickness	$50mm$
Total Pressure Drop of Collector	$5.304Pa$

CHAPTER 6

THERMAL STORAGE TANK AND INSULATION

6.1 Introduction

Solar energy is a time-dependent energy resource. Thermal storage tank is one of the major components in large scale solar water heating system to provide a thermal inertia or capacitance effect. The optimum capacity of an energy storage system depends on the expected time dependence of solar radiation availability, the nature of loads to be expected on the process, the degree of reliability needed for the process, the manner in which auxiliary energy is supplied, and an economic analysis that determines how much of the annual load should be carried by solar and how much by the auxiliary energy source [5].

Total hot water demand of Minilik II hospital is subjected to different hot water consumption patterns (two different final load system) in the hospital building. The first final load system is daily hot water consumption pattern and the second final load system is weekly hot water consumption pattern. For the design of thermal energy storage tank: total load used is the sum of the two final loads is considered. In this chapter; design of thermal energy storage tank is performed for total final load of solar thermal system in the hospital building and selection of storage tank and insulation material also included.

6.2 Material Selection

The materials must retain their shape and strength during repeated thermal expansion and contraction; all the while being exposed to the weather. The thermal energy storage tank is exposed to wind, rain, hail, temperature extremes and ultraviolet radiation. Materials for solar energy systems must be chosen very carefully. The most important factors are safety, performance, durability and cost [5].

6.2.1 Material Selection of Thermal Storage Tank

Thermal storage tank may be made from a wide range of materials. Storage tank with selective galvanization have high efficiency either in maintaining constant operating temperature of the storage tank by minimizing heat loss from the tank to the surrounding. Properties of selected thermal storage tank materials are listed in **ANNEX C-Table (C-1)**

Mild steel plate storage tank is selected because of the following reasons:

- Due to its low thermal conductivity.
- higher performance
- higher durability and
- Lower cost per unit area and Lower maintenance cost
- Higher safety
- Lower cost of heat loss per cost of thickness

Also steel jacket (outer cover) galvanization pre painting is used for the selected thermal storage tank material galvanization.

6.2.2 Material Selection of Thermal Storage Insulation

Heat losses from the thermal storage tank are reduced by the use of insulation. Because of the risks of water penetration in thermal storage tank consideration should be given to insulation material selection. At these high temperatures the insulation should not shrink, melt, or give off vapour (outgas), which could condense on the storage tank outer cover and increase its heat loss to the surrounding [10]. Properties of various insulation materials are listed in **ANNEX C-Table (C-4)**.

Glass fiber insulation material is selected for the following reasons:

- higher resistance to the water
- Lower thermal conductivity properties
- Higher durability in the presence of moisture.
- Higher temperature resistance
- Lower cost per unit area
- Higher ultraviolet radiation resistance

6.3 Optimization of Thermal Storage Tank

6.3.1 Volume of Storage Tank

When the daily hot water demand has been determined, the volume of the storage tank can be specified. It should be some 0.8 to 1.2 fold the daily demand for regions with high solar radiation and 2 to 2.5 fold the daily demand for regions with lower solar radiation respectively [10].

The volume of the storage tank (V_{St}) is thus calculated as follows:

$$V_{St} = THWD * 1.2 \quad (6.1)$$

For total daily hot water demand volume of the storage tank (V_{St}) is:

$$V_{St} = 30{,}475lt * 1.2 = \mathbf{36{,}570\ liter \approx 36.6m^3}$$

Two storage tank each with the capacity of ($\mathbf{18.3m^3}$) is needed.

6.3.2 Diameter and Height of Storage Tank

The shapes of the storage tanks are a right circular cylinder with height to diameter ratio of 2:1. For daily and weekly hot water consumption pattern of the hospital; thermal storage tank diameter and height determined as follows:

For circular cylinder with height to diameter ratio of 2:1 height of storage tank is given as:

$$h = 2 * D_i \quad (6.2)$$

By substituting equation (6.2) into equation (6.1) the volume of a single storage tank is rearranged as:

$$V_s = \pi \frac{{D_i}^2}{4} h = \pi \frac{{D_i}^3}{2} \quad (6.3)$$

From equation (6.3) the inner diameter of a cylindrical storage tank is given as:

$$D_i = \sqrt[3]{\frac{2V_s}{\pi}} \quad (6.4)$$

A singe thermal storage tank volume is ($V_{st} = 18.3m^3$);

Therefore, the diameter of storage tank is:

$$D_i = \sqrt[3]{\frac{2 * 18.3m^3}{\pi}} = \mathbf{2.2669m \approx 2.3m}$$

Therefore, the height of storage tank is:

$$h = 2 * 2.3m = \mathbf{4.6m}$$

6.3.3 Surface Area of Storage Tank

Determining the surface area of thermal storage tank is used to understand the space it occupies on the roof of hospital building: that helps for proper space consumption of the building roof.

The surface area of storage tank is given as:

$$A_s = \pi D_i h + 2 * \left(\frac{\pi {D_i}^2}{4}\right) = \frac{5}{2}\pi {D_i}^2 \quad (6.5)$$

The diameter of thermal storage tank is ($D_i = 2.3m$);

Therefore, the surface area of storage tank is:

$$A_s = \frac{5 * \pi * (2.3)^2}{2} = \mathbf{41.55}\boldsymbol{m^2}$$

6.4 Optimization of Insulation Thickness

The exterior of a storage tank should be well insulated to retain heat. Heat losses from the storage tank have great impact on the economic utilization of the system as a whole. For this reason thickness of insulation should be determined by considering it as one part of the storage tank design [5, 12].

The determination of the storage tank insulation can be made by using different consideration.

- In one case for example, the insulation thickness is taken as an utilizable parameter and then determined by considering the economic trade-off between the cost of the added insulation and the benefit gained from the saved solar heat.
- The other way of calculating the insulation thickness is as follows: The overall heat transfer coefficient U across the storage tank is assumed first. Then, the thickness of the insulation is determined.

For simplification of the problem, the first method is used for the determination of the required insulation thickness from the economic trade-off between the cost of the added insulation and the benefit gained from the saved solar heat. Therefore, there should be an ***optimum*** thickness of insulation that corresponds to a minimum combined cost of insulation and heat lost [12].

a) Cost of Insulation Thickness

Glass fiber material is selected for the insulation of thermal storage tank and the cost of glass fiber gathered from market that is given as 4.5 birr/thickness (mm) per unit area (m^2).

The relation between cost of glass fiber (CGF) and thickness is given by:

$$CGF = (Cost/mm) * (t_{in}\ mm) \quad (6.6)$$

By substituting the cost of insulation into equation (6.6); relation is rearranged as:

$$CGF = (4.5 * t_{in}) Birr \quad (6.7)$$

Notice: that the cost of insulation increases linearly with thickness.

b) Cost of Heat Loss

The cost of heat energy loss from the storage tank is determined based on the cost of energy in Ethiopia. The cost of energy per (KWh) in Ethiopia is equal ($0.46\ birr/KWh$).

The relation between cost of heat loss (CHL) and thickness of insulation is given by:

$$CHL = (Cost/KWh) * (\mathrm{Q}_L KWh) \quad (6.8)$$

Neglecting the effect of the storage tank material on heat transfer, the temperature difference across the insulation is taken as ($\Delta T = T_s - T_a$).

The rate of heat loss from the tank is then given by:

$$\mathrm{Q}_L = \mathrm{U}_L \mathrm{A}_s \Delta T \quad (6.9)$$

The overall heat loss coefficient (U_L) by the insulation of storage tank is then given by:

$$\mathrm{U}_L = \mathrm{U}_{in} + \mathrm{h}_{ina} \quad (6.10)$$

$\mathrm{U}_{in} = \frac{K_{in}}{t_{in}}$; heat loss coefficient through insulation and

$\mathrm{h}_{ina} = 2.8 + 3\mathrm{V}_w$; convective heat loss coefficient fron insulation to ambient

Where: $\mathrm{V}_w = 3m/s$, is average wind speed of the location and $K_{in} = 0.036\ W/Km$, is thermal conductivity of glass fiber.

Therefore, the overall heat loss coefficient (U_L) is equal to:

$$\mathrm{U}_L = \frac{0.036}{t_{in}} + 11.8 \quad (6.11)$$

Therefore rate of heat loss from the tank is then equal to:

$$\mathrm{Q}_L = \left[\left(\frac{0.036}{t_{in}} + 11.8\right) A_s \Delta T\right] KWh \quad (6.12)$$

Area of thermal storage tank and temperature of storage tank and average ambient is:

$A_s = 41.55m^2, T_s = 60℃$ and $T_a = 20℃$

By substituting the value of area (A_s) and change of temperature (ΔT) into equation (6.12); the rate of heat loss from the tank in a 24 hour is then given as:

$$Q_L = \left(\frac{1436}{t_{in}} + 255\right) KWh \quad (6.13)$$

By substituting cost of energy and equation (6.13) into equation (6.8); the cost of heat loss from the tank is then given as:

$$CHL = \left(\frac{661}{t_{in}} + 117\right) Birr \quad (6.14)$$

c) Total Cost

Total cost is the sum of insulation material cost and heat energy loss cost. The relation between total cost and thickness insulation of the storage tank is given as:

$$TC = CGF + CHL \quad (6.15)$$

By substituting equation (6.8) and (6.14) into equation (6.15); the total cost with thickness variation is given by:

$$TC = \left[(4.5 * t_{in}) + \left(\frac{661}{t_{in}} + 117\right)\right] Birr \quad (6.16)$$

The relation of insulation material cost, heat loss cost, and total cost with thickness of insulation is shown in fig. 6.1.

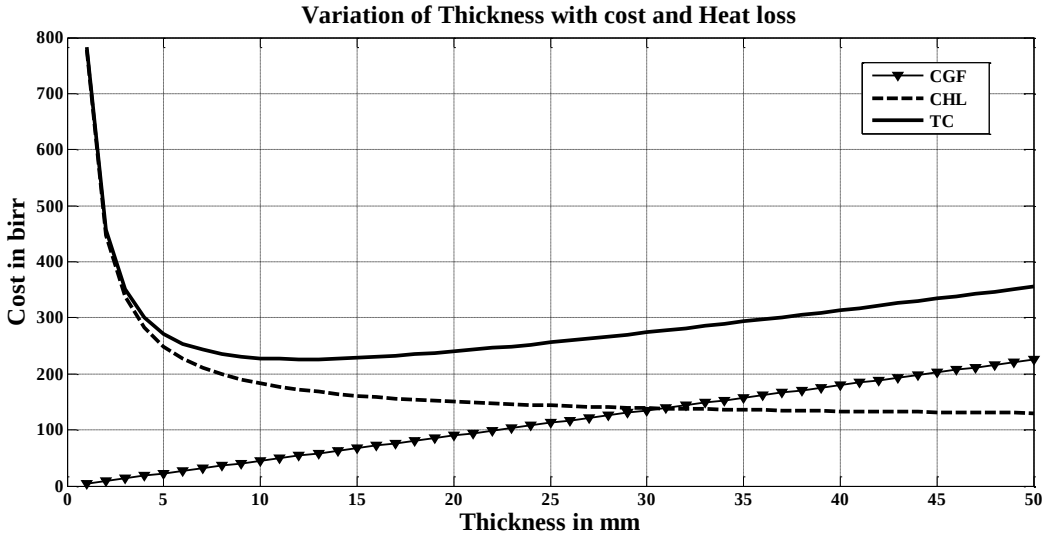

Figure 6.1: Optimum Thickness of Insulation on the Basis of Minimum Total Cost.

The total cost, which is the sum of the expressions for the lost heat cost and insulation cost as a function of thickness; differentiating the total cost equation (6.16) with respect to the thickness; and setting it equal to zero; is gives as:

$$\frac{-661}{t_{in}} + 4.5 = 0 \quad (6.17)$$

Rearranging equation (6.17) and equating to thickness; then the optimum thickness of the insulation is equal to:

$$t_{in} = \mathbf{12.12mm} \approx \mathbf{12.5mm}$$

The thickness value satisfying the resulting equation is the optimum thickness. For safety and long year operation storage tank insulation thickness ($t_{in} = \mathbf{15mm}$) is selected.

6.5 Optimization of Storage Tank Thickness and Outer Diameter

6.5.1 Optimum Storage Tank Thickness

It should be realized that thickness of the storage tank does not eliminate heat transfer; it merely reduces it. The thicker the storage tank, the lower the rate of heat transfer but also the higher the cost of storage tank material. Therefore, there should be an ***optimum thickness and outer diameter*** of storage tank that corresponds to a minimum combined cost of storage tank material and heat lost [27].

a) Cost of Storage Tank

Mild steel plate tank is selected for the design of this thermal storage tank and the cost of mild steel plate gathered from market that is given as 125 birr/thickness (mm) per unit area (m^2).

The relation between cost of mild steel plate (CMSP) and thickness is given by:

$$CMSP = (Cost/mm) * (t_t\ mm) \quad (6.18)$$

By substituting the cost into equation above; relation is rearranged as:

$$CMSP = (125 * t_t) Birr \quad (6.19)$$

Notice: that the cost of mild steel plate increases linearly with thickness

b) Cost of Heat Loss

The cost of heat energy loss from the storage tank is determined based on the cost of energy in Ethiopia. The cost of energy per (KWh) in Ethiopia is equal ($0.46\ birr/KWh$).

The relation between cost of heat loss (CHL) and thickness of the storage tank is given as:

$$CMSP = (Cost/KWh) * (\mathrm{Q}_L\ KWh) - (6.20)$$

The rate of heat loss from the tank is then given by:

$$\mathrm{Q}_L = \mathrm{U}_L \mathrm{A}_s \Delta T$$

The overall heat loss coefficient (U_L) is then given by:

$$\mathrm{U}_L = \mathrm{h}_{ws} + \mathrm{U}_s + \mathrm{U}_{in} + \mathrm{h}_{ina} - (6.21)$$

$\mathrm{U}_s = \frac{K_s}{t_t}$; heat loss coefficient through storage tank material and

$\mathrm{h}_{ws} = \frac{N_{uw} k_w}{d_i}$; convective heat loss coefficient from water to storage tank

Therefore, the overall heat loss coefficient (U_L) is equal to:

$$\mathrm{U}_L = \left(\frac{38}{t_t} + 18.6\right) W/mK\ - (6.22)$$

Therefore, the rate of heat loss from the tank is then equal to:

$$\mathrm{Q}_L = \left[\left(\frac{38}{t_t} + 18.6\right) A_S \Delta T\right] KWh - (6.23)$$

Surface area of thermal storage tank, temperature of storage tank and average ambient is:

$A_s = 41.55 m^2, T_s = 60℃$ and $T_a = 20℃$

By substituting the value of area (A_s) and change of temperature (ΔT) into equation (6.23); the rate of heat loss from the tank in a 24 hour is then given as:

$$\mathrm{Q}_L = \left(\frac{1436}{t_t} + 742\right) KWh - (6.24)$$

Therefore, the cost of heat loss from the tank is then equal to:

$$CHL = \left(\frac{697}{t_t} + 342\right) Birr - (6.25)$$

c) Total Cost

Total cost is the sum of insulation material cost and heat energy loss cost. The relation between total cost and thickness of the storage tank is given as:

$$TC = CMSP + CHL - (6.26)$$

Therefore, total cost with thickness variation is given as:

$$TC = \left[\left(\frac{697}{t_t} + 342\right) + (125 * t_t)\right] Birr \quad (6.27)$$

The relation of storage tank material cost, heat loss cost, and total cost with thickness of storage tank is shown in fig. 6.2.

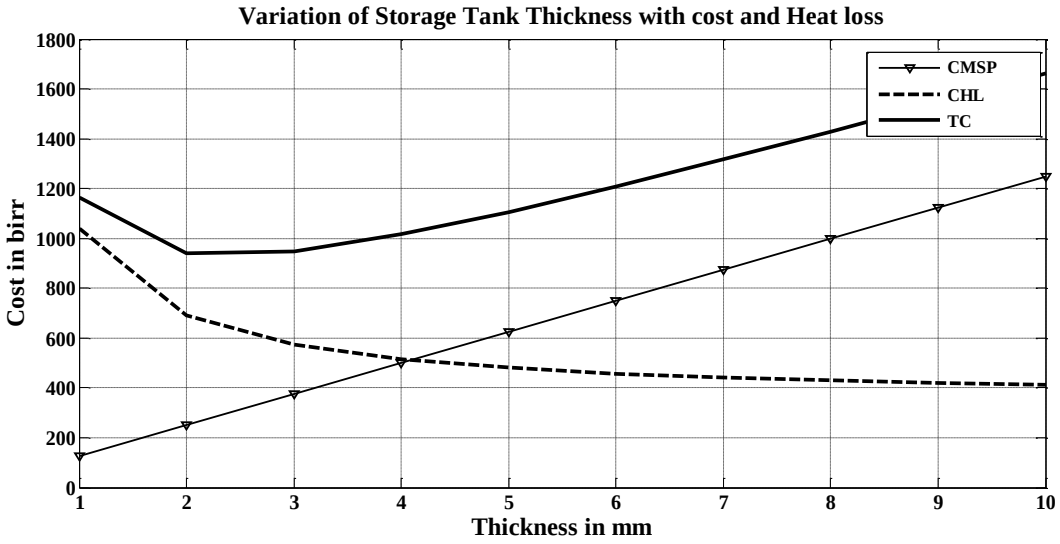

Figure 6.2: Optimum Thickness of Storage Tank on the Basis of Minimum Total Cost.

Differentiating the total cost equation (6.27) with respect to the thickness; and setting it equal to zero; is given as:

$$\frac{-697}{{t_t}^2} + 125 = 0 \quad (6.28)$$

Rearranging equation (6.28) and equating to thickness; then the optimum thickness of the storage tank material is equal to:

$$t_t = \mathbf{2.36mm} \approx \mathbf{2.5mm}$$

The thickness value satisfying the resulting equation is the optimum thickness. For strength of the tank thickness will be ($\boldsymbol{t_t = 2.5mm}$).

6.5.2 Outer Diameter of Storage Tank

Outer diameter of thermal energy storage tank is determined from the relation of inner diameter and thickness with outer diameter of the storage tank.

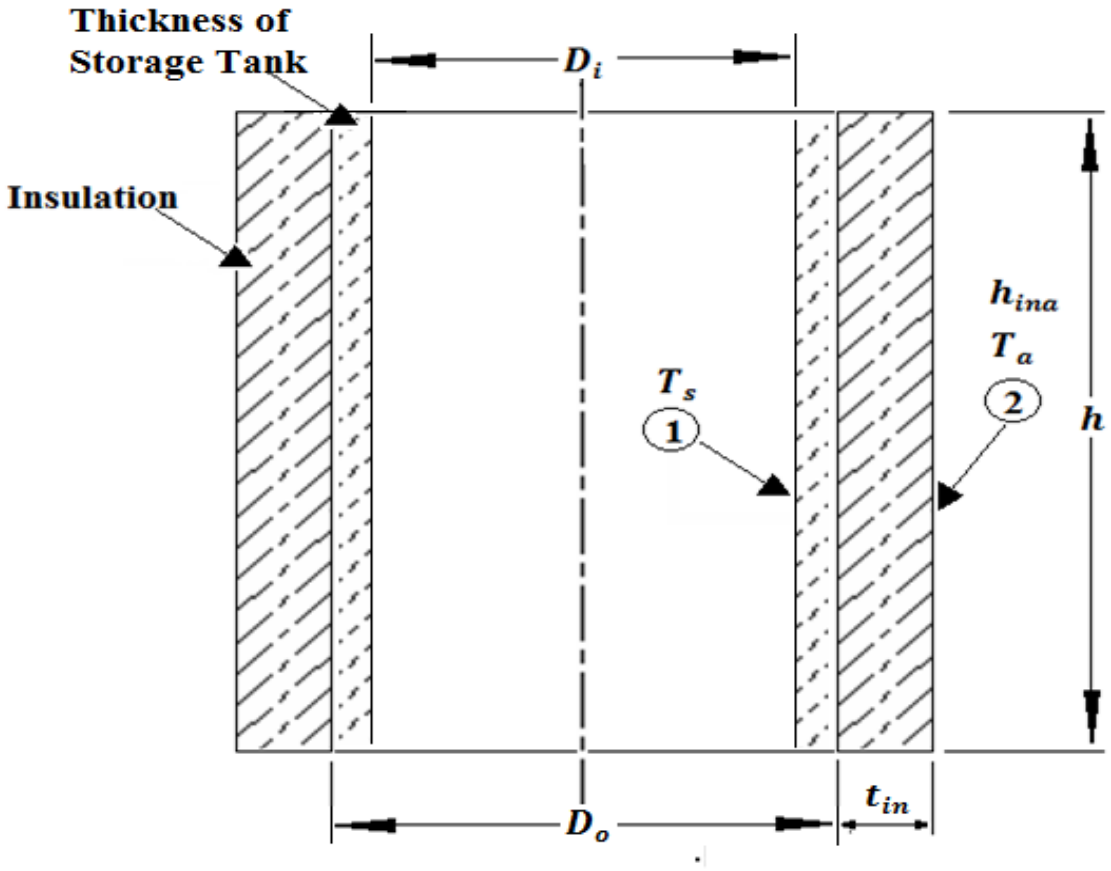

Figure 6.3: Thicknesses of the Storage Tank and Side Insulation

The outer diameter of the storage tank is given as:

$$D_o = D_i + 2t \quad (6.29)$$

Inner diameter (D_i) and thickness (t_s) of thermal storage tank is:

$D_i = 2.3m, t_t = 2.5\text{mm}, t_{in} = 15\text{mm}$ and $t_{gv} = 0.8\text{mm}$

Thickness of the thermal storage tank is given by:

$$t = t_t + t_{gv} + t_{in} \quad (6.30)$$

$$t = (2.5 + 15 + 0.8)mm = \mathbf{18.3mm}$$

Therefore, outer diameter of the storage tank is equals to:

$$D_o = 2.3m + 2 * (0.0183m) = \mathbf{2.3366m} \approx \mathbf{2.34m}$$

6.6 Technical Data of Storage Tank

Technical data of storage tank which can be used for solar thermal water heating system design is given as follows.

Table 6.1: Technical Data of Storage Tank

Technical Data of Storage Tank	
Hot water consumption pattern	Daily
Hot water consumption	$30.5m^3$
Number of storage tank	2
Volume (V_s)	$18.3m^3$
Surface Area (A_s)	$41.55m^2$
Height (h)	$4.6m$
Inner diameter (D_i)	$2.3m$
Outer Diameter (D_O)	$2.34m$
Storage Tank Material	Mild steel plate
Tank Thickness (t_t)	$2.5mm$
Galvanized pre painted	steel jacket (outer cover)
Galvanized Thickness (t_{gv})	$0.8mm$
Insulation Material	Glass fiber
Thermal Conductivity of Insulation	$k_{in} = 0.036W/mk$
Insulation Thickness (t_{in})	$15mm$
Storage Tank Thickness (t_s)	$18.3mm$

CHAPTER 7

TRANSIENT ANALYSIS OF FLAT-PLATE SOLAR COLLECTOR

The transient thermal performance of the solar collector is evaluated by applying energy balance on its components. The important parts of a typical liquid heating flat-plate solar collector, as shown in Figure 7.1. solar energy-absorbing surface with means for transferring the absorbed energy to a fluid, envelopes transparent to solar radiation over the solar absorber surface that reduce convection and radiation losses to the atmosphere, and back insulation to reduce conduction losses [5].

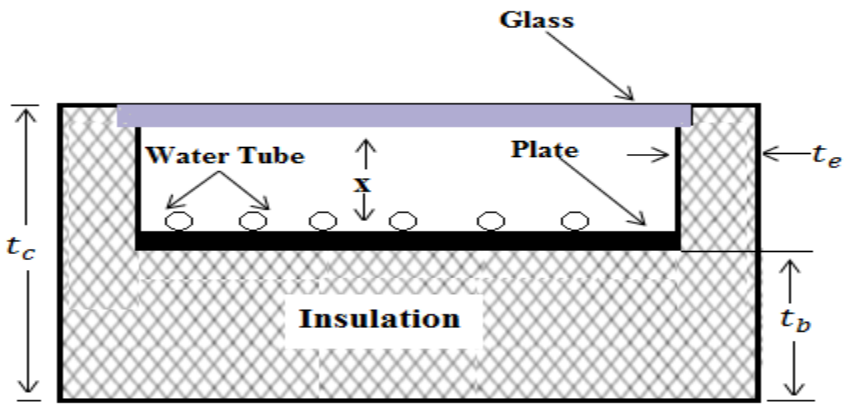

Figure 7.1: Cross-Section of the Flat Plat Collector

Flat-plate collectors are almost always mounted in a stationary position (e.g., as an integral part of a wall or roof structure) with an orientation optimized for the particular location in question for the time of year in which the solar device is intended to operate. Hence in this chapter the development of the simulation model will be discussed.

7.1 Transient Analysis of Solar Water Heater

In steady state, the performance of a solar collector is described by an energy balance that indicates the distribution of incident solar energy into useful energy gain, thermal losses, and optical losses. The thermal energy lost from the collector to the surroundings by conduction, convection, and infrared radiation can be represented as the product of a heat transfer coefficient (U_L) times the difference between the mean absorber plate temperature (T_{pm}) and the ambient temperature (T_a) varies as a function of time. The useful energy output per unit time of a

collector area (A_C) is the difference between the absorbed solar radiation and the thermal loss and is given by:

$$\dot{Q}_u = \dot{A}_C \dot{q}_u = A_C [\dot{q}_{ab} - U_L(T_P - T_a)] \quad (7.1)$$

Where: $\dot{q}_{ab}$ is solar energy absorbed by plate is given by:

$$\dot{q}_{ab} = (\tau_g \alpha_p) I_t \quad (7.2)$$

Where: (τ) and (α) is the transmissivity of the glass cover and absorptivity of the absorber.

A measure of collector performance is the collection efficiency, defined as the ratio of the useful gain over some specified time period to the incident solar energy over the same time period.

Therefore the instantaneous efficiency is given by:

$$\eta = \frac{Q_u}{A_c I_t} \quad (7.3)$$

The design of a solar energy system is concerned with obtaining minimum-cost energy. Thus, it may be desirable to design a collector with efficiency lower than is technologically possible if the cost is significantly reduced. In any event, it is necessary to be able to predict the performance of a collector.

7.2 Assumptions for Transient Analysis of Flat Plate Collector

To simplify the analysis of the solar collector, the following assumptions were made [5]:

1. Performance is steady state.
2. Uniform mass flow rate in the collector tubes.

   $$\dot{m}_f = \frac{\dot{m}_t}{n} \quad (7.4)$$

   Where: n = number of tubes in the solar collector, $\dot{m}_t$ = the total mass flow rate at the solar collector inlet and $\dot{m}_f$ = the mass flow rate in each tube
3. Construction is of sheet and parallel tube type.
4. Heat flow through a cover and insulation is one dimensional.
5. The covers are opaque to infrared radiation.
6. The sky can be considered as a blackbody for long-wavelength radiation at an equivalent sky temperature.

7. The temperature gradients in the direction of flow and between the tubes can be treated independently.
8. Properties are independent of temperature.
9. Loss through front and back are to the same ambient temperature.
10. Dust, dirt and Shading on the collector are negligible.

7.3 Basic Energy Balance Equation

The energy balance caused by the mass transfer during the circulating of the fluid within the solar collector is included by the definition that the collector's temperature depends on time variation (transient analysis) and the coordinates in the direction of the fluid flow. The governing equations were derived by applying the general energy balance for each zone in the analyzed control volume of the solar collector [5].

For one-dimensional heat transfer, the general energy balance is given by:

$$\frac{dU}{dx} = \dot{Q}_{in} + \dot{Q}_{v} - \dot{Q}_{out} \quad (7.5)$$

Where: $\frac{dU}{dx}$ = the change in the internal energy

$\dot{Q}_{in}$ = the heat transfer rate into the system

$\dot{Q}_{in}$ = the heat generation rate into the system

$\dot{Q}_{out}$ = the heat transfer rate out of the system

Generally thermal water heating system using flat plate collector's; heat energy balance of one-dimensional transient heat transfer system of solar collector leys on four main parts of the collector [10].

Main parts of flat plate solar collector which heat energy balance performed are Glass cover, Absorber plate, Water stream and Storage tank.

7.3.1 Energy Balance of Glass Cover

The small thickness of the cover makes it reasonable to consider a uniform glass temperature distribution through the whole part of the glass cover. Also by considering constant properties of glass material, the governing equation can be derived from an energy balance in a differential volume of thickness (t_g), area (A_c) and time variation over period of the day.

Thermal energy absorbed to the glass cover and lost form glass cover is shown by fig: 7.2:

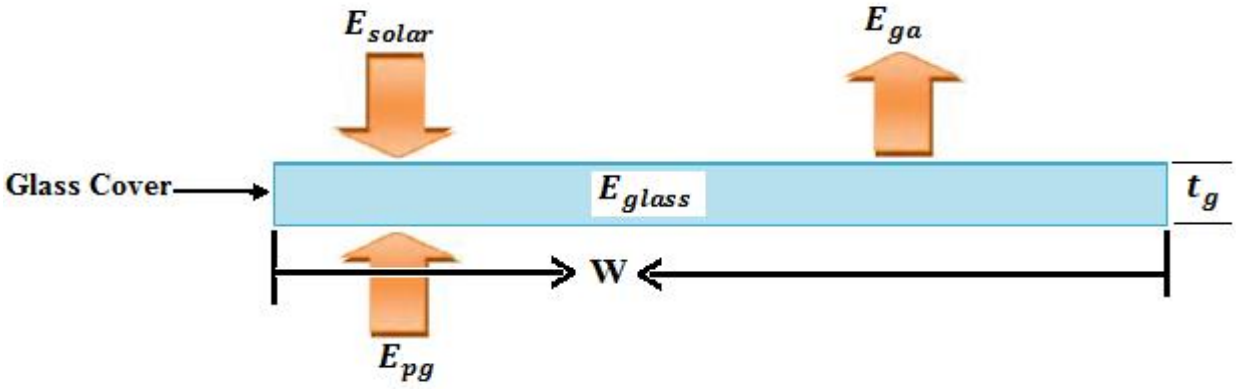

Figure 7.2: Heat Energy Balance of Glass Cover.

Making energy balance on the glass cover, assumed single glazed collector, its empirical equation at any time $(t + \Delta t)$ is determined from data at time (t) and energy absorbed and lost from the glass cover during the time interval (Δt) as follows:

$$\boldsymbol{E_{glass} = E_{solar} + E_{pg} - E_{ga}} \quad (7.6)$$

Where: $E_{glass} = \left(m_g C_{pg}\right)\frac{dT_g}{dt}$ ... heat energy gained by the glass

$E_{solar} = I_N A_c \alpha_g$ ... solar energy recived by the glass

$E_{pg} = A_c U_{pg}\left(T_{p0} - T_{g0}\right)$ ... heat energy gained from plate

$E_{ga} = A_c U_{ga}\left(T_{g0} - T_{a0}\right)$ ... heat loss to the ambient

By substituting the empirical equation of $(E_{glass}), (E_{solar}), (E_{pg})$ and (E_{ga}) into equation (7.6), yields the energy balance of the glass cover, given as:

$$\left(m_g C_{pg}\right)\frac{dT_g}{dt} = A_c I_N \alpha_g + A_c U_{pg}\left(T_{p0} - T_{g0}\right) - A_c U_{ga}\left(T_{g0} - T_{a0}\right) \quad (7.7)$$

7.3.2 Energy Balance on Absorber Plate

The small thickness of the absorber plate makes it reasonable to consider a uniform plate temperature distribution through the whole part of the absorber plate. Applying the heat energy balance for the absorber plate zone; taking the transient thermo-physical properties of the absorber plate material and considering the solar irradiance on the absorber plate zone in the

solar collector control volume, the radiation and convection heat transfer between the absorber and the glass cover, the conduction and convection heat transfer between the absorber and the insulation zone and the heat transfers by convection with the fluid flow, gives the relation below.

Thermal energy absorbed to the absorber plate and lost form absorber plate is shown by fig: 7.3:

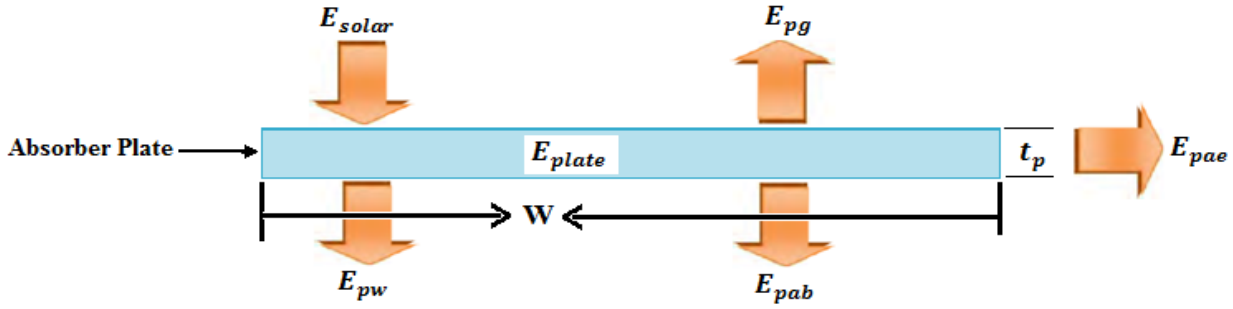

Figure 7.3: Heat Energy Balance of Absorber Plate.

The energy balance of plate at any time $(t + \Delta t)$ is estimated from energy absorbed during the time interval (Δt) and the energy losses at the same time interval given as:

$$\boldsymbol{E_{plate} = E_{solar} - E_{pg} - E_{pw} - E_{pab} - E_{pae}} \quad \text{(7.8)}$$

Where: $E_{plate} = (m_p C_{pp})\frac{dT_P}{dt}$ ... net energy gain of plate

$E_{solar} = A_c I_c$ ... solar energy absorbed by the plate

$E_{pw} = A_w U_{pw}\left(T_{p0} - \frac{T_{woo}+T_{wio}}{2}\right)$ ... heat energy loss to water

$E_{pab} = A_c U_{pab}(T_{p0} - T_{a0})$ ... back heat energy loss to ambient

$E_{pae} = A_c U_{pae}(T_{p0} - T_{a0})$ ... edge heat energy loss to ambient

By substituting empirical equation of (E_{plate}), (E_{solar}), (E_{pg}), (E_{pw}), (E_{pab}) and (E_{pae}) into equation 7.8, yields the energy balance equation of the absorber plate, is give as:

$$(m_p C_{pp})\frac{dT_p}{dt} = A_c I_c - A_c U_{pg}(T_{p0} - T_{g0}) - A_w U_{pw}\left[T_{p0} - \frac{T_{woo}+T_{wio}}{2}\right] - A_c U_{pab}(T_{p0} - T_{a0}) - A_l U_{pae}(T_{p0} - T_{a0}) \quad \text{(7.9)}$$

7.3.3 Energy Balance on Water Stream

Figure 7.4 shows the energy balance in a control volume of the working fluid in a flat-plate solar collector.

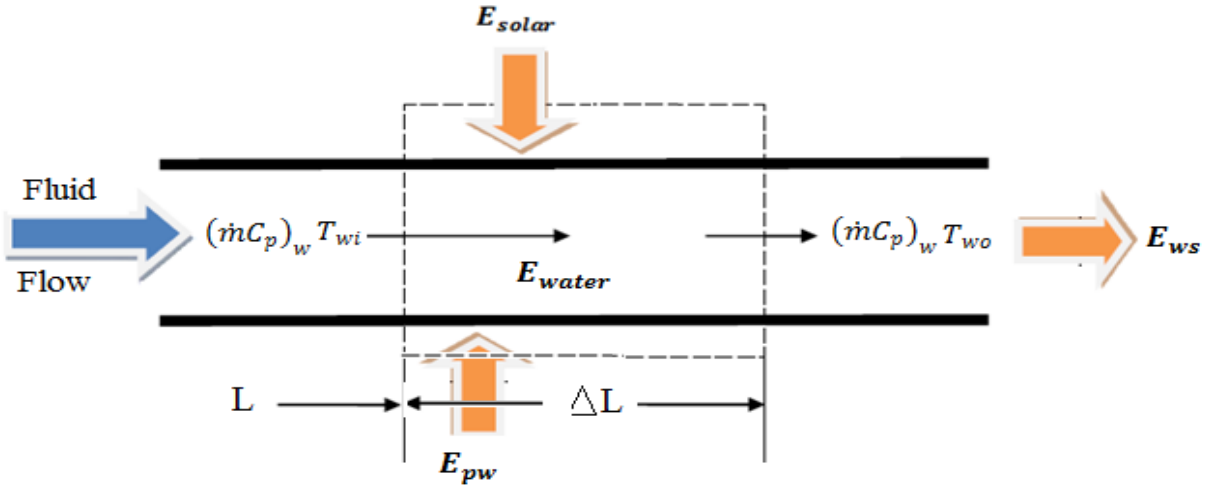

Figure 7.4: Energy balance of the working fluid in flat-plate solar collector

Taking in consideration the change in total energy with time and the total heat transferred into the fluid control volume, the energy balance under transient properties of the working fluid can be written as:

$$\boldsymbol{E_{water} = E_{sw} + E_{pw} - E_{ws}} \quad \text{(7.10)}$$

Where: $E_{water} = \left(m_w C_{pw}\right)\frac{dT_{wo}}{dt}$ ... net heat energy gain by water

$E_{sw} = A_w I_N \alpha_t \tau_g$ ... solar energy absorbed by the water

$E_{ws} = \dot{m} C_{pw}(T_{wo0} - T_{wi0})$ ... out put heat energy stored in storage

By substituting empirical equation of (E_{water}), (E_{sw}), (E_{pw}) and (E_{ws}) into equation 7.10, yields the energy balance of the working fluid, is given as:

$$\left(mC_p\right)_w \frac{dT_{wo}}{dt} = A_w I_N \alpha_t \tau_g + A_w U_{pw}\left(T_p - \frac{T_{wo}+T_{wi}}{2}\right) - \left(\dot{m}C_p\right)_w (T_{wo} - T_{wi}) \quad \text{(7.11)}$$

7.3.4 Energy Balance on Storage Tank

The energy balance of the water in the storage tank is evaluated by taking the hot water extracted from the solar collector and the heat losses across the storage tank to the ambient into account. In the model, the level of water in the storage tank is to be controlled by a float valve keeping the

mass of water in the storage constant. Figure 7.5 shows the conservation of energy in a control volume of the storage tank.

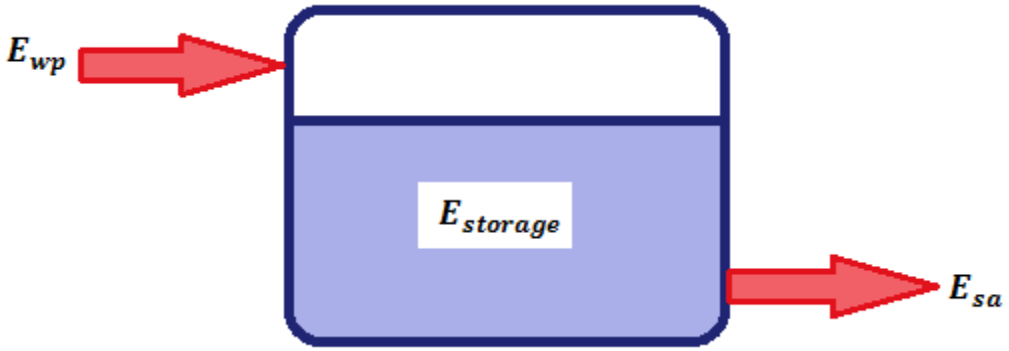

Figure 7.5: Energy balance in a control volume of storage tank.

Applying the first low of thermo dynamics over the tank control volume gives as the thermal energy balance of the storage tank.

$$\boldsymbol{E_{storage} = E_{wp} - E_{sa}} \quad (7.12)$$

Where: $E_{storage} = (\rho C_p)_w V_s \frac{dT_s}{dt}$ ... net energy gain of storage tank

$E_{wp} = \dot{m} C_{pw}(T_{wo} - T_{wi})$ ... input energy to storage tank

$E_{sa} = U_{sa} A_s (T_s - T_a)$ ... heat energy loss to the ambient

By substituting empirical equation of $(E_{storage})$, (E_{wp}) and (E_{sa}) into equation (7.12), yields the energy balance of the storage tank, is given as:

$$(\rho C_p)_w V_s \frac{dT_s}{dt} = (\dot{m} C_p)_p (T_{wo} - T_{wi}) - U_{Ls} A_s (T_s - T_a) \quad (7.13)$$

7.4 Transient Temperature Analysis of Collector System

This section presents a mathematical model describing the flat-plate solar collector system considering the transient properties of its different zones. In the proposed model, the analyzed control volume of the flat-plate solar collector (glass cover, absorber plate, fluid stream and storage tank) perpendicular to the liquid flow direction. The transient analysis of flat plate solar collector temperature varies for each zone of the collector, having a maximum temperature on absorber plate and water stream zone, minimum temperature on the glass cover and insulation zone of a collector and also varies through the time of the day.

7.4.1 Glass Cover

The transient analysis of glass cover temperature varies across the width of the glass, having a maximum on the centerline between the fluid riser tubes and also varies through the time of the day. The temperature of glass cover derived from the energy balance of the glass zone at any time $(t + \Delta t)$, energy absorbed and lost from the glass cover during the given time interval (Δt). Upon integrating energy balance equation (7.7), yields the equation of transient temperature (T_{g1}) variation of glass cover, after time interval of (Δt) is given as:

$$T_{g1} = \frac{A_c I_N (1-\tau_g)\Delta t}{(mC_p)_g} + \left\{1.0 - \left(\frac{A_c U_{pg}}{(mC_p)_g} + \frac{A_c U_{ga}}{(mC_p)_g}\right)\Delta t\right\} T_{g0} + \left(\frac{A_c U_{pg}\Delta t}{(mC_p)_g}\right) T_{p0} + \left(\frac{A_c U_{ga}\Delta t}{(mC_p)_g}\right) T_{a0} \quad (7.14)$$

7.4.2 The Absorber Plate

The transient temperature of the absorber plate varies across the width of the fin, having a maximum on the centerline between the fluid riser tubes and varies through the time of the day that varies solar radiation energy. The absorber plate temperature T_{p1} at any time $(t + \Delta t)$ can be determined from conditions at time t and energy absorbed during the time interval Δt and the energy losses at the same time interval (Δt).

Upon integrating energy balance equation (7.9), yields the equation of transient temperature (T_{p1}) variation of absorber plate, after time interval of (Δt) is given as:

$$T_{p1} = \frac{A_c I_c\, \Delta t}{(mC_p)_p} + \left\{1.0 - \left(\frac{A_c U_{pg}}{(mC_p)_p} + \frac{A_w U_{pw}}{(mC_p)_p} + \frac{A_c U_{pab}}{(mC_p)_p} + \frac{A_l U_{pae}}{(mC_p)_p}\right)\Delta t\right\} T_{p0} + \left(\frac{A_c U_{pg}\Delta t}{(mC_p)_p}\right) T_{g0} \left(\frac{A_w U_{pw}\Delta t}{2(mC_p)_p}\right) T_{wo0} + \left(\frac{A_w U_{pw}\Delta t}{2(mC_p)_p}\right) T_{wi0} \left(\frac{A_c U_{pab}}{(mC_p)_p} + \frac{A_l U_{pae}}{(mC_p)_p}\right) \Delta t T_{a0} - \quad (7.15)$$

7.4.3 The Water Stream

The transient temperature of the water stream varies across the length of the riser tube, having a maximum at the middle point of the water riser tube and varies through the time of the day that varies solar radiation energy. Water stream temperature (T_{wo1}) at any time $(t + \Delta t)$ can be determined from data at time t and energy absorbed during the time interval (Δt).

Upon integrating energy balance equation (7.11), yields the equation of transient temperature (T_{wo1}) variation of water stream, after time interval of (Δt) is given as:

$$T_{wo1} = \left(\frac{(A_w U_{pw}\Delta\tau)}{(mC_p)_w}\right) T_{p0} + \left(1.0 - \left(\frac{A_w U_{pw}}{(2mC_p)_w} + \frac{(\dot{m}C_p)_w}{(mC_p)_w}\right)\Delta\tau\right) T_{wo0} + \left(\frac{(\dot{m}C_p)_w}{(mC_p)_w} - \frac{A_w U_{pw}}{(2mC_p)_w}\right) \Delta\tau T_{wi0} - - - - \quad (7.16)$$

7.4.4 The Storage Tank

The transient temperature of the storage tank varies across the width of the tank, having a maximum on the middle point of the storage tank and varies through the time of the day that varies solar radiation energy. Storage tank temperature (T_{s1}) at any time ($t + \Delta t$) can be determined from conditions at time (t) and energy absorbed during the time interval (Δt) and the energy losses at the same time interval (Δt).

Upon integrating energy balance equation (7.13), yields the equation of transient temperature (T_{s1}) variation of storage tank, after time interval of (Δt) is given as:

$$T_{s1} = \left\{\left(\frac{(\dot{m}C_p)_w}{(\rho C_p)_w V_s}\right)(T_{wo0} - T_{wi0})\Delta\tau\right\} + \left(\frac{A_s U_{Ls}\Delta\tau}{(\rho C_p)_w V_s}\right)T_{a0} + \left\{1.0 - \left(\frac{A_s U_{Ls}\Delta\tau}{(\rho C_p)_w V_s}\right)\right\}T_{s0} - - - -(7.17)$$

7.5 The Heat Transfer Correlations

At some typical location on the plate solar energy of amount (S) is absorbed by the plate is equal to the incident solar radiation reduced by optical losses. This absorbed energy (S) is distributed to thermal losses and to useful energy gain [10]. Thermal losses from the plate through the glass cover and the insulation and take place by conduction, convection and radiation.

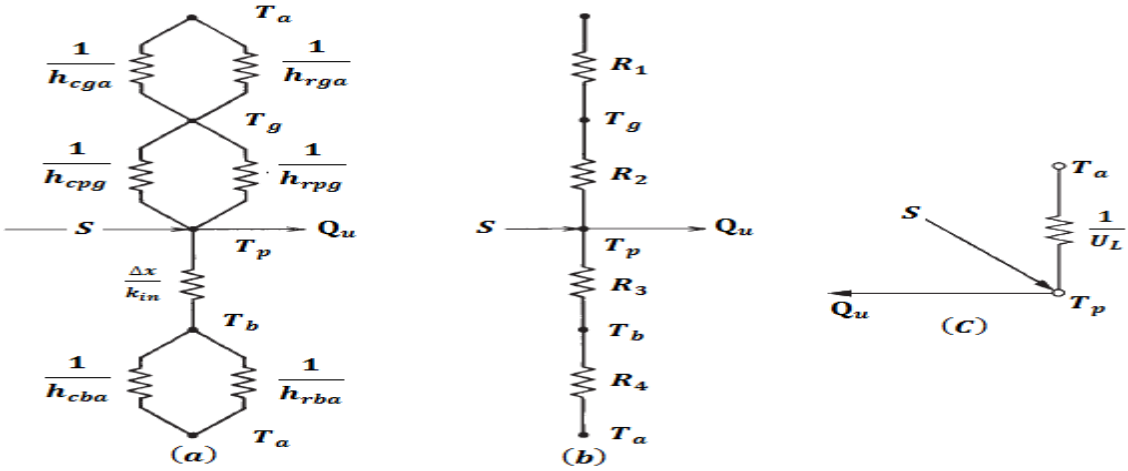

Figure 7.6: Thermal Networks for a One-Cover Flat-Plate Collector

7.5.1 Top Loss Coefficients

The energy loss through the top is the result of convection and radiation between parallel plates. The steady-state energy transfer between the plate at (T_p) and the first cover at (T_g) is the same as between any other two adjacent covers and is also equal to the energy lost to the surroundings

from the top cover. The energy loss through the top is the result of convection and radiation from glass cover to the ambient and between absorber plate and glass cover.

Top heat loss to the surroundings from the plate has two zones:

1. From absorber plate to the glass cover and
2. From glass cover to the ambient

A) From Absorber Plate to Glass Cover

The heat transfer coefficient from absorber plate to the glass cover includes the thermal energy loss by convection and radiation.

a) Convective Heat Transfer Coefficient

Convective heat transfer coefficient (h_{1c}) of top heat loss from collector plate to the cover can be expressed as:

$$h_{1c} = N_u \frac{K}{t_{pg}} \quad (7.18)$$

The Nu can be obtained from the expression (Hollandet. al. (1976)).

$$N_u = 1 + 1.44\left[1 - \frac{1708}{R_a \cos(\beta)}\right]^{+}\left[1 - \frac{1708\sin(1.8\beta)^{1.6}}{R_a\cos(\beta)}\right] + \left[\left\{\frac{R_a\cos(\beta)}{5830}\right\}^{1/3} - 1\right]^{+} \quad (7.19)$$

"+" exponent means only the positive value of the term in square bracket is to be considered, Zero is to be used for negative values, and The angle of inclination (β) can vary between $0 - 90^o$.

- The Rayleigh number Ra is given by:

$$R_a = G_r P_r = \frac{g\beta' \Delta T L^3 P_r}{v^2} \quad (7.20)$$

- The volume expansion coefficient β' is given by:

$$\frac{1}{\beta'} = \frac{(T_p + T_g)}{2} \quad (7.21)$$

b) Radiation Heat Transfer Coefficient

Radiation heat transfer coefficient (h_{1r}) of radiation heat loss from collector plate to the cover can be expressed as:

$$h_{1r} = E_{eff}\sigma\left\{\frac{(T_p+273)^4 - (T_g+273)^4}{T_p - T_g}\right\} \quad (7.22)$$

- The effective emissivity (E_{eff}) of plate-glazing system is given by:

$$E_{eff} = \left[\frac{1}{E_p} + \frac{1}{E_g} - 1\right]^{-1} \quad (7.23)$$

c) Total heat loss coefficient from Plate to Glass

The total heat transfer coefficient from collector plate to cover is expressed as the sum of convection (h_{1c}) and radiation (h_{1r}) heat loss coefficient.

$$h_1 = h_{1c} + h_{1r} = \frac{1}{R_1} + \frac{1}{R_2} \quad (7.24)$$

The total heat transfer coefficient from collector plate to cover can be simplified as:

$$U_{pg} = N_u \frac{K}{t_{pg}} + E_{eff}\sigma\left\{\frac{(T_p+273)^4 - (T_g+273)^4}{T_p - T_g}\right\} \quad (7.25)$$

B) From Absorber Plate to Water Stream

The heat loss coefficient from absorber plate to the water stream includes the thermal energy loss by convection and conduction modes of heat transfer. The thickness of absorber plate and riser tubes is very small that implies transient temperature through the thickness of absorber plate and riser tube is constant and conduction heat transfer coefficient almost equal to zero, for the mathematical modeling of temperature only convective method of heat loss coefficient is applied.

Heat transfer coefficient on the internal surface of the collector tube is given as:

$$U_{pw} = h_{cw} = \frac{N_{uw}\, k_w}{d_{in}} \quad (7.26)$$

Where the Nusselt number calculated using the empirical Heaton formula suggested by Duffie and Beckman [2006] is given by:

$$N_{uw} = N_{u\infty} + \frac{a\left(R_{ew} P_{rw} (d_{in}/L_t)\right)^m}{1 + b\left(R_{ew} P_{rw} (d_{in}/L_t)\right)^n} \quad (7.27)$$

$$1 < R_{ew} P_{rw} \frac{d_{in}}{L_t} \leq 1000 \quad (7.28)$$

With the assumption that the flow inside of tubes is fully developed,

Therefore values of constants in equation (7.27):

- $(N_{u\infty} = 4.4,\ a = 0.00398,\ b = 0.0114,\ m = 1.66 \text{ and } n = 1.12)$ respectively, for the constant heat flux boundary condition.

C) From Glass Cover to Ambient

The heat transfer coefficient from glass cover to the ambient includes the thermal energy loss by convection and radiation.

a) Convective Heat Transfer Coefficient

Convective heat transfer coefficient (h_{2c}) of convective heat loss from collector cover to the ambient can be expressed as:

$$h_{2c} = 2.8 + 3V_w \quad (7.29)$$

b) Radiation Heat Transfer Coefficient

Radiation heat transfer coefficient (h_{1r}) of radiation heat loss from collector cover to the ambient can be expressed as:

$$h_{2r} = E_g \sigma \left\{ \frac{(T_g+273)^4 - (T_{sky}+273)^4}{T_g - T_a} \right\} \quad (7.30)$$

- The sky temperature T_{sky} is given by:

$$T_{sky} = T_a - 6 \quad (7.31)$$

c) Total Heat Loss Coefficient from Glass to Ambient

The total heat transfer coefficient from the cover to ambient is expressed as:

$$h_2 = h_{2c} + h_{2r} = \frac{1}{R_3} + \frac{1}{R_4} \quad (7.32)$$

The total heat transfer coefficient from collector cover to ambient can be simplified as:

$$U_{ga} = (2.8 + 3V_w) + \left(E_g \sigma \left\{ \frac{(T_g+273)^4 - (T_{sky}+273)^4}{T_g - T_a} \right\} \right) \quad (7.33)$$

The effective top heat transfer coefficient from plate to ambient is given by:

$$U_t = U_{pg} + U_{ga} + U_{pw} \quad (7.34)$$

The rate of heat loss from the top per unit area can be given as:

$$\dot{q}_{loss,top} = U_t(T_p - T_a) \quad (7.35)$$

The value of (U_t) is calculated by the method of iteration. In general, the cover temperature (T_g) is unknown. An arbitrary value of (T_g) is assumed and (h_{1c}), (h_{1r}), (h_{2r}) are calculated at the mean temperature (T_m), and Then using these values, the top loss coefficient is calculated.

7.5.2 Back Loss Coefficient

The energy loss through the bottom of the collector is represented by two series resistors, *R*3 and *R*4, in Figure 6.4.1, where *R*3 represents the resistance to heat flow through the insulation by conduction and *R*4 represents the convection and radiation resistance to the environment.

Back heat loss from the plate to the surrounding through insulation:

1. Bottom insulation and
2. Edge insulation

a) Bottom Heat Loss Coefficient

Heat is lost from the plate to ambient by conduction through the insulation and subsequently by convection and radiation from the bottom surface casing. The bottom loss heat coefficient is given by:

$$U_b = \left[\frac{L_{in}}{K_{in}} + \frac{1}{h_b}\right]^{-1} \quad (7.36)$$

b) Edge Loss Heat Coefficient

Energy lost from the side of the collector casing may be taken to have exactly the same value as that from the back, if the thickness of the edge insulation is the same as that of the back insulation (Tabor, 1958). The edge loss is given as:

$$U_e = U_b \left(\frac{A_e}{A_c}\right);\ A_c = A_b \quad (7.37)$$

7.5.3 Overall Heat Loss Coefficient

The overall heat loss coefficient U_L is the sum of the top, bottom and edge loss coefficient.

$$U_L = U_t + U_b + U_e \quad (7.38)$$

The overall heat lost by the absorber to the ambient per unit area per can be expressed as:

$$\dot{q}_L = U_L\left(T_p - T_a\right) \quad (7.39)$$

In the proposed solution method the heat transfer coefficients were calculated using the above formulas.

CHAPTER 8

MATHEMATICAL MODEL PROGRAMING

Transient analysis of absorber plate, glass cover, water stream, and storage tank temperature of flat plate solar collector is performed by using simulation software's. This study uses mathematical model programing for a flat-plate solar collector with single glass cover working in parallel channel arrangement model. All designed physical dimensions of the collector can be entered as inputs, which make it suitable to any single glass cover flat-plate solar collector without any modifications.

There are different types of software's used to code mathematical model for numerical problem solution; which are MATLAB, C, C++ and FORTRAN. For this study mathematical model programing software package used to code the model is MATLAB version R2011a. MATLAB is a programming package that can be used for algorithm development, data analysis, visualization, and numerical computation. The software is faster than traditional programming languages including C, C++, and FORTRAN.

The MATLAB code numerically solves the derived model and computes the transient temperature distributions for any cross-section at the collector beginning at time (t = 0), that is from the onset of the process till the total time of calculations that entered by user. The detailed MATLAB code developed for the model is presented in ANNEX (A-10).

8.1 MATLAB Input Parameters

The parameters read from input files at the beginning of the simulation process include:

- Latitude of the site, azimuth and slope of the solar collector,
- Geometric dimensions and thermophysical properties of the absorber plate, the glazing and the insulation,
- Thermophysical properties of water,
- Storage capacity, daily hot water consumption pattern and hot water delivery and cold water supply temperatures,
- Global and diffuse solar radiation and ambient temperature for every hour of the day, and

- Initial assumption of absorber plate, glass cover, water stream and storage tank temperature.

8.2 Expected Output of MATLAB

By considering all the boundary conditions in the proposed model taken to be time dependent, the inputs data used for the numerical code and the mathematical model of numerical equation described in previous chapters; the expected output from the analysis of MATLAB simulation is includes:

- Hourly temperature of absorber plate, glass cover, water stream and storage tank for the selected days in each month of the year 2015,
- The amount of hot water generated per a unit collector, for the desired output temperature of hot water per day (the amount of mass flow rate of hot water flow to storage tank per a collector per day),
- The actual performance of designed solar collector; fin efficiency factor (F), collector efficiency factor (F'), collector heat removal factor (F_R) and collector flow factor (F''),
- Total solar heat energy input to the system (Q_{in}), the maximum actual useful heat energy gain (Q_u) and the maximum heat energy loss in and out of the system (Q_L) per a unit collector, and
- The maximum actual instantaneous efficiency (η_{in}), average hourly collector efficiency (η_{eff}) and average day-long collector efficiency (η_{day}).

8.3 Procedure for Simulation of Solar Thermal Water Heater

The simulation program is used to predict the monthly and annual performance of the solar water heating system includes the following procedures:

i. Properly writing the programing code of input parameters; basic angles (latitude, azimuth and slope angles), the solar collector parameters and solar radiation data.

ii. The fraction of the total daily hot water load that occurs in the hour should also be specified in the simulation process.

iii. Determining sun basic angles (declination, hour, zenith, and incident angle), total and Incident solar radiation, for each hour of the day.

iv. Starting the system simulation by assuming the following initial temperatures for the various components of the solar-collector model.

- Ambient temperature: T_{a0} = value read from solar radiation data on January 01 at 01:00 AM,
- Glass temperature: $T_{g0} = T_{a0} + 0.25$,
- Plate temperature: $T_{p0} = T_{a0} + 1.0$,
- Temperature of water at collector inlet: $T_{wi0} = T_{a0}$,
- Temperature of water at collector outlet: $T_{wo0} = T_{a0} + 0.5$, and
- Storage tank temperature: $T_{s0} = T_{a0} + 0.5$

v. Evaluate temperatures (T_{p1}) of the plate, (T_{g1}) of the glass cover, (T_{wo1}) of the water at outlet from the collector and (T_{s1}) of the storage tank at time ($t + \Delta t$) applying Equations (7.17), (7.18), (7.19) and (7.20), respectively,

vi. Since the assumed temperatures for the various components of the collector are too crude, they have to be refined by taking average values of the assumed temperatures and the evaluated temperatures at time ($t + \Delta t$) and substituted for temperature values at time t.

vii. Temperature variations (T_{p1}), (T_{g1}), (T_{wo1}) and (T_{s1}) during a period of 24 hours over the year are then estimated by substituting the new values of (T_{p1}), (T_{g1}), (T_{wo1}) and (T_{s1}) respectively, for (T_{p0}), (T_{g0}), (T_{wo0}) and (T_{s0}), for the next time interval.

viii. Evaluate the possible performance of solar collector.

ix. Finally the expected output of the MATLAB simulation displayed using graph.

The flow chart describes the procedure that can be implemented for transient simulation of water heating system is shown by fig. 8.1 (Dr.-Ing. Demiss Alemu).

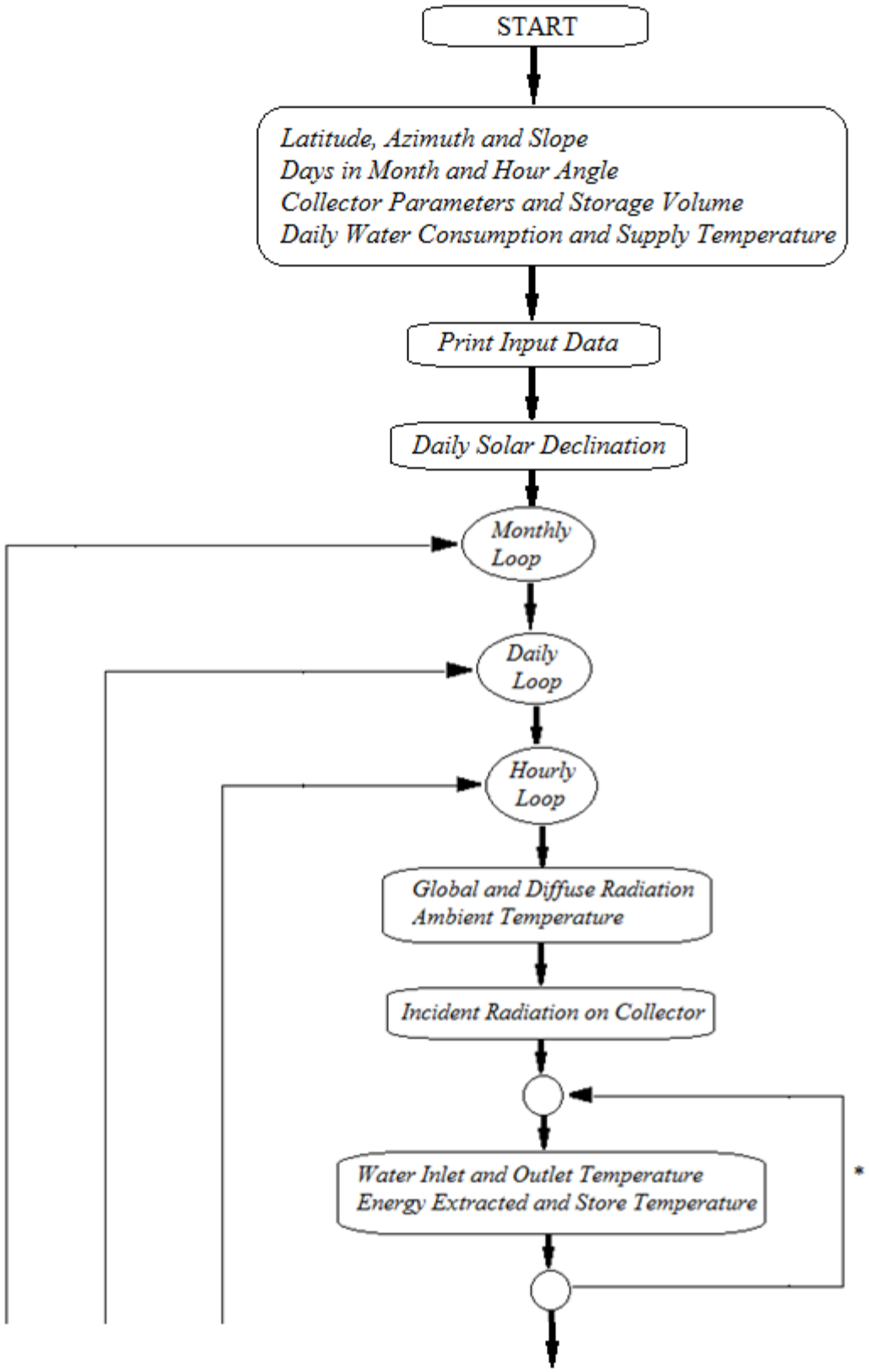

Figure 8.1 (a) Flowchart of Simulation Programme

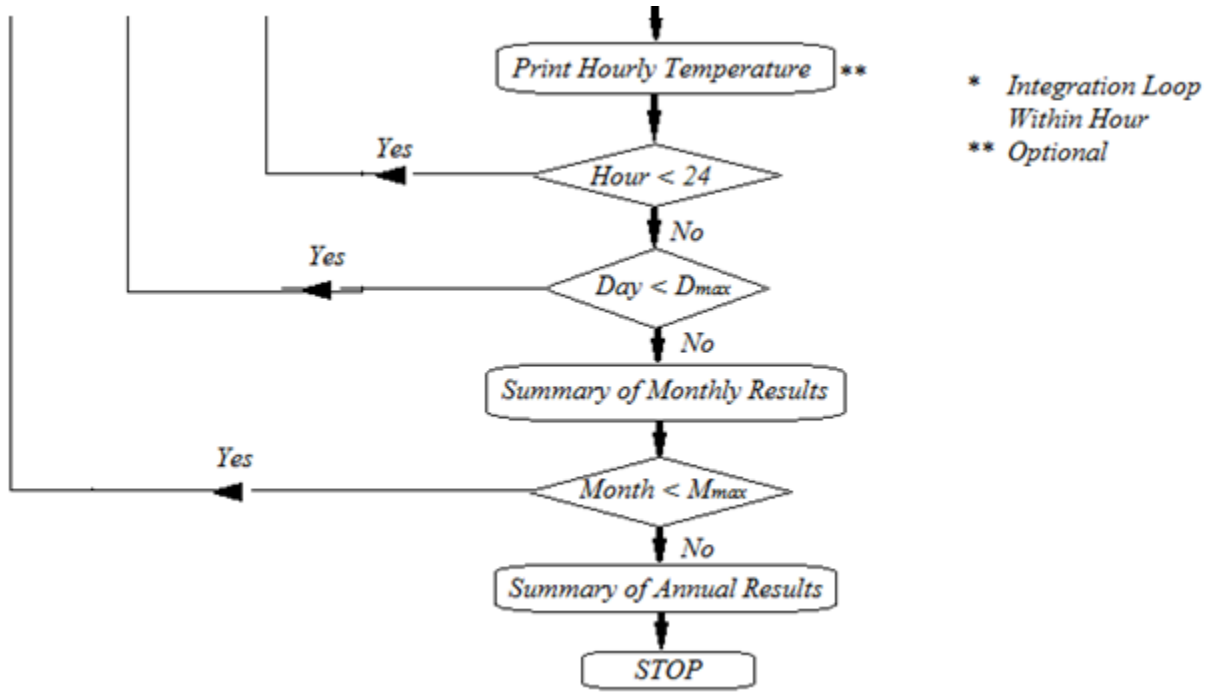

Figure 8.1 (b) Flowchart of Simulation Programme (contd.),

CHAPTER 9

RESULTS AND DISCUSSION

This chapter presents the results obtained from the theoretical works in previses chapter and MATLAB simulation. The first part of the analysis was a convergence study for the proposed numerical code. The second part presents a discussion on numerical obtained temperature histories, mass flow rate, collector factors, total heat gain, collector system efficiency and annual solar radiation contribution to heating load. The following sections present the details of each section.

9.1 Solar Contribution to the Heating Load

Hot water at collector outlet and delivered to thermal energy storage tank at temperature of 60ºc for the maximum solar contribution to the heating load is achieved during the winter season in the month February and the minimum is achieved during the summer season in the month of July.

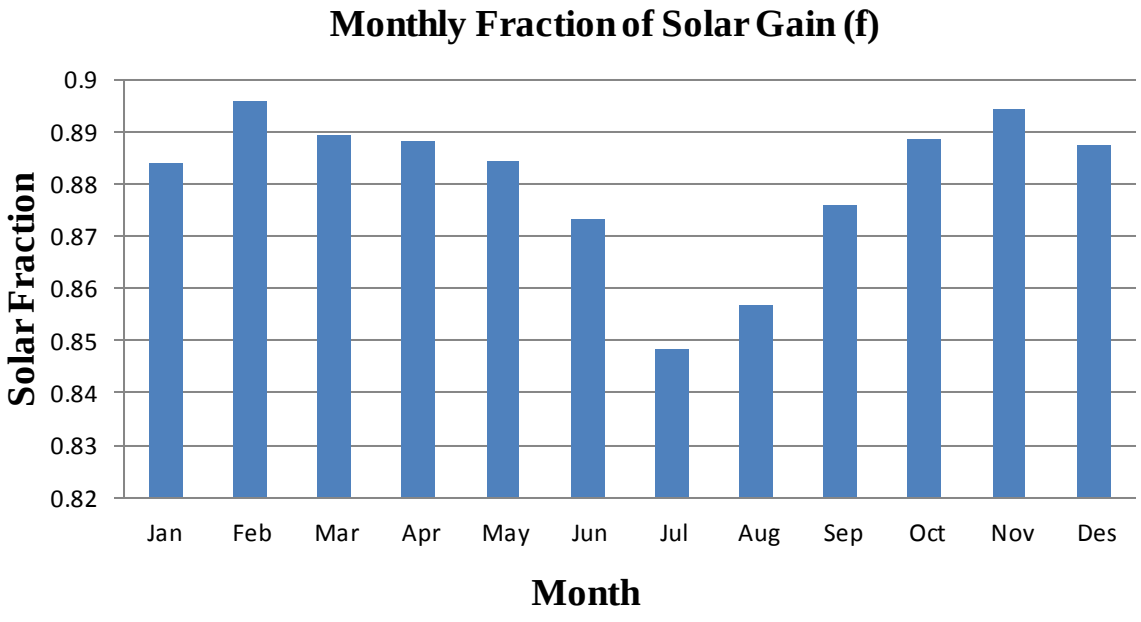

Figure 9.1: Solar Radiations for Minilik II Hospital

For the analysis of this study solar thermal water heating system 12 month is selected, but for July and August months auxiliary heating system is needed additional to solar thermal water

heating system; because in Ethiopia these months are covered by clouds and fogs, also heavy rain recorded in these months and minimum solar radiation available at this month.

- The annual solar contribution to heating load is summarized in the table below.

Table 9.1: Summery of Annual Fraction of Solar Contribution to Load

Project Site	Annual Solar Contribution		
	Solar Fraction	Heating Load [MWh]	Heating Load [KWh/m^2]
Minilik II Hospital	0.882	18.05	9023.944

9.2 Outlet Water Temperature Graph

Outlet water temperature result graph shows that the outlet temperature depends on the hourly solar radiation on tilted surface and the mass flow rate of water stream for each collector. Fig. 9.2 shows the outlet water Temperature distribution obtained by the MATLAB code for different number of nodes (n = 12, 24 and 36) along the flow direction, for each number of nodes at constant flow rate ($0.03Kg/s$) and for the selected time period of ($t = 1.5min$).

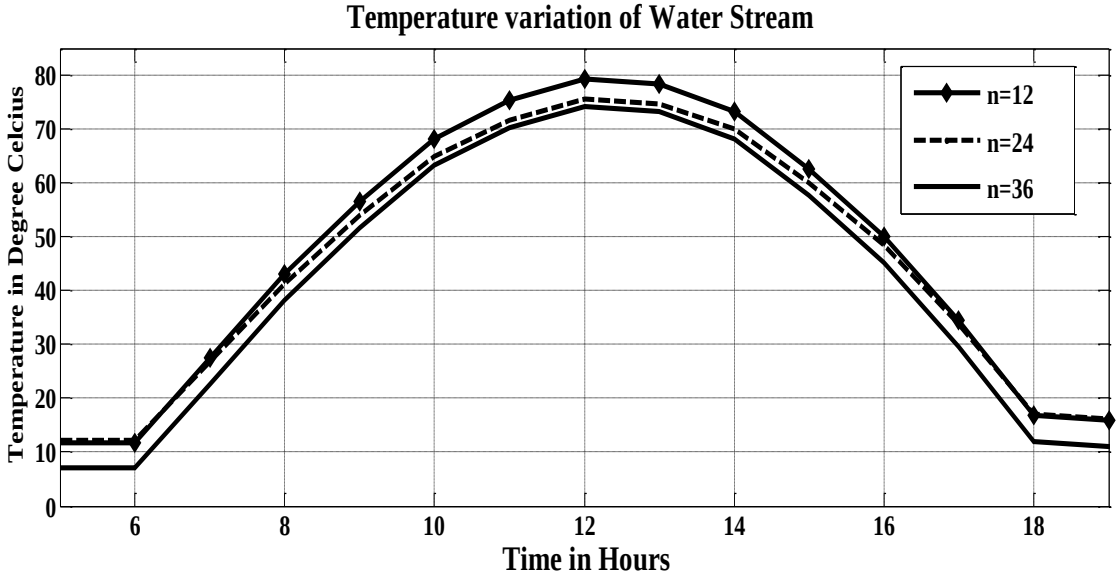

Figure 9.2: Outlet Water Temperatures for Different Number of Nodes

Figure 9.2 shows that the hourly water temperature at collector outlet increases from morning up to mid-day and then decreases from mid-day up to night forming downward parabola. Outlet water temperature reaches at the maximum point at the mid-day and at the minimum point

morning and night hour s of the day. As shown on fig. 9.2; when the number of nodes increases outlet water temperature decreases and converges to the exact outlet water temperature. For this transient analysis of outlet water temperature; ($\boldsymbol{n = 36}$).number of nodes are selected.

Figure 9.3 shows the result of outlet water Temperature distribution obtained by the MATLAB code for different time periods ($t = 1min, t = 1.5\,\text{min}\ and\ t = 2min$) along the flow direction, for each number of time period at constant mass flow rate ($0.03Kg/s$) and for the selected number of nodes ($n = 36$).

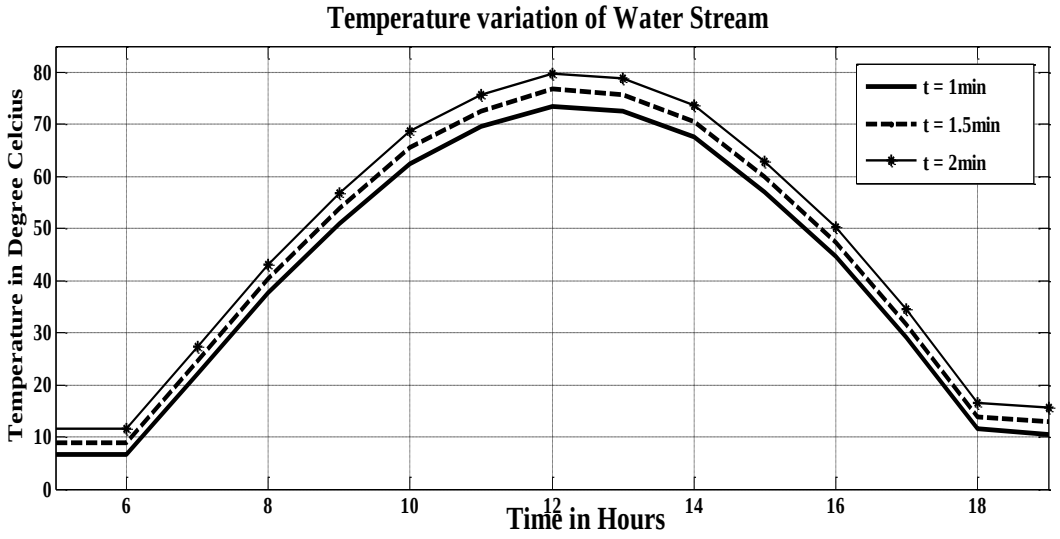

Figure 9.3: Outlet Water Temperatures for Different time period

As shown on fig. 9.2; when the gap of time period decreases outlet water temperature decreases and converges to the exact outlet water temperature. For this transient analysis of outlet water temperature; ($\boldsymbol{t = 1min}$) time period is selected which is the minimum time step satisfies the stability condition in the flow direction.

9.2.1 Water Stream Temperature

Outlet water temperature result graph shows that the outlet temperature depends on the hourly solar radiation on tilted surface and the mass flow rate of water stream for each collector. Figure 9.4 shows the result of outlet water Temperature distribution obtained by the MATLAB code for selected time period ($t = 1min$), mass flow rate ($0.03Kg/s$) and number of nodes ($n = 36$) along the flow direction. Outlet water Temperatures are plotted on the figure below for the representative days of selected months at various seasons of a year

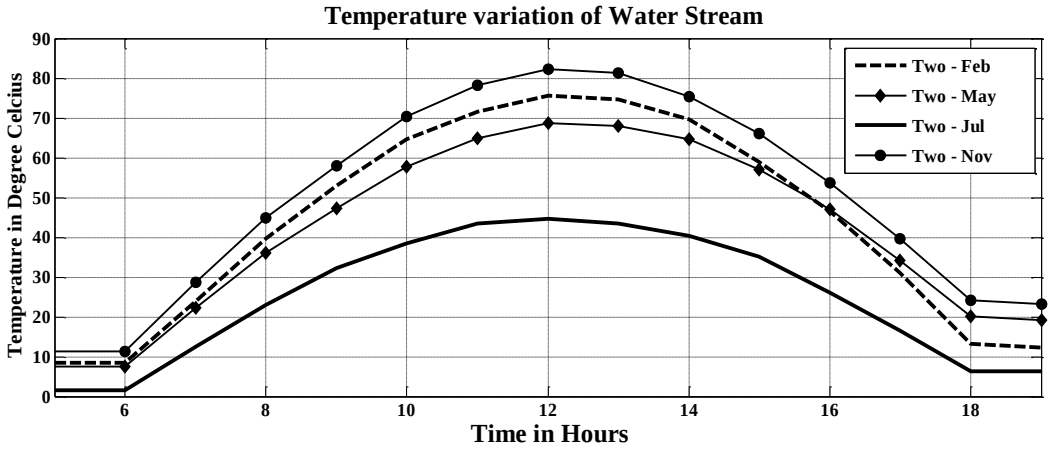

Figure 9.4: Simulated Hourly Outlet Water Temperatures for Various Seasons

Hot water at collector outlet at temperature of 60ºc the maximum solar contribution to the heating load is achieved during the autumn season in the month November and the minimum is achieved during the summer season in the month of July.

Temperature distribution of water in a collector per a day:

- For July month temperature of water stream below 60℃ for all hours of the day
- For November month temperature of water stream above 60℃ for 7 hours of the day

The maximum and minimum outlet water temperature is 83℃ and 10℃ for November month, for July month 45℃ and 8℃ respectively.

9.2.2 Storage Tank Temperature

Temperatures of the water in the storage tank at various seasons of a year are plotted in the figure below.

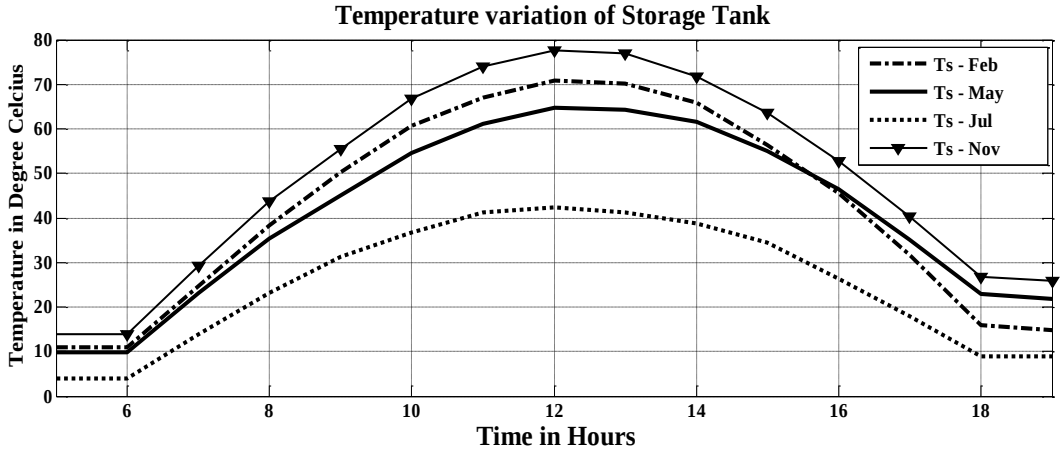

Figure 9.5: Simulated Hourly Storage Tank Temperatures for Various Seasons

For the storage tank hot water delivery temperature of 60ºc the maximum solar contribution to the heating load is archived during the autumn season in the month November and the minimum is achieved during the summer season in the month of July.

Temperature distribution of water in storage tank per a day:

- For June month temperature of water stream below 60℃ for all hours of the day
- For November month temperature of water stream above 60℃ for 6 hours of the day

The maximum and minimum hot water temperature in storage tank is 76℃ and 15℃ for November month, for July month 41℃ and 8℃ respectively.

9.3 Hourly Useful Heat Gain

Hourly Solar thermal energy gain mainly depends on the available solar radiation of the location, mass flow rate and outlet water temperature. Fig. 9.6 shows hourly useful heat gain of a single collector for November autumn season and July summer season.

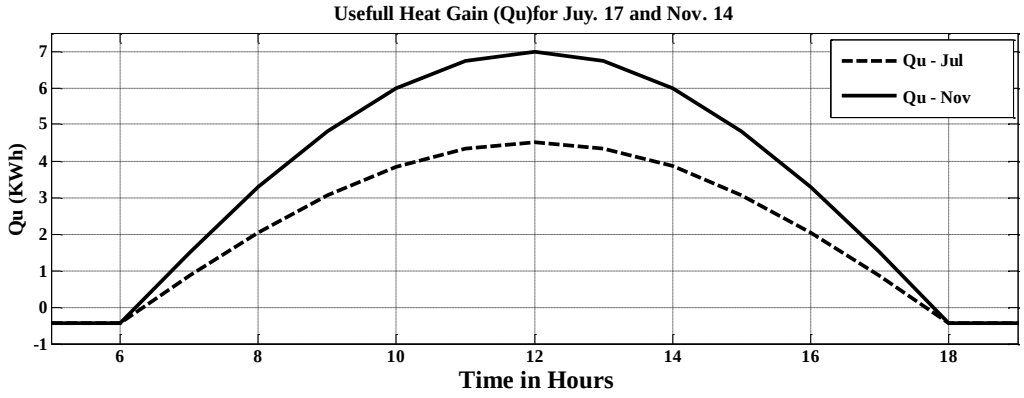

Figure 9.6: Hourly Useful Heat Gain

As shown on the figure 9.6; maximum useful heat is gained at the mad-day hours of the day. The maximum useful heat gain for November is 7KWh and for July is 4.5KWh. Monthly Useful Heat Gain is shown in table below.

Table 9.2: Monthly Useful Heat Gain

Monthly Useful Heat Gain [MWh]											
Month	Jan	Feb	Mar	Apr	May	Jun	Jul	Aug	Sep	Oct	Nov
$\mathbf{Q_u}$	1.56	1.6	1.65	1.58	1.57	1.37	1.15	1.23	1.41	1.64	1.68

9.4 Collector Efficiency

The instantaneous efficiency of the single collector depends on mass flow rate, water temperature at collector outlet and available solar radiation. Fig. 9.7 shows collector instantaneous efficiency for selected month July and November which are the minimum and maximum solar radiation available months of a year.

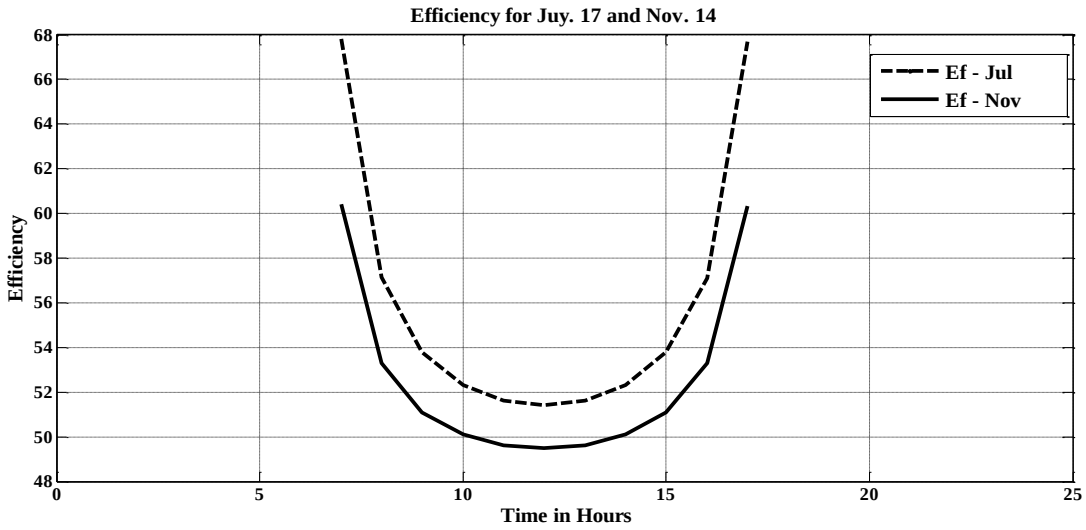

Figure 9.7: Efficiency for July 17 and November 14

Figure 9.7 shows that the maximum instantaneous efficiency is achieved at the sunshine and sunset hours and the minimum is achieved at the mid-day hours of the day. For November 14, maximum instantaneous efficiency is 60.2% and minimum is 49%; also for July 17 maximum instantaneous efficiency is 67% and minimum is 51.88%.

CHAPTER 10

PUMP AND CONTROL SYSTEM SELECTION

In Chapters 3 through 9 performed the development of mathematical models for two of the key components in solar energy systems: collectors and storage units. In this chapter mainly included how other components can be modeled and how the component models can be combined into system models. With information on the magnitude and time distribution of the system loads and the weather, it is possible to simultaneously solve the set of equations to estimate the thermal performance of a solar process over any time period. These estimates (simulations) are usually done numerically and provide information on the expected dynamic behavior of the system and long-term integrated performance.

10.1 Arrays of Collectors

Collector modules in arrays may be connected in series, in parallel, or in combinations. The performance of collectors in arrays is dependent on how they are arranged, that is, on the flow rate through risers and on the inlet temperatures to individual modules. Fig. 10.1 shows arrays of two modules (or two groups of modules) with parallel and series connections [5].

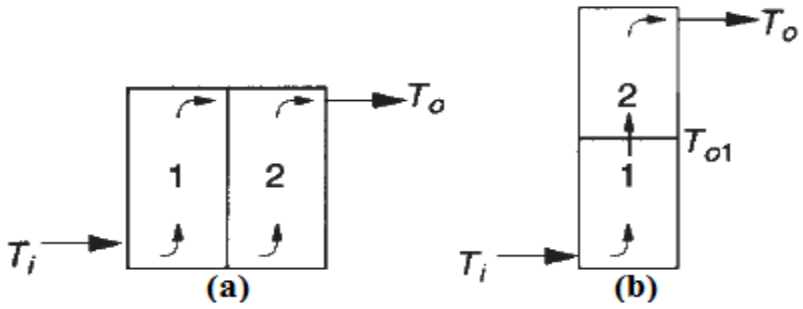

Figure 10.1: Collector modules in parallel (a) and series (b).

Flow divides in the parallel set; full flow goes through each module in the series set. For this study parallel arrangement is selected for the analysis of solar thermal water heating system component and collector arrangement [5].

According to the results of computer simulation, the daily hot water demand of the Minilik II hospital is fulfilled by the use of 108 collectors. There are two storage tanks, where each of the two storage tanks are connected to 54 collectors where there are 27 collectors are on both side of

the storage tank. There are 6 arrays on each side of the storage tank and the first 5 arrays contain 12 collector modules and the last array contains 4 collector modules for the total of 54 collectors. The collector array layout is shown in fig. 10.2.

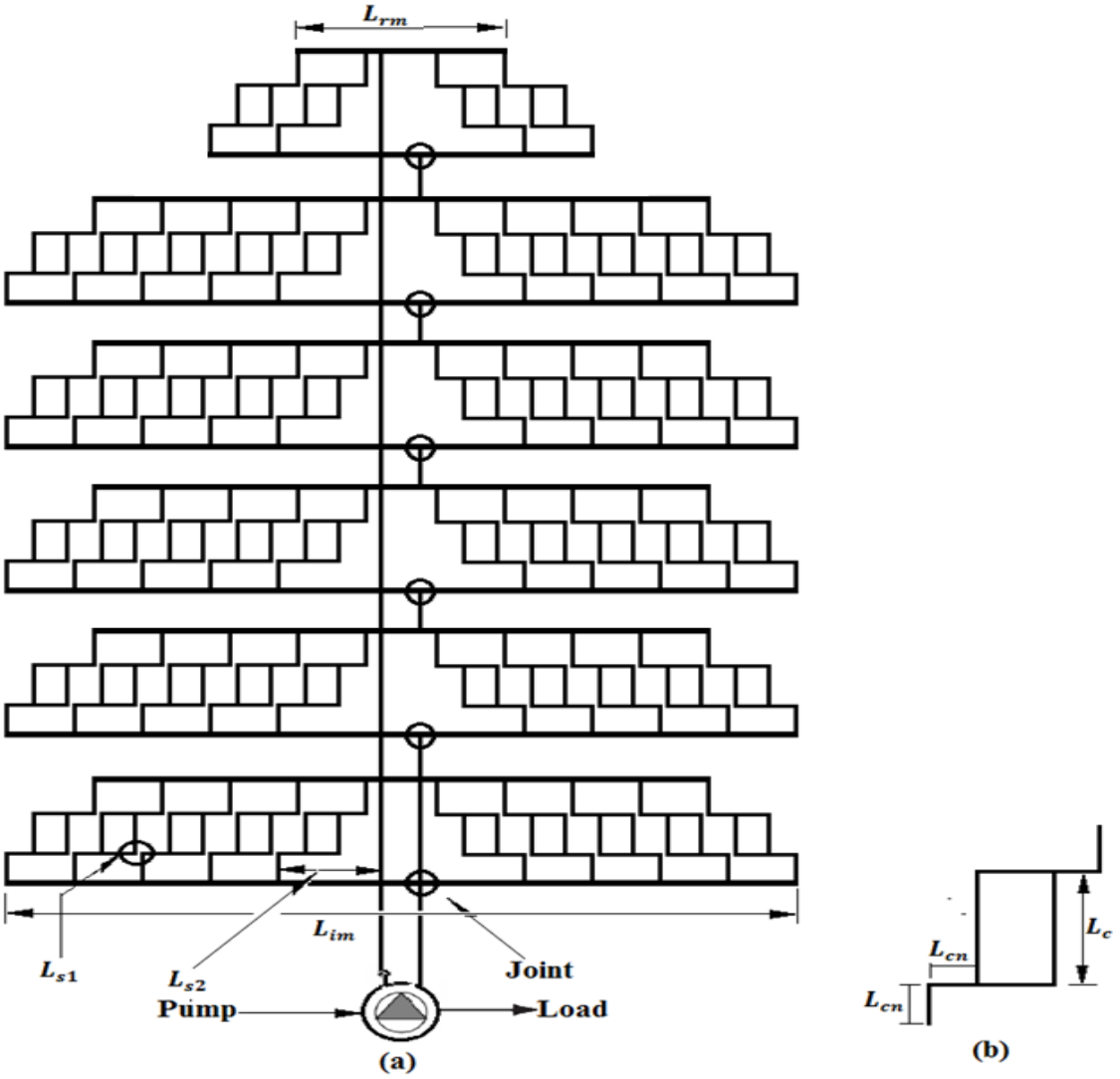

Figure 10.2: Collector Array (a) and Collector Module with Connection Line (b)

10.1.1 Clearance Inside Collector Arrays

When installing several rows of collectors in series behind each other, behind building height in the roof top and behind thermal storage tank, suitable clearance to prevent shading must be maintained. Determining this clearance requires the angle of the sun at midday on the 12, the shortest day of the year. In Ethiopia this angle (subject to latitude), in Addis Ababa the angle of sun (Altitude) for maximum solar radiation day, February 16 is equals to ($\alpha = 14.05°$).

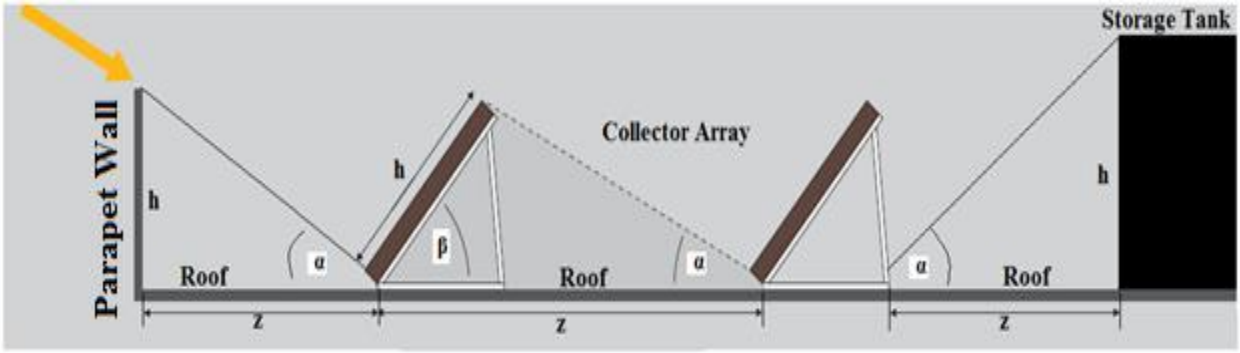

Figure 10.3: Clearance of Collector Array System

The resulting clearance between rows is calculated as follows:

$$\frac{z}{h} = \frac{\sin(180-(\alpha+\beta))}{\sin(\alpha)} \quad (10.1)$$

By rearranging equation (10.1), clearance between array systems is:

$$z = \frac{h*\sin(180-(\alpha+\beta))}{\sin(\alpha)} \quad (10.2)$$

a) Clearance Between Collector Arrays

When installing several rows of collectors in series behind each other, suitable clearance to prevent shading must be maintained.

For collector inclination angle ($\beta = 22°$), sun angle ($\alpha = 14.05°$) and ($h = 2.054m$), distance between two collector array is:

$$z = \frac{2.054m * \sin(180-(14.05+22))}{\sin(14.05)} = \mathbf{4.979m \approx 5m}$$

b) Clearance Between Collector Arrays and Storage Tank

When installing several collector arrays behind storage tank, suitable clearance between last array and storage tank is essential to prevent shading must be maintained.

For collector inclination angle ($\beta = 22°$), sun angle ($\alpha = 14.05°$) and ($h = 2m$), distance between last collector array and storage tank is:

$$z = \frac{2m * \sin(180-(14.05+22))}{\sin(14.05)} = \mathbf{4.848m \approx 5m}$$

c) Clearance Between Collector Arrays and Parapet Wall

When installing several collector arrays behind building roof height, suitable clearance between the first collector array and building is essential to prevent shading must be maintained.

For collector inclination angle ($\beta = 22°$), sun angle ($\alpha = 14.05°$) and (h = 0.5m), distance between the first collector array and building height is:

$$z = \frac{0.5\text{m} * \sin\left(180 - (14.05 + 22)\right)}{\sin(14.05)} = \mathbf{1.212m} \approx \mathbf{1.5m}$$

10.2 Pipe Length

The energy lost from ducts and pipes leading to and returning from the collector in a solar energy system can be significantly related to the length of the pipe, material property and insulation thickness. Length of pipe determined based on fig. 10.3.

10.2.1 Length of Intake Manifold

a) Length of Collectors Mudale in Array

There are 12 number of collector module in each array and the width of one collector module is ($W = 1.054m$).

Total length of collectors (L_c) is equal to:

$$L_c = Number\ of\ collector * Width \quad (10.3)$$

$$L_c = 10 * 1.054m = \mathbf{10.54m}$$

b) Length of Connection Pipes

There are 12 numbers of connectors between each collector's module inlet and pipe bend to intake manifold in the array and the length of one connector is ($L_{cn} = 0.1m$).

Total length of connectors (L_{cn}) is equal to:

$$L_{cn} = Number\ of\ connector * Length\ of\ connector$$

$$L_{cn} = 10 * 0.1m = \mathbf{1m}$$

c) Space Between Two Collector Module

There are 10 spaces between each collector's module edge and pipe bend to intake manifold in both collector array and the width of each space is ($W_{s1} = 0.05m$).

Total length of space (L_{s1}) is equal to:

$$L_{s1} = Number\ of\ space * Width\ of\ space$$

$$L_{s1} = 8 * 0.05m = \mathbf{0.4m}$$

d) Space Between Pipe Bend and Pipe Joint

There are 2 spaces between the joint of (intake manifold and supply pipe) and connector pipe in both collector array of a system and the width of each space is ($W_{s2} = 0.15m$).

Total length of space (L_{s2}) is equal to:

$$L_{s2} = Number\ of\ space * Width\ of\ space$$

$$L_{s2} = 2 * 0.15m = \mathbf{0.3m}$$

Therefore the total length of intake manifold (L_{im}) is:

$$L_{im} = L_c + L_{cn} + L_{s1} + L_{s1} \quad (10.4)$$

$$L_{im} = (10.54 + 1 + 0.4 + 0.3)m = \mathbf{12.24m} \approx \mathbf{12.5m}$$

10.2.2 Length of Return Manifold

Total length of space one (between each collector's edge and pipe bend to intake manifold) and space two (between the joint of intake manifold and supply pipe and connector pipe) is: $L_{s1} = 0.5m\ and\ L_{s2} = 0.3m$

a) Length of Collectors Module

There are 10 number of collector module in the length of return manifold pipe and the width of one collector is ($W = 1.054m$).

Total length of collectors (L_c) is equal to:

$$L_c = Number\ of\ collector * Width$$

$$L_c = 8 * 1.054m = \mathbf{8.432m}$$

b) Length Between Collector Inlet and Pipe Bend to Intake Manifold

There are 10 numbers of connectors between each collector's inlet and pipe bend to intake manifold and the length of one connector is ($L_{cn1} = 0.1m$).

Total length of connectors (L_{cn}) is equal to:

$$L_{cn} = Number\ of\ connector * Length\ of\ connector$$

$$L_{cn} = 8 * 0.1m = \mathbf{0.8m}$$

Therefore the total length of return manifold (L_{rm}) is:

$$L_{rm} = L_c + L_{cn} + L_{s1} + L_{s1}$$

$$L_{rm} = 8.432m + 0.8m + 0.4m + 0.3m = \mathbf{9.932m \approx 10m}$$

10.2.3 Distance Between Storage Tank and Collector Array

a) Length of Supply Pipe

Distance between two collector arrays, distance between the last collector module array and thermal storage tank, and length of connector (between two storage tank) is:

$D_{CA} = 5m, D_{CS} = 5m\ and\ L_{cns} = 2.5m$

Therefore total distance between storage tank and collector array inlet (supply pipe) is:

$$L_{SP} = (5 * D_{CA}) + D_{CS} + L_{cns}$$

$$L_{SP} = 5 * 5m + 5m + 2.5m = \mathbf{32.5m \approx 35m}$$

b) Length of Return Pipe

Distance between two collector arrays, distance between the last collector module array and thermal storage tank, length of connector one (return manifold and return pipe line) and length of connector two (between two storage tank) is:

$D_{CA} = 5m, D_{CS} = 5m, L_{cns1} = 0.8m\ and\ L_{cns2} = 2.5m$

Therefore total distance between storage tank and collector array inlet (supply pipe) is:

$$L_{RP} = D_{CA} + D_{CS} + L_{cns1} + L_{cns2}$$

$$L_{RP} = 5m + 5m + 0.8m + 2.5m = \mathbf{13.3m \approx 15m}$$

Table 10.1: Summery of Length of Pipes

Summary of Length of Pipes				
	Intake Manifold	**Return Manifold**	**Supply Pipe**	**Return Pipe**
Length	$\boldsymbol{L_{im} = 12.5m}$	$\boldsymbol{L_{rm} = 10m}$	$\boldsymbol{L_{sp} = 40m}$	$\boldsymbol{L_{rp} = 15m}$

10.3 Selection of Pump

Solar water heating systems are classified depending on how the domestic water is heated or how the heat transfer fluid (water or antifreeze fluid) flows through the collector. Factors that influence the selection of a specific system type include:

- The amount of water that needs to be heated,
- Relative cost and efficiency,
- Simplicity of operation, and
- Climate conditions in which the system will be used.

Based on the above factors an active water circulation system is selected to complete solar thermal water heating system components. Pumps are sized to overcome static and head pressure requirements in order to meet specific system design and performance flow rates. This requires a centrifugal pump or other pump that will provide adequate pressure. Most active solar systems use centrifugal pumps.

Pump selection depends on the following factors:

- System type (direct or indirect) and Heat collection fluid.
- Operating temperatures and Required fluid flow rates.
- Head or vertical lift requirements and Pressure drop due to friction losses.

The most common pump (circulator) used in solar systems is the "wet rotor" type in which the moving part of the pump, the rotor, is surrounded by liquid. The pump that circulates water through each collector is related based on the total pressure drop that occurs following the longest path to the farthest collector.

10.3.1 Total Pressure Drop

a) Pressure Drop in the Intake Manifold

Length of intake manifold is: $L_{im} = 12.5m$

Average volume flow rate through the manifold is:

$$\dot{Q}_{im} = Number\ of\ manifold * \frac{\dot{Q}_{cn}}{2}$$

$$\dot{Q}_{im} = 6 * \frac{(3.04 * 10^{-5}) m^3/S}{2} = \mathbf{9.12 * 10^{-5} m^3/s}$$

For 32 mm diameter pipe, area of intake manifold is:

$$A_{im} = \frac{\pi {D_{im}}^2}{4} = \frac{\pi * 0.032^2}{4} = \mathbf{8.043 * 10^{-4} m^2}$$

The average velocity of intake manifold is:

$$V_{avim} = \frac{\dot{Q}_{im}}{A_{im}}$$

$$V_{avim} = \frac{9.12 * 10^{-5} m^3/s}{8.043 * 10^{-4} m^2} = \mathbf{0.1134 m/s}$$

Reynolds number,

$$R_e = \frac{\rho V_{av} D}{\mu} = \frac{988 * 0.1134 * 0.032}{5.47 * 10^{-4}} = \mathbf{6555}$$

$R_e > 2300$, it is turbulent flow

For the tube material of galvanized steel the equivalent roughness is, ($\varepsilon = 0.15mm$).

$\frac{\varepsilon}{D} = \frac{0.00015}{0,032} = \mathbf{0.00469}$,

Therefore, from the Moody Chart or by using the explicit Haaland formula with the corresponding Reynolds number f = 0.041 (ANNEX D).

The pressure drops in the supply manifold is:

$$\Delta P_{ms} = f \frac{L}{D} \frac{\rho {V_{av}}^2}{2}$$

$$\Delta P_{ms} = 0.041 * \left(\frac{12.5}{0.032}\right) * \frac{988 * 0.1134^2}{2} = \mathbf{102 Pa}$$

b) Pressure Drop in the Return Manifold

Length, diameter and average velocity of return array manifold is:

$L_{rm} = 12.5m, D_{rm} = 0.032m \; and \; V_{avrm} = 0.1134m/s$

The pressure drops in the return manifold is:

$$\Delta P_{rm} = 0.041 * \left(\frac{10}{0.032}\right) * \frac{988 * 0.1134^2}{2} = \mathbf{81.4 Pa}$$

c) Pressure Drop in the Supply and Return Pipe Line

The total closed loop length will be:

$$L_{cl} = L_{sp} + L_{rp}.$$

$$L_{cl} = 35m + 15m = \mathbf{50m}$$

The total volume flow rate in the storage outlet and inlet pipes is:

$\dot{Q}_p = Number\ of\ collector * \dot{Q}_{cn}$

$\dot{Q}_p = 54 * (3.04 * 10^{-5}) m/s = \mathbf{1.642 * 10^{-3} m^3/s}$

For 51 mm diameter pipe, area of pipe lines is:

$$A_p = \frac{\pi {D_p}^2}{4} = \frac{\pi * 0.051^2}{4} = \mathbf{2.043 * 10^{-3} m^2}$$

The average velocity in pipe line is:

$$V_{avp} = \frac{\dot{Q}_p}{A_p}$$

$$V_{avp} = \frac{1.642 * 10^{-3} m^3/s}{2.043 * 10^{-3} m^2} = \mathbf{0.804 m/s}$$

Reynolds number,

$$R_e = \frac{\rho V_{avp} D_p}{\mu} = \frac{988 * 0.804 * 0.051}{5.47 * 10^{-4}} = \mathbf{74{,}062.07}$$

$R_e > 2300$, it is turbulent flow

For the tube material of galvanized steel the equivalent roughness is, ($\varepsilon = 0.15mm$).

$\frac{\varepsilon}{D} = \frac{0.00015m}{0.051m} = \mathbf{0.00294}$,

Therefore, from the Moody Chart or by using the explicit Haaland formula with the corresponding Reynolds number f = 0.021 (ANNEX D).

The pressure drops in the supply manifold is:

$$\Delta P_p = f \frac{L}{D} \frac{\rho {V_{avp}}^2}{2}$$

$$\Delta P_p = 0.021 * \left(\frac{50}{0.051}\right) * \frac{988 * 0.804^2}{2} = \mathbf{6574.43 Pa}$$

d) Pressure Drop Through the Collector

Pressure drop through a 20 collector is:

$\Delta P_c = 54 * 5.304Pa = \mathbf{286.42Pa}$

e) Pressure Drop due to the Inclination of the Collector to the Horizontal

The height of a single collector is:

$h_c = 0.85m$

Pressure drop due to the inclination of the collector to the horizontal is:

$\Delta P_h = \rho g h$ ---------- (10.5)

$\Delta P_h = 988 * 9.81 * 0.85 = \mathbf{8238.44Pa}$

f) Pressure Drop in the Bend

Based on the layout there are 6 bends:

Pressure loss in bends,

$$\Delta P_b = K_f \frac{\rho V_1^{\,2}}{2}$$

Where: K_f = pressure loss factor

V_1 = average velocity in the tube up stream of the fitting.

For 90º standard elbow, $K_f = 0.9$

$$\Delta P_b = 6 * (0.9) \frac{988 * 0.242^2}{2} = \mathbf{156.24Pa}$$

g) Total Pressure Drop in the System

Total pumping pressure needed for design is the sum of all the above pressure drops.

$\Delta P_{total} = \Delta P_{sm} + \Delta P_{rm} + \Delta P_p + \Delta P_c + \Delta P_h + \Delta P_b$

$\Delta P_{total} = (102 + 81.4 + 6574.43 + 286.42 + 8238.44 + 156.24)Pa = \mathbf{15,439Pa}$

i) Total Specific Work

Total pressure drop is:

$\Delta P_{total} = 15{,}439Pa$

Therefore total specific work is given by:

$Y = \frac{\Delta P_{total}}{\rho} = \frac{15{,}439Pa}{988} = \mathbf{15.63m^2/s^2}$

ii) Total Head

Total Specific Work is ($Y = 15.63 m^2/s^2$); therefore total head is:

$$H = \frac{Y}{g} = \frac{15.63}{9.81} = \mathbf{1.593m \approx 2m}$$

iii) Total Volume Flow Rate for the Pump

Volume flow rate of a collector is ($\dot{Q}_c = (3.04 * 10^{-5}) m^3/s$)

The total volume flow rate for the pump is:

$$\dot{Q} = 10 * \dot{Q}_c = 10 * (3.04 * 10^{-5}) m^3/s = (3.04 * 10^{-4}) m^3/s = \mathbf{1.095 m^3/h}$$

The proper centrifugal electric drive pump satisfying the requirement of Head = 2 m and flow rate = 1.095 m3/ h are:

Table 10.2: Specification of Selected Pump

Specification of Selected Pump			
Type	**Electric Drive Pump**	**The proper motor data**	
Model	MEC-A 1/40A	Frequency	50 Hz
Normal Speed	1450 rpm	Rated Voltage	400 V
Shaft Power	0.39 KW	Rated power	0.55 KW
Efficiency	42.3 %	Motor Type	3~

10.4 Control Element

10.4.1 Pump Control

The use of pump in thermal collection system increases the efficiency of the system. However the operation of the pump should be designed only when solar collection is feasible. To determine whether solar collection is feasible or not, measuring collector temperature and comparing it with the storage tank bottom temperature is necessary. If the energy obtained from solar collection is not relatively greater than the pumping cost, the pump should be off until sufficient energy is obtained, and on elsewhere. This can be done by the use of differential controller.

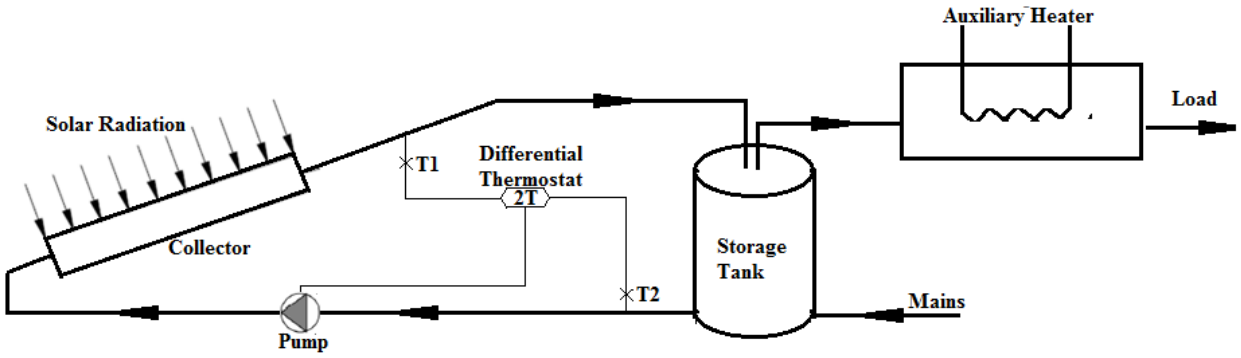

Figure 10.4: Positioning of Differential Controller

For this case the use of a differential thermostat fulfills the requirement. A thermostat whose electrical resistance varies with temperature messages the differential temperature at a two specified points. The differential thermostat which is preset for maximum and minimum temperature difference closes or opens the electric pump circuit.

For this model one end of the thermistor sensors is placed at the bottom of the storage tank and the other end at the collector outlet pipe and set to start the pump when the water outlet temperature is 5ºc hotter than the storage medium. The pump will stop its operation when the temperature difference is below 1ºc. In order to avoid continuous off and on operation of the pump, 1 – 3 minutes delay increases the life of the motor.

10.4.2 Drain Valve and Vacuum Air Vent

Maintenance and avoidance of freezing in cold weather require a water draining system at each collector. A drain valve is installed to fulfill this purpose at the entrance of a collector. For the proper function of the drain valve a vacuum air vent is provided at the headers of the arrays of collectors.

10.4.3 Pressure Relief Valve

A pressure relief valve is a valve used in liquid systems that opens whenever the pressure in the system is greater than some safe maximum. It guards against destructive pressures that could build up if the system is overheated. The design is based on a spring action for a maximum pressure of 3 bars.

10.4.4 Air Vent

The amount of air which can be contained in water decreases with the temperature of the water. Therefore, a large amount air from the water may develop a higher pressure in the storage tank

and the pipes. Therefore this air should be vented through an air vent. Air vent designed at the header and top of the storage tank is in coincidence with a lighter density of air.

10.4.5 Check Valves

Check valves allow fluid to flow in only one direction. In solar systems, these valves prevent thermosiphoning action in the system plumbing. Without a check valve, water that cools in the elevated collector at night will fall by gravity to the storage tank, displacing lighter, warmer water out of the storage tank and up to the collector. Once begun, this thermosiphoning action can continue all night, continuously cooling all the water in the tank.

Corrosion and scale may build up on the internal components of a check valve; therefore, a regular service schedule should be maintained.

CHAPTER 11

FINANCIAL ANALYSIS

Economics play a central role in any customer's decision to purchase a solar water heater system. The customer, or a corporation, is unlikely to buy a solar energy system if they know that its only benefits are to the environment. Obviously, any company considering solar power generation is going to look very carefully at economics to ensure that such a project will be profitable to them.

Solar processes are generally characterized by high first cost and low operating costs. Thus the basic economic problem is one of comparing an initial known investment with estimated future operating costs. The cost of any energy delivery process includes all of the items of hardware and labor that are involved in installing the equipment plus the operating expenses. Factors which may need to be taken into account include interest on money borrowed, property and income taxes, resale of equipment, maintenance, insurance, fuel, and other operating expenses [5].

In this chapter we note several ways of doing economic evaluations, with emphasis on the life cycle savings method. This method takes into account the time value of money and allows detailed consideration of the complete range of costs. It is introduced by an outline of cost considerations, note of economic figures of merit (design criteria), and comments on design variables which are important in determining system economics.

11.1 Costs of Solar Process Systems

Investments in buying and installing solar energy equipment are important factors in solar process economics. These include the delivered price of equipment such as collectors, storage unit, pumps and controls, pipes and ducts, and all other equipment associated with the solar installation.

Table 11.1: Price for Solar Water Heating System

Cost of Solar Water Heating System				
No	**Item**	**Specification**	**Unit Price [birr]**	**Total Price [birr]**
1	**Collector**	1m*2m flat plat		
	Tube of riser and	Riser (t=1mm, Dr=15mm and L=1.9m)	204.25	44,118

	header	Header (t=1mm, Dh=24mm and L=0.736m) Both copper material (L=6m)	270	58,320
	Plate material	Chrome coated Copper (t=0.4mm, L=1m and W=1m)	451.5	97,524
	Glass material	Low iron timbered (t=4mm, L=2m and W=1m)	844	182,304
	Insulation	Rockwool (t=40mm, L=2m and W=1m)	95	20,520
	Casing	Aluminium for 2m2 collector and t=4mm	471.75	101,898
	Sealing	Silicone for 2m2 collector	43.2	9331.2
	Manufacturing	50% of Material Cost	1,189.85	257,007.6
	Total cost	Total cost of collector	**3569**	**770,904**
2	**Storage tank**	Cylindrical		
	Inside material	2mm Thick Sheet Steel	250	3927.5
	Insulation	Glass Fiber (t = 15 mm W = 1m, L=2m)	1653	25,968.63
	Insulation cover	0.8 mm Thick Galvanized Pre Painted Steel (1m*1m)	150	2356.5
	Manufacturing	25% of Material Cost	514.5	8082.8
	Total cost	Total storage tank cost	**2572.5**	**40,335.5**
3	**Piping Material**	L=6m		
		1" Galvanized Steel	143	2,145
		1 1/2" Galvanized Steel	230	8,625
		2" Galvanized Steel	345	7762.5
	Total cost	Total pipe line cost	**718**	**18,532.5**
4	**Elbows and Fittings**	1 " Elbows, Tees 1 1/2" Elbows, Tees 2 " Elbows, Tees	4 7 16	160 280 192
	Total cost	Total elbow and fitting cost	**27**	**632**
5	**Pump (Electric Drive)**	MEC-A 1/40A (with full accessories)	**11600**	**23,200**
6	**Supporting**	Aluminium (6m and t=5mm) L-shape	**3,225**	**16,125**

	Structure	frame		
7	**Controlling system**	Drain, pressure relief and check valves, vacuum and air vent, and pump control.	**4,300**	**21,500**
8	**Labor and Installation Cost**	15 % of Collector Cost	**535.35**	**115,635.6**

11.2 Operating, Maintenance and Replacement Cost

Operating costs are associated with a solar process. These continuing costs include cost of auxiliary energy, energy costs for operation of pumps and others often termed parasitic energy, which should be minimized by careful design [5].

Repair and replacement costs are so central to the success of solar water heating. On the other hand they are difficult to obtain. It has to be mentioned that the replacement and repair cost depends on the manufacturer and the type of the system used. The reason for this is the best approximation of the life cycle costing.

a) Pumps

Pumps are the solar water heater components most frequently replaced. Various companies working with solar water heaters recommend that the average age of pumps replaced varies between 5-10 years.

The most common reasons causing a pump failure according to various researches are:

- Plumping leaks, affecting pump and electrical.
- Air in the pump (cavitation).
- Overheating which is a product of poor system design, such as undersize pump or improper collector area to storage volume ratio.

b) Controls

According to controllers manufacturing company's information most controls are a matter of replacement. It could be possible to have the electronic circuit repaired but that happens very rarely. A large part of the repairs involving simple controls had to do with sensors (thermo resistors) replacement and not the control itself. Actual control failures were rather uncommon.

So replacement of thermostats is quite cheap and reasonable and would not cost much.

c) Collectors

In terms of lifetime and replacement this is the most difficult section solar water heating system component to evaluate. From the various companies manufacturing solar collectors just a few of them were notable to give an exact average replacement age. Most of them certified that the solar collectors would last for at least 20-25 years.

d) Storage Tanks

Various companies recommend the average age of tanks replacement varies between 10-15 years.

Table 11.2: Operating, Maintenance and Replacement Cost

No	Item	Specification	Unit Price [birr]	Total Price [birr]
1	Operating Cost (Maintenance & Pumping Cost)	10% of system Cost	**2655**	**100,685**

11.3 Investment cost

Investments in buying and installing solar energy equipment are important factors in solar process economics. These include the delivered price of equipment such as collectors, storage unit, pumps and blowers, controls, pipes and ducts, heat exchangers, and all other equipment associated with the solar installation [7].

Installed costs of solar equipment can be shown as the sum of two terms, one proportional to collector area and the other independent of collector area:

$$CI = C_A A_C + C_E \quad (11.1)$$

Where CI = total cost of installed solar energy equipment

C_A = total area-dependent costs (cost/m^2)

A_C = collector area (m^2)

C_E = total cost of equipment which is independent of collector area

$$CI = (3569 * 216) + 235{,}960.6 = \mathbf{1{,}006{,}865\ Birr}$$

11.4 Economic Analysis

11.4.1 Economic Analysis Parameters

Life time of the investment is 20 years; most of them certified that the solar collectors would last for at least 20-25 years.

Table 11.3: Economic Analysis Parameters

Parameters	Value
Inflation Rate	10%
Discount Rate	10%
Salvage Rate	10%
Debt Ratio	50%
Debt Interest Rate	8.5%
Loan Period	10 year
Rate of Energy Escalation	15%
Cost of Electricity	0.46Birr/KWh

11.4.2 Life Cycle Cost

The life cycle cost includes investment capital and present worth of operating cost during the useful life of the plant. The operating cost of solar water heating system is mainly the maintenance and pumping cost. The life cycle cost of solar water heating system is determined from the investment cost and the present value of maintenance and pumping cost distributed over the life as follows [10, 13].

$$LCC = CI + C_m \frac{1}{i}\left(1 - \frac{1}{(1+i)^n}\right) \quad (11.2)$$

Where: CI = is the investment cost of solar water heating system, and

C_m = is annual maintenance and pumping cost.

n = is the years of economic analysis

Therefore the life cycle cost of solar water heating system of the project is:

$$LCC = 1{,}006{,}865 + \left[100{,}685 * \left(\frac{1}{0.1} * \left(1 - \frac{1}{(1+0.1)^{20}}\right)\right)\right]$$

$$LCC = \mathbf{1,864,054}\boldsymbol{Birr}$$

11.4.3 Life Cycle Saving of Energy

The life cycle saving of solar water heater is the energy cost saved due to replacement of electricity by solar [10].

The annual energy saving is,

$$ES = f_a Q_a \quad (11.3)$$

The life cycle saving of energy:

$$LCS = P_e f_a Q_a \left(\frac{1+i_e}{i-i_e}\right)\left[1-\left(\frac{1+i_e}{1+i}\right)^n\right] \quad (11.4)$$

Where: - LCS is the life cycle saving of a solar water heating system [kWh]

- f_a is annual fraction of load supplied by solar energy
- Q_a is the annual heating load [kWh].
- i is the annual market discount rate.
- i_e is the annual market rate of energy escalation, and

11.4.4 Unit price of Solar Energy

To determine the unit price of solar energy cost, P_e the life cycle cost has to be equal to the life cycle savings of the solar water heater during its life time [10].

To determine the unit price:

$$LCS = LCC \quad (11.5)$$

By substituting equation (11.2) and (11.4) into equation (11.5), (P_e) determined as follows:

$$CI + C_m \frac{1}{i}\left(1-\frac{1}{(1+i)^n}\right) = P_e f_a Q_a \left(\frac{1+i_e}{i-i_e}\right)\left[1-\left(\frac{1+i_e}{1+i}\right)^n\right]$$

The unit price of solar energy for water heating is:

$$P_e = \frac{CI + C_m \frac{1}{i}\left(1-\frac{1}{(1+i)^n}\right)}{f_a Q_a \left(\frac{1+i_e}{i-i_e}\right)\left[1-\left(\frac{1+i_e}{1+i}\right)^n\right]} \quad (11.6)$$

Therefore the unit price of solar energy for water heating is equals to:

$$P_e = \mathbf{0.033}\boldsymbol{Birr/KWh}$$

If solar energy has to be economically viable, the unit cost of water heating system must be less than that of other alternatives [10].

Therefore the life cycle saving of energy is equals to:

$$LCS = \mathbf{1,869,571}$$

11.5 Payback Period

To determine the pay-back period, the maintenance cost is neglected. Hence the investment of the solar water heater has to be pay-backed by the life cycle saving of electric cost [10, 13].

$$LCCS = C_f f_a Q_a \left(\frac{1+i_e}{i-i_e}\right)\left[1-\left(\frac{1+i_e}{1+i}\right)^n\right] \quad (11.7)$$

Where: $LCCS = CI \qquad at\ n = N_p$

$$C_f f_a Q_a \left(\frac{1+i_e}{i-i_e}\right)\left[1-\left(\frac{1+i_e}{1+i}\right)^{N_p}\right] = CI$$

$$N_p = \frac{ln\left[1+\frac{CI\left(\frac{i_e-i}{1+i_e}\right)}{C_f f_a Q_a}\right]}{ln\left[\frac{1+i_e}{1+i}\right]} \quad (11.8)$$

Where: - $LCCS$ is the life cycle saving of electric cost [Birr]

- C_f is the unit cost of electricity for the first year of analysis [Birr / kWh].

Therefore the pay-back period is equals to:

$$N_p = \mathbf{2.2Year}$$

Table 11.4: Financial Analysis Summary

Cost Summary of the Project				
Total Initial Cost of SWHS [Birr]	**Total life cycle cost of SWHS [Birr]**	**Unit Cost of Solar Energy [Birr/kWh]**	**Unit Cost of Electricity [Birr/kWh]**	**Pay Back Period [Years]**
1,006,865	**1,864,054**	**0.033**	**0.46**	**2.2**

CHAPTER 12

CONCLUSIONS AND RECOMMENDATIONS

12.1 Conclusion

This project presents design and analysis of solar thermal system for Hot water supply to Minilik II hospital new building. To achieve the objective of the study different approaches are performed.

A detailed mathematical derivation for the flat-plate solar collector cross sections (glass cover, absorber plate, water stream, and thermal storage tank) was presented. A one dimensional mathematical model with distributed parameters that combines the solar collector's tank model and the flat-plat model is derived to simulate the collector process. All the thermo-physical properties of the water stream and the storage tank are computed in time dependent mode. The transient heat transfer coefficients are also computed in real time.

To solve the derived system of equations, the implicit finite-difference scheme was suggested. The proposed method allows the transient processes occur in the flat-plate solar collector to be simulated. The time dependent flow rate, variable ambient temperature, and variable solar irradiance have been taken in consideration. The proposed solution method was implemented by utilizing the MATLAB software. The code mathematically solves the model and iteratively evaluates the temperature histories for each analyzed cross section of the solar collector at any selected point along the flow direction.

It was found that for Minilik II hospital of total daily hot water consumption of 30.475 m^3, a total of 108 collectors with two storage tanks of each capacity 18.3 m^3 are needed with initial capital cost of 1,006,865 Birr per project, which will cost a total of 1,864,054 Birr per project through-out its life time and the life cycle cost saving will be 1,869,571 Birr per project. The unit price of solar thermal energy is 0.033 Birr per KWh and the payback period of the project is 2.2 year.

Since the unit cost of solar energy (0.033 Birr/KWh) is less than the unit cost of electricity (0.46 Birr/KWh) in Ethiopia, therefore water heating by solar energy is a viable alternative to heating by electricity and fossil fuel (furnace oil).

12.2 Recommendation

The following points can be recommended for the future work.

- More experimental investigations are needed to confirm the performance and efficiency of the proposed model, by testing the code for different cases.
- The same work can also be done using parabolic trough collectors or vacuum tube collectors system.
- Parametric studies can be done using the flat-plate, vacuum tube or concentric type solar collectors.
- Optimizing of the solar thermal system.
- Use of insulated pipe line for the collector to minimize the approximation error in the ambient-pipe free convection coefficient.
- Improving the running time of the code by using the inner product function instead of the loops.

REFERENCE

1. "**Solar Thermal Combined Heat and Power Project at the Energy Resource Center**", Southern California Gas Company, August 2014.
2. "**Solar Thermal Systems: Solar Heating R&D**", U.S. Department of Energy Solar Energy Technologies
3. Maxi Brochure 05: "**Energy Efficiency in Hospitals**", December 2015.
4. **Ministry of water and Energy, Ethiopian national energy policy,** (2nd draft), Ethiopia Addis Ababa, 2013, February.
5. Duffie, J. A. and Beckman W. A. (1991): **Solar Engineering of Thermal Processes.** 4th edition, J. Wiley and Sons, New York.
6. Christopher A. Homola, PE: **Solar Domestic Hot Water Heating Systems Design, Installation and Maintenance.**
7. Dimitrios Panapakidis: **Solar Water Heating Systems Study Reliability, Quantitative Survey and Life Cycle Cost Method**, MSc. thesis, Department of Mechanical eng., University of Strathclyde in Glasgow.
8. John R. Howell, Richard B. Bannerot, Grary C. Vliet: **Solar Thermal Energy System**, USA, 1982.
9. RAI, G.D.: **Solar Energy Utilization**, fifth edition, Delhi, 2001.
10. Demiss Alemu: **Optimal Design of Solar Water Heating System**, Zede, No.15, Addis Ababa, 1998.
11. Vonal.com (**Manufacturer of Flat-Plate Solar Collectors in Ethiopia**).
12. Yunus A. Cengel: **Heat Transfer an Engineering Approach**, 5th edition.
13. Collares-Pereira, Gordan, J. M., Rabi and Zarmi, Y.: **Design and Optimization of Solar Industrial Hot Water System**, Solar Energy, Vol. 32, 1984.
14. Abebayehu Assefa and Demiss Alemu : **The Viability of Solar Energy for Domestic Water Heating in Ethiopian Cities**, Zede, No.9, Addis Ababa, 1992.
15. **Alternative Energy Sources (AES):** ''solar heating'' (accessed: 09-02-2011) www.hk-phy.org/energy/alternate/.../act_water_heating_e.htm. (2008),
16. ASHRAE (1995): ''**Handbook of Heating and Ventilation of Air Conditioning Applications**", Atlanta.

17. Benz N, Gut M, and Rub W.: **Solar process heat in breweries and dairies**, Portoroz, Slovenia: Eurosun 1998; 1998.

18. Brandemuehl, M.J. and Beckman, W.A.: **Economic Evaluation and Optimization of Solar Water heating Systems**, Solar Energy, Vol. 23, No. 1, 1979.

19. Fisch, M.N., Guigas, M. and Dalenback, J.O.: **A Review of Large-Scale Solar Heating System in Europe**, Solar Energy, Vol. 63, No. 6, pp. 355-366, 1998.

20. Hottel, H.C. and Woertz, B.B.: **Performance of Flat-Plate Solar-Heat Collectors**, Trans. ASME, 64, 91 (1942).

21. **''International Journal of Climatology'',** 26: 75–89 (2006), Published online 7 November 2005 in Wiley Inter Science (www.interscience.wiley.com).

22. **"Introduction to Solar Thermal"**, Sun Water Solar.

23. Kalogirou S. A. (2003): **The potential of solar industrial process heat applications". Application Energy**, pp76:337–61.

24. Lex Bosselaar and He Zinian: **"Integration of Solar Water Heating into Residential Building",** September 2014.

25. Sodha, M.S., Tiwari, G.N., Sawhney, R.L., Sharma, A.K., Singh, A.K. and Goya, R.K.: **Sizing of a Multi-Tank Solar Water Heater**, Int. J. Energy Res., 22, 777 - 790 (1998), India.

26. "**The Potential of Solar Heat in the Future Energy System**" Faculty for Interdisciplinary Research and Continuing Education, IFF-University of Klagenfurt, Austria(E-mail: gerhard.faninger@uni -klu.ac.at)

27. Tsilingiris, P.T.: **Solar Water-Heating Design – A New Simplified Dynamic Approach**, Solar Energy, Vol. 57, No. 1 pp. 19-28,1996.

APPENDIX

ANNEX A: MATLAB PROGRAM CODE

ANNEX (A-1): Mass flow rate

```
%%%%%%%%%%%%%%%%%%%%%%%%%%%%%%%%%%%%%%%%%%%%%%%%%%%%%%%%%%%%%%%%%%%%%%%%%%%%%%%%
% Variation of Collector Efficiency with Mass Flow Rate
% Steady State Analysis
% Input Parameters
cp=4200;            % Specific Heat Capacity of Water at 60oC [J/Kg.k]
To=340;             % Outlet Water Temperature [K]
Ti=293;             % Inlet Water Temperature [K]
I=700;              % Incident Solar Radiation [W/m2]
Ac=1;               % Area of Collector [m2]
eff1=0.5;           % Collector Efficiency
%%%%%%%%%%%%%%%%%%%%%%%%%%%%%%%%%%%%%%%%%%%%%%%%%%%%%%%%%%%%%%%%%%%%%%%%%%%%%%%%
mf=(0.009:0.001:0.03);          % Input Data of Mass Flow Rate
%%%%%%%%%%%%%%%%%%%%%%%%%%%%%%%%%%%%%%%%%%%%%%%%%%%%%%%%%%%%%%%%%%%%%%%%%%%%%%%%
% efficiency and outlet water temperature
eff=((mf*cp*(To-Ti))/(I*Ac))*100;
Two=((eff1*I*(Ac))./(mf*cp))+Ti;
Two1=Two-273;
mf=(0.009:0.001:0.03);
plot(mf,eff,'r',mf,Two1,'-','linewidth',3)
   xlabel('Mass Flow Rate','fontsize',20)
   ylabel('Efficiency and Temperature','fontsize',20)
   title('Variation of Eff and Two with Mass Flow Rate','fontsize',20)
   legend('eff','Two')
   grid on
   pause
   clf
```

ANNEX (A-2): Plate Thickness

```
%%%%%%%%%%%%%%%%%%%%%%%%%%%%%%%%%%%%%%%%%%%%%%%%%%%%%%%%%%%%%%%%%%%%%%%%%%%%%%%%
% Variation of Collector Efficiency with Absorber Plate Thickness
% Steady State Analysis
% Input Parameters
Gt=0.94;            % Transmittance of Glass Cover
Pa=0.95;            % Absorbance of Absorber Plate
UL=6;               % Overall Heat Transfer Coefficient [W/K.m2]
Ac=1;               % Collector Area [m2]
I=745.3;            % Average Daily Solar Radiation [W/m2]
To=333;             % Outlet Water Temperature [K]
Ta=293;             % Inlet Water Temperature [K]
mf=0.03;            % Mass Flow Rate [Kg/s]
cp=4200;            % Specific Heating Capacity of Water at 60oC [J/Kg.m]
W=0.0756;           % Space Between Riser Tube [m]
```

```
Di=0.015;           % Inner Diameter of Riser Tube [m]
Do=Di+0.001;        % Outer Diameter of Riser Tube [m]
hfi=1500;           % Heat Transfer Coefficient Inside the Tube [W/oC.m2]
k=401;              % Thermal Conductivity of Plate [J/K.m]
%Plate Thickness Data Input
load pla.m;
data1=zeros(24,1,5);
for j=1:5
    data1(:,:,j)=pla(j+(23*(j-1)):j*24,:);
end
%%%%%%%%%%%%%%%%%%%%%%%%%%%%%%%%%%%%%%%%%%%%%%%%%%%%%%%%%%%%%%%%%%%%%%%%%%%%
Eff1=zeros(24,5);
% main program
for i=1:5
    t=data1(:,1,i);
for j=1:24
    tp=t(j);
    m=sqrt(UL./(k*tp));
    F=(tanh(m*((W-Do)/2)))/(m*((W-Do)/2));
    F2=(1/UL)/(W*((1./(UL*(Do+((W-Do)*F))))+(1/(pi*hfi*Di))));
    FR=((mf*cp)/(Ac*UL))*(1-(exp((-Ac*UL*F2)/(mf*cp))));
    Eff=(FR*Gt*Pa)-((UL*FR*(To-Ta))/(Ac*I));
    % Efficiency stored as;
    Eff1(j,i)=Eff*100;
end
end
% store
    Eff11=Eff1(:,1);
    j=1:24;
plot(j,Eff11,'k','linewidth',3)
   xlabel('Plate Thickness (mm)','fontsize',16)
   ylabel('Efficiency','fontsize',16)
   title('Variation of Efficiency with Plate Thickness','fontsize',16)
   legend('Eff')
   grid on
   pause
   clf
```

ANNEX (A-3): Riser Tube Inner Diameter

```
%%%%%%%%%%%%%%%%%%%%%%%%%%%%%%%%%%%%%%%%%%%%%%%%%%%%%%%%%%%%%%%%%%%%%%%%%%%%
% Efficiency, Pressure Drop and Velocity with Header Tube Diameter
% Steady State Analysis
% Input Parameters
Gt=0.94;              % Transmittance of Glass Cover
Pa=0.95;              % Absorbance of Plate
UL=6;                 % Overall All Heat Transfer Coefficient [W/K.m2]
Ac=1;                 % Collector Area [m2]
I=745.3;              % Average Daily Solar Radiation [W/m2]
To=333;               % Outlet Water Temperature [K]
```

```
Ta=293;                % Inlet Water Temperature [K]
mf=0.03;               % Mass Flow Rate [Kg/s]
cp=4200;               % Specific Heating Capacity of Water at 60oC [J/Kg.m]
tp=0.0004;             % Plate Thickness [m]
Wdens=988;             % Density of Water at 60oC [Kg/m3]
mu=5.47e-4;            % Dynamic Viscosity of Water at 60oC [m2/s]
L=1.8;                 % Length of Riser Tube [m]
hfi=1500;              % Heat Transfer Coefficient Inside the Tube [W/oC.m2]
k=401;                 % Thermal Conductivity of Plate [J/K.m]
N1=10;                 % Number of Riser Tube
% Inner Diameter of Riser Tube data input
load nrt.m;
data1=zeros(15,1,1);
for j=1
    data1(:,:,j)=nrt(j+(14*(j-1)):j*15,:);
end
%%%%%%%%%%%%%%%%%%%%%%%%%%%%%%%%%%%%%%%%%%%%%%%%%%%%%%%%%%%%%%%%%%%%%%%%%%%%%%%
Eff1=zeros(15,1);
Pr1=zeros(15,1);
Vavr1=zeros(15,1);
% main program
for i=1
    D=data1(:,1,i);
for j=1:15
    Di=D(j);
    Do=Di1+0.001;
    W=(0.81-Do)/9;
    Ar=(pi*(Di1^2))/4;
    Vfr=(mf/Wdens)/N;
    Vavr=Vfr/Ar;
    Re=(Wdens*Vavr*Di1)/mu;
    f=64/Re;
    Pr=f*(L/Di1)*((Wdens*(Vavr^2))/2);
    m=sqrt(UL./(k*tp));
    F=(tanh(m*((W-Do)/2)))/(m*((W-Do)/2));
    F2=(1/UL)/(W*((1./(UL*(Do+((W-Do)*F))))+(1./(pi*hfi*Di1))));
    FR=((mf*cp)/(Ac*UL))*(1-(exp((-Ac*UL*F2)/(mf*cp))));
    Eff=(FR*Gt*Pa)-((UL*FR*(To-Ta))/(Ac*I));
    % Efficiency stored as;
    Eff1(j,i)=Eff*100;
    Pr1(j,i)=Pr;
    Vavr1(j,i)=Vavr*10000;
end
end
% store
    Eff11=Eff1(:,1);
    Pr11=Pr1(:,1);
    Vavr11=Vavr1(:,1);
   j=1:15;
```

```
plot(j,Eff11,'k','linewidth',3)
   xlabel(''Inner Diameter of Riser Tube','fontsize',16)
   ylabel('Efficiency','fontsize',16)
   title('Efficiency with 'Inner Diameter of Riser Tube','fontsize',16)
   legend('Eff')
   grid on
   pause
   clf
plot(j,Pr11,'k',j,Vavr11,'-*','linewidth',3)
   xlabel('Inner Diameter of Riser Tube','fontsize',16)
   ylabel('Pressure Drop and Velocity','fontsize',16)
   title('Pr and Vavr with 'Inner Diameter of Riser Tube','fontsize',16)
   legend('Pr','Vavr')
   grid on
   pause
   clf
```

ANNEX (A-4): Riser Tube Outer Diameter

```
%%%%%%%%%%%%%%%%%%%%%%%%%%%%%%%%%%%%%%%%%%%%%%%%%%%%%%%%%%%%%%%%%%%%%%%%%%%%%%%
% Variation of Efficiency with Riser Tube Outer Diameter
% Steady State Analysis
% Input Parameters
Gt=0.94;              % Transmittance of Glass Cover
Pa=0.95;              % Absorbance of Plate
UL=6;                 % Overall All Heat Transfer Coefficient [W/K.m2]
Ac=1;                 % Collector Area [m2]
I=745.3;              % Average Daily Solar Radiation [W/m2]
To=333;               % Outlet Water Temperature [K]
Ta=293;               % Inlet Water Temperature [K]
mf=0.03;              % Mass Flow Rate [Kg/s]
cp=4200;              % Specific Heating Capacity of Water at 60oC [J/Kg.m]
tp=0.0004;            % Plate Thickness [m]
Wdens=988;            % Density of Water at 60oC [Kg/m3]
mu=5.47e-4;           % Dynamic Viscosity of Water at 60oC [m2/s]
L=1.8;                % Length of Riser Tube [m]
hfi=1500;             % Heat Transfer Coefficient Inside the Tube [W/oC.m2]
k=401;                % Thermal Conductivity of Plate [J/K.m]
N1=10;                % Number of Riser Tube
Di1=0.015;            % Inner Diameter of Riser Tube [m]
% Riser Outer Diameter data input
load ORTD.m;
data1=zeros(19,1,1);
for j=1
    data1(:,:,j)=ORTD(j+(18*(j-1)):j*19,:);
end
%%%%%%%%%%%%%%%%%%%%%%%%%%%%%%%%%%%%%%%%%%%%%%%%%%%%%%%%%%%%%%%%%%%%%%%%%%%%%%%
Eff1=zeros(19,1);
% main program
for i=1
```

```
    D=data1(:,1,i);
for j=1:19
    Do=D(j);
    W=(0.81-Do)/9;
    m=sqrt(UL./(k*tp));
    F=(tanh(m*((W-Do)/2)))/(m*((W-Do)/2));
    F2=(1/UL)/(W*((1./(UL*(Do+((W-Do)*F))))+(1./(pi*hfi*Di1))));
    FR=((mf*cp)/(Ac*UL))*(1-(exp((-Ac*UL*F2)/(mf*cp))));
    Eff=(FR*Gt*Pa)-((UL*FR*(To-Ta))/(Ac*I));
    % Efficiency stored as;
    Eff1(j,i)=Eff*100;
end
end
% store
    Eff11=Eff1(:,1);
   j=1:19;
plot(j,Eff11,'k','linewidth',3)
   xlabel('Outer Diameter of Riser (mm)','fontsize',16)
   ylabel('Efficiency','fontsize',16)
   title('Efficiency with Outer Diameter of Riser','fontsize',16)
   legend('Eff')
   grid on
   pause
   clf
```

ANNEX (A-5): Number of Riser Tube

```
%%%%%%%%%%%%%%%%%%%%%%%%%%%%%%%%%%%%%%%%%%%%%%%%%%%%%%%%%%%%%%%%%%%%%%%%%%%
% Variation of Pressure Drop and Velocity with Number of Riser Tube
% Stady State Analysis
% Input Parameters
mf=0.03;              % Mass Flow Rate [Kg/s]
Wdens=988;            % Density of Water at 60oC [Kg/m3]
mu=5.47e-4;           % Dynamic Vescociyt of Water at 60oC [m2/s]
L=0.736;              % Length of Header Tube [m]
N1=10;                % Number of Riser Tube
Di=0.015;             % Inner Diameter of Riser Tube [m]
%Number of Riser Tube data input
load nrt.m;
data1=zeros(15,1,1);
for j=1
    data1(:,:,j)=nrt(j+(14*(j-1)):j*15,:);
end
%%%%%%%%%%%%%%%%%%%%%%%%%%%%%%%%%%%%%%%%%%%%%%%%%%%%%%%%%%%%%%%%%%%%%%%%%%%
Pr1=zeros(15,1);
Vavr1=zeros(15,1);
% main program
for i=1
    n=data1(:,1,i);
for j=1:15
```

```
    N=n(j);
    Ar=(pi*(Di^2))/4;
    Vfr=(mf/Wdens)/N;
    Vavr=Vfr/Ar;
    Re=(Wdens*Vavr*Di1)/mu;
    f=64/Re;
    Pr=f*(L/Di1)*((Wdens*(Vavr^2))/2);
    % Pressure Drop and Velocity stored as;
    Pr1(j,i)=Pr;
    Vavr1(j,i)=Vavr*10000;
end
end
% store
    Pr11=Pr1(:,1);
    Vavr11=Vavr1(:,1);
   j=1:15;
plot(j,Pr11,'k',j,Vavr11,'-*','linewidth',3)
   xlabel('Number of Riser Tube','fontsize',16)
   ylabel('Pressure Drop and Velocity','fontsize',16)
   title('Pr and Vavr with Number of Riser Tube','fontsize',16)
   legend('Pr','Vavr')
   grid on
   pause
   clf
```

ANNEX (A-6): Header Tube Diameter

```
%%%%%%%%%%%%%%%%%%%%%%%%%%%%%%%%%%%%%%%%%%%%%%%%%%%%%%%%%%%%%%%%%%%%%%%%%%%%%%%
% Variation of Pressure Drop and Velocity with Header Tube Diameter
% Steady State Analysis
% Input Parameters
mf=0.03;           % Mass Flow Rate [Kg/s]
Wdens=988;         % Density of Water at 60oC [Kg/m3]
mu=5.47e-4;        % Dynamic Viscosity of Water at 60oC [m2/s]
L=0.736;            % Length of Header Tube [m]
%Header Tube data input
load head.m;
data1=zeros(24,1,2);
for j=1:2
    data1(:,:,j)=head(j+(23*(j-1)):j*24,:);
end
%%%%%%%%%%%%%%%%%%%%%%%%%%%%%%%%%%%%%%%%%%%%%%%%%%%%%%%%%%%%%%%%%%%%%%%%%%%%%%%
Ph1=zeros(24,2);
Vavh1=zeros(24,2);
% main program
for i=1:2
    Dhh=data1(:,1,i);
for j=1:24
    Dh=Dhh(j);
    Ah=(pi*(Dh^2))/4;
```

```
    Vfh=(mf/Wdens)/2;
    Vavh=Vfh/Ah;
    Re=(Wdens*Vavh*Dh)/mu;
    f=64/Re;
    Ph=f*(L/Dh)*((Wdens*(Vavh^2))/2);
    % Header Diameter, Velocity and Pressure Drop stored as;
    Ph1(j,i)=Ph;
    Vavh1(j,i)=Vavh*10;
end
end
% store
    Ph11=Ph1(:,1);
    Vavh11=Vavh1(:,1);
   j=1:24;
plot(j,Ph11,'k',j,Vavh11,'-*','linewidth',3)
   xlabel('Header Diameter (mm)','fontsize',16)
   ylabel('Pressure and Velocity','fontsize',16)
   title('Relation Pressure and Velocity with Header Diameter','fontsize',16)
   legend('Ph','Vavh')
   grid on
   pause
   clf
```

ANNEX (A-7): Insulation Thickness Optimization

```
%%%%%%%%%%%%%%%%%%%%%%%%%%%%%%%%%%%%%%%%%%%%%%%%%%%%%%%%%%%%%%%%%%%%%%%%%%%%%%%
% Insulation Thickness Optimization
% input
t=(1:1:50);
p=length(t);
N=zeros(p);
i=1:p;
tin=t(i);
% calculation
    CGF=4.5*tin;
    CHL=(661./tin)+217;
    TC=CGF+CHL;
tin=1:50;
plot(tin,CGF,'-*',tin,CHL,'--',tin,TC,'-k','linewidth',3)
   xlabel('Thickness in mm','fontsize',20)
   ylabel('Cost in birr','fontsize',20)
   title('Variation of Thickness with cost and Heat loss','fontsize',20)
   legend('CGF','CHL','TC')
   grid on
   pause
   clf
```

ANNEX (A-8): Storage Tank Thickness Optimization

```
%%%%%%%%%%%%%%%%%%%%%%%%%%%%%%%%%%%%%%%%%%%%%%%%%%%%%%%%%%%%%%%%%%%%%%%%%%%%%%%
% Storage Tank Thickness Optimization
```

```
% input
t=(0:10);
p=length(t);
N=zeros(p);
i=1:p;
ts=(t(i));
% calculation
    CMSP=100.*ts;
    CHL=(697./ts)+342;
    TC=CMSP+CHL;
ts=0:10;
plot(ts,CMSP,'-*',ts,CHL,'--',ts,TC,'-k','linewidth',3)
   xlabel('Thickness in mm','fontsize',20)
   ylabel('Cost in birr','fontsize',20)
   title('Variation of Thickness with cost and Heat loss','fontsize',20)
   legend('CMSP','CHL','TC')
   grid on
   pause
   clf
```

ANNEX (A-9): Transient Analysis of Temperature

```
%%%%%%%%%%%%%%%%%%%%%%%%%%%%%%%%%%%%%%%%%%%%%%%%%%%%%%%%%%%%%%%%%%%%%%%%%%%%%%%
% Hourly Temperature Variation of Water Stream and Storage Tank
% Given Global Radiation and Ambient Temperature Values for a Year
% Consider a Single Glass Cover and Absorber Plate
% Design Parameters
ts=0.0025;          % Storage Tank Thickness [ m ]
tsin=0.015;         % Storage Insulation Thickness [ m ]
Lt=2;               % Length of Collector [ m ]
Lin=0.05;           % Insulation Thickness [ m ]
tp=0.0005;          % Plate Thickness [ m ]
di=0.015;           % Inner Diameter of Riser Tube [m]
ds=2.3;             % Diameter of Storage Tank [m]
Aa=2;               % Absorber Plate Area [ m2 ]
Ae=0.24;            % Collector Edge Area [ m2 ]
Aw=0.895;           % Riser Tube Surface Area [ m2 ]
As=41.55;           % Storage Tank Surface area [ m2 ]
Vs=12.2;            % Storage Tank Volume [ m3 ]
Gabso=0.02;         % Absorivity of Glass
Pabso=0.95;         % Absorivity of Plate
Tabso=0.95;         % Absorivity of Riser Tube
Gtrans=0.94;        % Transmissivity of Glass
rho=0.2;            % Ground Reflectivity Factor
Ep=0.03;            % Emissivity of Plate
Eg=0.04;            % Emissivity of Glass
Vw=3;               % Wind Speed [ m/s ]
sigma=5.67e-8;      % Boltzmann Constant [ W/m2K4 ]
tpg=0.03;           % Distance b/n Glass and Plate [ m ]
phi=9.03*(pi/180);  % Latitude of Addis Ababa (Minilik II) [ rad ]
```

```
beta=22*(pi/180);   % Collector Slope (South Facing) [ rad ]
mg=18.8;            % Mass of Glass [ Kg ]
mp=8.933;           % Mass of Plate [ Kg ]
mw=1.3;             % Mass of Water [ Kg ]
mf=0.03;            % Mass Flow Rate of a Water [ m/s ]
mfs=0.6;            % Mass Flow Rate to Storage Tank [ m/s ]
cpw=4180;           % Sp.Heat of Water [ J/Kg.K ]
cpp=8933;           % Sp.Heat of Plate [ J/Kg.k ]
cpg=840;            % Sp.Heat of glass [ J/Kg.K ]
kg=1.7;             % Thermal Conductivity of Glass [ W/mK ]
ka=0.03;            % Thermal Conductivity of Air [ W/m2K ]
kin=0.037;          % Thermal Conductivity of Insulation [ W/m2K ]
kw=0.625;           % Thermal Conductivity of Water [ W/m2K ]
ks=0.036;           % Thermal Conductivity of Storage Tank [ W/mK ]
ksin=0.032;         % Thermal Conductivity of Storage Insulation [ W/mK ]
kp=401;             % Thermal Conductivity of Plate [ W/mK ]
prw=4.772;          % Prantdl Number of Water
pr=0.708;           % Prantdl Number of Air
Re=733;             % Reynolds Number
dv=1.754e-5;        % Dynamic Viscosity of Water [ Kg/ms ]
g=9.81;             % Gravity [ m.s2 ]
Nuinf=4.4;          % Nusselt Number @ Infinity
a=0.00398;          % Nusselt Number Constant
b=0.0114;           % Nusselt Number Constant
m=1.6;              % Nusselt Number Constant
n=1.12;             % Nusselt Number Constant
W=0.08;             % Space B/n Riser Tubes [ m ]
D=0.016;            % Outer Diameter of Riser Tubes [ m ]
hfi=1500;           % Heat Transfer Coefficient Inside the Tube [ W/oC.m2]
N=10;               % Number of Riser Tube
Wdens=988;          % Density of Water [ Kg/m3 ]
deltt=60;           % Time Step
%%%%%%%%%%%%%%%%%%%%%%%%%%%%%%%%%%%%%%%%%%%%%%%%%%%%%%%%%%%%%%%%%%%%%%%%%%%%
%solar radiation data input
load SolDat.m;
data1=zeros(24,3);
for j=1:365
    data1(:,:,j)=SolDat(j+(23*(j-1)):j*24,:);
end
%%%%%%%%%%%%%%%%%%%%%%%%%%%%%%%%%%%%%%%%%%%%%%%%%%%%%%%%%%%%%%%%%%%%%%%%%%%%
Tp=zeros(24,365);Tp1=zeros(24,365);Tp2=zeros(24,365);Tp3=zeros(24,365);
Tg=zeros(24,365);Tg1=zeros(24,365);Tg2=zeros(24,365);Tg3=zeros(24,365);
Two=zeros(24,365);Two1=zeros(24,365);Two2=zeros(24,365);Two3=zeros(24,365);
Ts=zeros(24,365);Ts1=zeros(24,365);Ts2=zeros(24,365);Ts3=zeros(24,365);
Upw1=zeros(24,365);Upw2=zeros(24,365);UL1=zeros(24,365);ULs1=zeros(24,365);
UL2=zeros(24,365);ULs2=zeros(24,365);It1=zeros(24,365);It2=zeros(24,365);
Ic1=zeros(24,365);Ic2=zeros(24,365);Qu1=zeros(24,365);Ef1=zeros(24,365);
%%%%%%%%%%%%%%%%%%%%%%%%%%%%%%%%%%%%%%%%%%%%%%%%%%%%%%%%%%%%%%%%%%%%%%%%%%%%
% Sun Basic Angles
```

```
  % Declination Angle(Deltt)of the sun every day over the year
    for j=1:365
        decl(j)=(pi/180)*(23.45*sin((2*pi/365)*(284+j)));
    end
  % Calculation of the hour angle for each hour of the day.
    for i=1:24
        omega(i)=(i-12)*pi/12;
    end
  % Incidence angle of the sun every hour and day of the year
    IA=(((cos(phi)*cos(beta))+(sin(phi)*sin(beta)))*(cos(decl(j))*...
        cos(omega(i))))+(sin(decl(j))*((sin(phi)*cos(beta))-...
        (sin(beta)*cos(phi))));
  % Zenith angle of the sun every hour and day of the year
    ZA=(cos(phi)*cos(decl(j))*cos(omega(i)))+(sin(decl(j))*sin(phi));
% Radiation factors
  % Beam radiation factor
    Rb=IA/ZA;
  % Diffuse radiation factor
    Rd=(1+cos(beta))/2;
  % Reflectivity radiation factor
    Rr=(1-cos(beta))/2;
% This Approximates the Plate, Glass, Water and Storage Temperature
%=========================================================================
for j=1:365
Grr=data1(:,1,j); Drr=data1(:,2,j); Taa=data1(:,3,j);
for i=1:24
Gr=Grr(i); Dr=Drr(i); T=Taa(i);
% Initial Temperature Assumption
Ta0=T+273;               % Ambient Air Temperature [ K ]
Tg0=Ta0+0.25;            % Initial Glass Temperature [ K ]
Tp0=Ta0+1.0;             % Initial Plate Temperature [ K ]
Twi0=Ta0;                % Initial Inlet Water Temperature [ K ]
Two0=Ta0+0.75;           % Initial Outlet Water Temperature [ K ]
Ts0=Ta0+0.75;            % Initial Storage Tank Temperature [ K ]
% Beam and Total Radiation
Ib=Gr-Dr;
It=(Rb*Ib)+(Rd*Dr)+(rho*Rr*Gr);
Ic=It*Gtrans*Pabso;
for vv=1:100
    vbeta=2/(Tp0+Tg0);
    deltT=Tp0-Tg0;
    Ra=(g*vbeta*deltT*(tpg^3)*pr)/(dv^2);
    Epg=((1/Ep)+(1/Eg)-1)^-1;
    Tsky=Ta0-6;
    A=1.44*(1-(1708/(Ra*cos(beta))));
    C=((((Ra*cos(beta))/5830)^(1/3))-1);
    if (A>0 && C>0)
       A=1.44*(1-(1708/(Ra*cos(beta))));
       C=((((Ra*cos(beta))/5830)^(1/3))-1);
```

```
    else
        A=0;
        C=0;
    end
    B=1-((1708*(sin((1.8*beta)^1.6)))/(Ra*cos(beta)));
    Nu=1+(A*B)+C;
    F=Re*prw*(di/Lt);
    if (1<F<=1000)
        Nuw=Nuinf+((a*(F^m))/(1+(b*(F^n))));
    else
        Nuw=Nuinf;
    end
    hcga=2.8+(3*Vw);
    hcpg=Nu*(ka/tpg);
    hrga=Eg*sigma*(((Tg0^4)-(Tsky^4))/(Tg0-Ta0));
    hrpg=Epg*sigma*(((Tp0^4)-(Tg0^4))/(Tp0-Tg0));
    hws=Nuinf;
    Upab=(kin/Lin)+hcia;
    Upae=Upab*(Ae/Aa);
    Uga=((1/hcga)+(1/hrga))^-1;
    Upg=((1/hcpg)+(1/hrpg))^-1;
    Upw=(Nuw*kw)/di;
    hsa=2.8+(3*Vw);
    Us=ks/ts;
    Usin=ksin/tsin;
    ULs=((1/hws)+(1/hsa)+(1/Us)+(1/Usin))^-1;
    UL=(Uga+Upg);
    %=======calculation of Tp1, Tao1 and Tg1  for the firts day =========
Tg1=((deltt*Aa*It*Gabso)/(mg*cpg))+((deltt*Aa*Upg*Tp0)/(mg*cpg))+...
    ((deltt*Aa*Uga*Ta0)/(mg*cpg))+((1-(((Aa*Upg)+(Aa*Uga))*...
    (deltt/(mg*cpg))))*Tg0);
Tp1=((Aa*4.*deltt*Ic)/(mp*cpp))+((4.*deltt*Aa*Upg*Tg0)/(mp*cpp))+...
    (((4.*deltt*Aw*Upw)/(2*mp*cpp))*(Two0+Twi0))+(((Aa*Upab)+(Ae*Upae))*...
    ((4.*deltt*Ta0)/(mp*cpp)))+((1-(((Aa*Upg)+(Aw*Upw)+(Aa*Upab)+...
    (Ae*Upae))*(4.*deltt/(mp*cpp))))*Tp0);
Two1=((deltt*It*Gtrans*Tabso*Aw)/(mw*cpw))+((deltt*Aw*Upw*Tp0)/(mw*...
    cpw))+(((mf*cpw)-((Aw*Upw)/2))*((deltt*Twi0)/(mw*cpw)))+...
    ((1-(((mf*cpw)+((Aw*Upw)/2))*(deltt/(mw*cpw))))*Two0);
Ts1=(1-((ULs*As*deltt)/(Wdens*cpw*Vs)))*Ts0+((mfs*cpw*deltt*Two0)/...
    (Wdens*cpw*Vs))+((ULs*As*deltt*Ta0)/(Wdens*cpw*Vs))-...
    ((mfs*cpw*deltt*Twi0)/(Wdens*cpw*Vs));
end
% Temperature for each day of the year are stored as;
   Tp2(j,i)=Tp1;Tg2(j,i)=Tg1;Two2(j,i)=Two1;Ts2(j,i)=Ts1;
   Upw1(j,i)=Upw;UL1(j,i)=UL;ULs1(j,i)=ULs;It1(j,i)=It;Ic1(j,i)=Ic;
end
end
%==================================Main Program=========================
for j=1:365
```

```
Grr=data1(:,1,j); Drr=data1(:,2,j); Taa=data1(:,3,j);
for i=1:24
Gr=Grr(i); Dr=Drr(i); T=Taa(i); Ta0=T+273;
% define input variable
Lm=1.9;                              % Length of Riser Tube [ m ]
Hm=4;                                % Height of Storage Tank [ m ]
n=36;                                % Number of Nodes
del_i=Lm/(n-1); del_s=Hm/(n-1);      % Length Input
% Initial temperature assumption
Tw_i=Ta0; T_s=Ta0;
% Time Gradiant
t_2=60; del_t=t_2/(n-1); t(1)=0;
% Temperature Variation of Water Stream, Absorber Plate and Glass Cover
Tp3=Tp2(i,j);Upw2=Upw1(i,j);Uls2=ULs1(i,j);UL2=UL1(i,j);It2=It1(i,j);
Ic2=Ic1(i,j);
% Initial Temperature
Two(n,:)=Ta0;                % Inlet Water Temperature [ K ]
Ts(n,:)=Ta0;                 % Inlet Storage Temperature [ K ]
for z=1:n           % Loop to Generate (x) Position Matrix
    x(z)=del_i*(z-1);
    x(z)=del_s*(z-1);
end
% Initiate Iteration Variable
m=1;                          % Time Counter
mm=1;                         % Plot Counter
% Start While Loop to Run Until Convergence it Met
while t(m)<t_2
    % Loop to Calculate Updated Temperature Based on Governing Equation
    for k=1:n
        if k==1
        Two(k,m+1)=Two(k,m)+((pi*di*N*(del_i)*It2*Tabso*Gtrans*del_t)/...
            (cpw*Wdens*N*(del_i)*((pi*(di^2))/4)))+(((Upw2*del_t*pi*...
            di*N*(del_i))/(cpw*Wdens*N*(del_i)*((pi*(di^2))/4)))*(Tp3-...
            ((Two(k,m)+Tw_i)/2)))-(((mf*del_t)/(Wdens*(del_i)*N*...
            ((pi*(di^2))/4)))*(Two(k,m)-Tw_i));
        Ts(k,m+1)=Ts(k,m)+(((mfs*cpw*9.*del_t)/(cpw*Wdens*del_s*...
            ((pi*(ds^2))/4)))*(Two(k,m)-Tw_i))-(((Uls2*9.*del_t*pi*ds*...
            (del_s))/(cpw*Wdens*del_s*((pi*(ds^2))/4)))*(T_s-Ta0));
        elseif k==n
        Two(k,m+1)=Two(k,m)+((pi*di*N*(del_i)*It2*Tabso*Gtrans*del_t)/...
            (cpw*Wdens*N*(del_i)*((pi*(di^2))/4)))+(((k*Upw2*del_t*pi*...
            di*N*(del_i))/(cpw*Wdens*N*(del_i)*((pi*(di^2))/4)))*(Tp3-...
            ((Two(k,m)+Two(k-1,m))/2)))-(((mf*del_t)/(Wdens*N*(del_i)*...
            ((pi*(di^2))/4)))*(Two(k,m)-Two(k-1,m)));
        Ts(k,m+1)=Ts(k,m)+(((mfs*cpw*9.*del_t)/(cpw*Wdens*del_s*...
            ((pi*(ds^2))/4)))*(Two(k,m)-Tw_i))-(((k*Uls2*9.*del_t*pi*ds*...
            (del_s))/(cpw*Wdens*del_s*((pi*(ds^2))/4)))*(Ts(k,m)-Ta0));
        else
        Two(k,m+1)=Two(k,m)+((pi*di*N*(del_i)*It2*Tabso*Gtrans*del_t)/...
```

```
            (cpw*Wdens*N*(del_i)*((pi*(di^2))/4)))+(((k*Upw2*del_t*pi*...
            di*N*(del_i))/(cpw*Wdens*N*(del_i)*((pi*(di^2))/4)))*(Tp3-...
            ((Two(k,m)+Two(k-1,m))/2)))-(((mf*del_t)/(Wdens*N*(del_i)*...
            ((pi*(di^2))/4)))*(Two(k,m)-Two(k-1,m));
        Ts(k,m+1)=Ts(k,m)+(((mfs*cpw*9.*del_t)/(cpw*Wdens*del_s*...
            ((pi*(ds^2))/4)))*(Two(k,m)-Tw_i))-(((k*Uls2*9.*del_t*pi*ds*...
            (del_s))/(cpw*Wdens*del_s*((pi*(ds^2))/4)))*(Ts(k,m)-Ta0));
        Qu=(mf*cpw*(Two(k,m)-Ta0))/1000;
        Eff=Qu/(Aa*It2);
        end
    end
    t(m+1)=t(m)+del_t;
    % Important to put all the (m+1) variable before the m=m+1 line
    m=m+1;                  % Update Time Counter
    mm=mm+1;                % Update Plot Counter
    % Conditional statement to check and make sure while loop does not run
    % Indefinitely (Use Control C to stop infinite loop)
    if m==2001
        fprintf('Autobreak')
        break
    end
end
% Temperature for each day of the year are stored as;
Two3(i,j)=Two(k,m)-273;
Ts3(i,j)=Ts(k,m)-273;
Qu1(i,j)=Qu;
Ef1(i,j)=Eff*100;
end
end
% Print the number of iteration used to command window
fprintf('Number of Iteration was % 0.2\n\n',m)
%%%%%%%%%%%%%%%%%%%%%%%%%%%%%%%%%%%%%%%%%%%%%%%%%%%%%%%%%%%%%%%%%%%%%%%%%%%%
% Generate Figure and Results
figure(1)
plot (Two3);
plot (Ts3);
plot (Qu1);
plot (Ef1);
% This stores for the selected day for plotting.
% Water Stream
TwJ17=Two3(:,17);TwF16=Two3(:,47);TwM16=Two3(:,75);TwA15=Two3(:,105);
TwM1=Two3(:,121);TwJ11=Two3(:,162);TwJu17=Two3(:,199);TwA16=Two3(:,228);
TwS15=Two3(:,258);TwO15=Two3(:,288);TwN14=Two3(:,318);TwD10=Two3(:,344);
% Storage Tank
TsJ17=Ts3(:,17);TsF16=Ts3(:,47);TsM16=Ts3(:,75);TsA15=Ts3(:,105);
TsM1=Ts3(:,121);TsJ11=Ts3(:,162);TsJu17=Ts3(:,199);TsA16=Ts3(:,228);
TsS15=Ts3(:,258);TsO15=Ts3(:,288);TsN14=Ts3(:,318);TsD10=Ts3(:,344);
% Useful Heat Gain
QuJ17=Qu1(:,17);QuF16=Qu1(:,47);QuM16=Qu1(:,75);QuA15=Qu1(:,105);
```

```
QuM1=Qu1(:,121);QuJ11=Qu1(:,162);QuJu17=Qu1(:,199);QuA16=Qu1(:,228);
QuS15=Qu1(:,258);QuO15=Qu1(:,288);QuN14=Qu1(:,318);QuD10=Qu1(:,344);
% Efficiency of Collector
EfJ17=Ef1(:,17);EfF16=Ef1(:,47);EfM16=Ef1(:,75);EfA15=Ef1(:,105);
EfM1=Ef1(:,121);EfJ11=Ef1(:,162);EfJu17=Ef1(:,199);EfA16=Ef1(:,228);
EfS15=Ef1(:,258);EfO15=Ef1(:,288);EfN14=Ef1(:,318);EfD10=Ef1(:,344);
i=1:24;
 % Plots plate, exit air and glass temperature for Jan.17
plot(i,real(TwF16),'r',i,real(TwM1),'b',i,real(TwJu17),'k',...
    i,real(TwN14),'g','linewidth',2)
   xlabel(' Time in Hours','fontsize',12)
   ylabel('Temperature in Degree Celcius','fontsize',12)
   title('Temperature variation of Water Stream ','fontsize',12)
   legend('Two-Feb','Two-May','Two-Jul','Two-Nov')
   grid on
   pause
   clf
plot(i,real(TsF16),'r',i,real(TsM1),'b',i,real(TsJu17),'k',...
    i,real(TsN14),'g','linewidth',2)
   xlabel(' Time in Hours','fontsize',12)
   ylabel('Temperature in Degree Celcius','fontsize',12)
   title('Temperature variation of Storage Tank ','fontsize',12)
   legend('Ts-Feb','Ts-May','Ts-Jul','Ts-Nov')
   grid on
   pause
   clf
plot(i,real(QuJu17),'r',i,real(QuN14),'b','linewidth',2)
   xlabel(' Time in Hours','fontsize',12)
   ylabel('Qu (KWh)','fontsize',12)
   title('Usefull Heat Gain (Qu)for Juy. 17 and Nov. 14','fontsize',12)
   legend('Qu-Jul','Qu-Nov')
   grid on
   pause
   clf
plot(i,real(EfJu17),'r',i,real(EfN14),'b','linewidth',2)
   xlabel(' Time in Hours','fontsize',12)
   ylabel('Efficiency','fontsize',12)
   title('Efficiency for Juy. 17 and Nov. 14','fontsize',12)
   legend('Ef-Jul','Ef-Nov')
   grid on
   pause
   clf
```

ANNEX B: GRAPHS OF OUTLET WATER TEMPERATURE ANALYSIS

ANNEX (B-1): Outlet Water Temperature for Winter Season

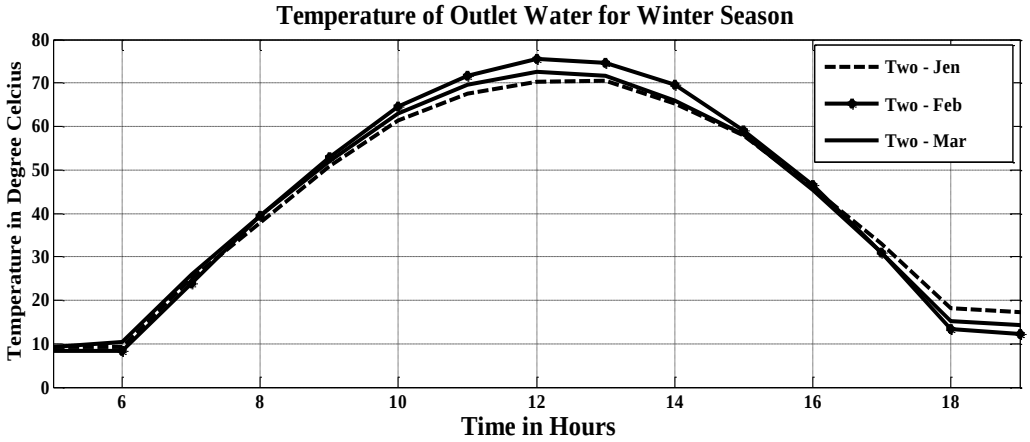

Figure (B-1): Outlet Water Temperature for Winter Season

ANNEX (B-2): Outlet Water Temperature for Spring Season

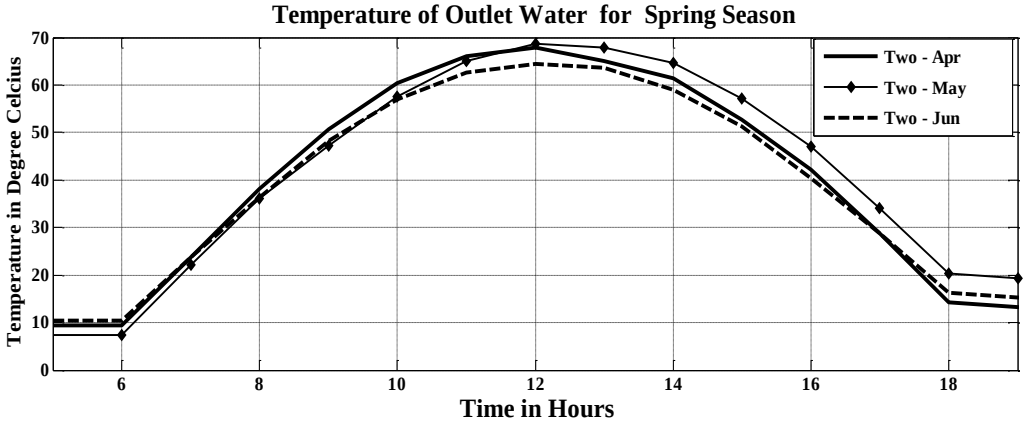

Figure (B-2) Outlet Water Temperature for Spring Season

ANNEX (B-3): Outlet Water Temperature for Summer Season

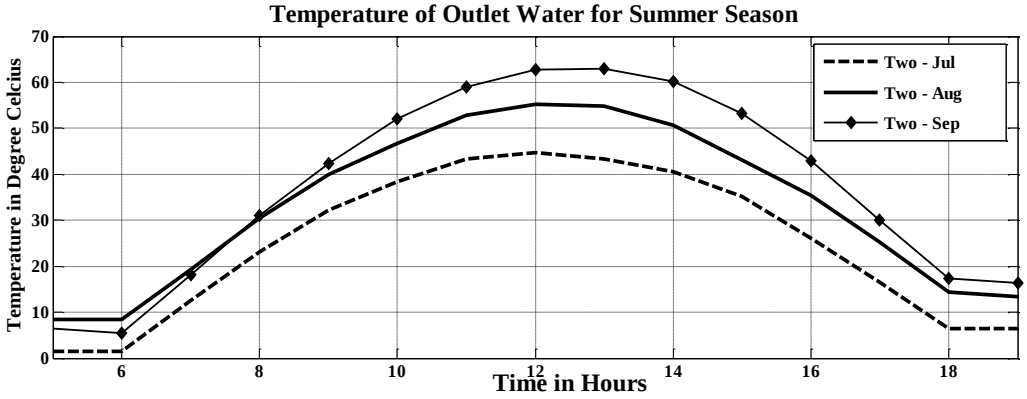

Figure (B-3) Outlet Water Temperature for Summer Season

ANNEX (B-4): Outlet Water Temperature for Autumn Season

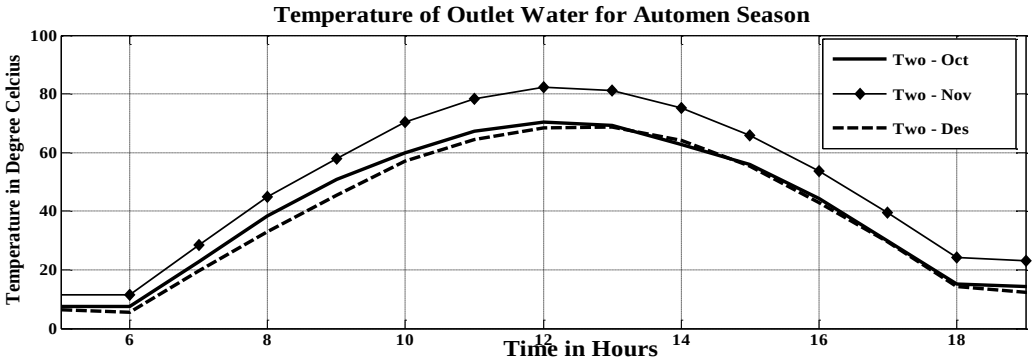

Figure (B-4) Outlet Water Temperature for Autumn Season

ANNEX C: PROPERTIES OF VARIOUS MATERIALS

Table (C-1): Thermal Conductivities of Absorber Materials

		Properties at 300 K				Property of K/C_p $[W/Km]/[J/KgK]$
Substance	**Melting point[K]**	ρ $[Kg/m^3]$	C_p $[J/KgK]$	K $[W/Km]$	$\alpha * 10^6$ $[m^2/s]$	**At 400 K**
Copper	**1358**	**8933**	**385**	**401**	**117**	**393**
Aluminium	**933**	**2702**	**903**	**237**	**97.1**	**240**
Mild Steel	**1810**	**7832**	**434**	**63.9**	**18.8**	**58.7**
Stainless steel	**1670**	**7913**	**477**	**14.6**	**3.95**	**16.6**
Lead	**601**	**11,340**	**129**	**35.3**	**24.1**	**34**
Nickel	**1728**	**8900**	**444**	**90.7**	**23**	**80**
Iron	**1810**	**7870**	**447**	**80.2**	**23.1**	**69.5**

Table (C-2): Properties of Glass Cover Materials

Material	Transmittance (τ)	Absorption (α)	Emissivity (ε)
Crystal Glass	**0.91**	**0.04**	**0.05**
Window Glass	**0.85**	**0.06**	**0.09**
Polyamide	**0.8**	**0.08**	**0.14**
Low Iron Tempered Glass	**0.94**	**0.02**	**0.04**
Polycarbonate	**0.84**	**0.1**	**0.06**
Polyvinyl fluoride	**0.93**	**0.04**	**0.03**
Fluorinated	**0.96**	**0.03**	**0.01**
Polymethyl	**0.89**	**0.05**	**0.06**

Table (C-3): Properties of Sealing Materials

Material	Working temp. Range (° c)		Elongation To Failure (%)	Resistance to Compression Set	Resistance to Creep	Resistance to Weather	Resistance to Water
	Min	Max					
Acrylic	-40	130	400	3	2	4	1
Butyl	-50	125	800	2 – 3	2	4	2 – 4
EPDM	-40	150	600	3 – 4	2	4	4
Fluroelastomers	-40	230	300	3 – 4	3	4	4
Silicone	-60	230	700	2 – 4	3	4	3 – 4
Urethanes	-50	100	700	1 – 4	3	4	1 – 2
(4=excellent, 3=good, 2=fair, 1=poor)							

Table (C-4): Properties of Insulation Materials

Materials	K @ 25 °C $[W/Km]$	Maximum Service Temperature (° C)	ρ $[Kg/m^3]$	C_p $[J/KgK]$
Glass Fiber	0.032	343	56 – 72	38 – 39
Mineral Fiber	0.036 - 0.055	649 – 1037	4.8 - 32	710 – 960
Calcium Silicate	0.055 (@90°C)	649	2330	712
Perlite	0.048	816	16	1260
Foamed Glass	0.058	565	144	1000
Polystyrene Foam	0.029 - 0.039	74	16	1200
Polyurethane Foam	0.023	104	24 – 40	1600
Isocyanurate Foam	0.025	121	70	1045
Phenolic Foam	0.033	135	136	1000
Cellular Plastic	0.040	100	37 – 51	39 – 46

Table (C-5): Lists Properties of Some Selective Coatings

Coating	Type	Absorbance (α)	Emissivity (ε)
Black Chrome	**Electroplated**	**0.96**	**0.10**
Black Nickel	**Electroplated**	**0.9**	**0.1**
Black Copper	**Copper oxide**	**0.87-0.92**	**0.07-0.35**
Black Anodize	**Aluminium oxide**	**0.94**	**0.07**
Solar Foil	**Black chrome over copper**	**0.96**	**0.10**
Enersorb*	**Urethane paint**	**0.97**	**0.90**
Nextel*	**Paint**	**0.98**	**0.89**
*** Non-Selective**			

ANNEX D: MOODY CHART

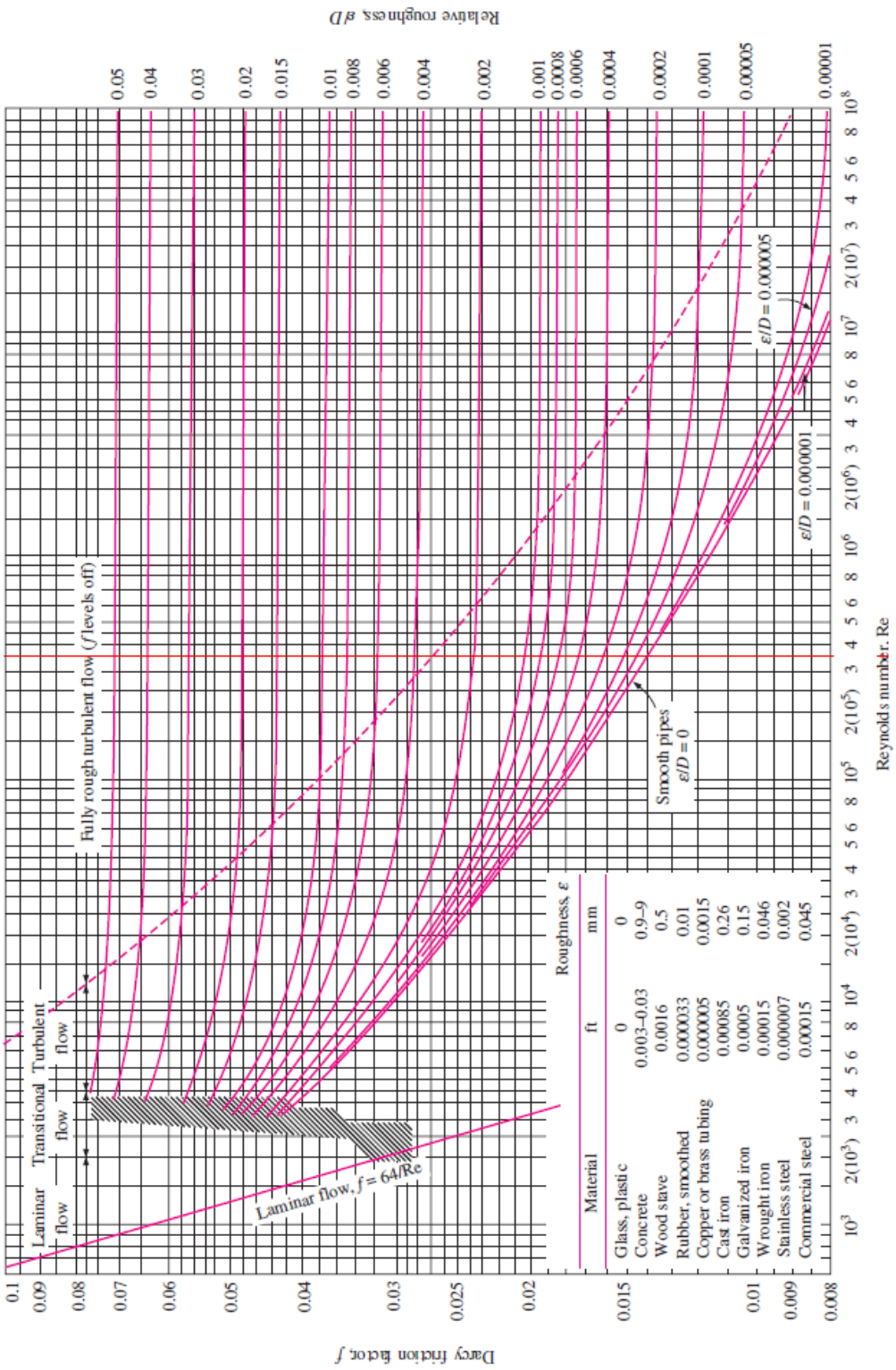

The Moody chart for the friction factor for fully developed flow in circular pipes for use in the head loss relation $\Delta P_L = f\frac{L}{D}\frac{\rho V^2}{2}$. Friction factors in the turbulent flow are evaluated from the Colebrook equation $\frac{1}{\sqrt{f}} = -2\log_{10}\left(\frac{\varepsilon/D}{3.7} + \frac{2.51}{\mathrm{Re}\sqrt{f}}\right)$.

Figure (D-1): Moody Chart